Evaluation of Natural and Synthetic Sorbents for Oil Spill Clean-up Applications

by

Abdulelah Ali Hakami

A thesis

presented to the University of Waterloo

in fulfillment of the

thesis requirement for the degree of

Master of Applied Science

in

Chemical Engineering

Waterloo, Ontario, Canada, 2020

Author’s Declaration

I hereby declare that I am the sole author of this thesis. This is a true copy of the thesis, including any required final revisions, as accepted by my examiners. I understand that my thesis may be made electronically available to the public.

Abstract

Oil products have become an important commodity in the world. However, the world oil demand has been increased due to the growing global population, and as long as oil transportation worldwide continues to increase, many communities are at high risk of oil products spill disasters, which can produce severe damage to the ecosystem and loss to human society. Different response methods have been used for removing oil from the sea surface, such as dispersants, mechanical recovery methods. But, these kinds of methods have several disadvantages that are difficult to address including their complicated operation, high cost, oxygen content, organic species, and high energy required. Currently, sedimentation, filtration, and absorption are physical methods that have been used for cleaning up oil-polluted water. Of these methods, absorption methods are received a lot of critical attention because of their simple operation, low energy consumption, high efficiency and superiority with organic materials that are difficult to degrade. This thesis evaluated the behavior of six fibers with respect to their behavior as sorbents for oil products. The fibers were used to build a porous medium and to study the efficiency for each fiber materials applying for oil products or water absorption applications. Methods for characterizing the fiber materials were studied and experiments were performed to evaluate the efficiency of these fiber. The research enabled selection of fiber media with best probertites for absorbing oil products. Some fibers proved that they are an excellent choice for resolving the problem of oil/water pollution. Traditional models such as Lucas-Washburn and Darcy-based models were used to provide a theoretical framework for the experimental results. These two models were used to fit the experimental data and determined the theoretical average porous size in sorbent materials. The character of hydrophobic and oleophilic for the fiber materials was successfully confirmed by spontaneous imbibition. The spontaneous imbibition equipment was performed to determine the wetting behavior of the fiber materials with different hydrocarbon oils.

Acknowledgement

I would like to express my sincere gratitude to Prof. Leonardo Simon for giving me the opportunity to work under his supervision since advancing my engineering training, helping me in doing a lot of research in my thesis, and becoming to know about so many new things. I am thankful to him for his continuous support, patience, and guidance.

I would like to thank Prof. Xianshe Feng and Prof. Aiping Yu for their valuable time and agreeing to become evaluators as part of the reading and examination committee for my thesis.

I am highly indebted to Jazan University and the Saudi Arabian Cultural Bureau (SACB) for their guidance and continuous supervision as well as for providing necessary information regarding this research, and for supporting me financially and giving me the opportunity to pursue my graduate studies in Canada.

Last but not least, I would like to thank everyone that helped me, but I have not previously mentioned him/her by the name, mainly to those who supported and motivated me throughout writing my thesis.

Dedication

To my beloved Mom and siblings, eternal love and respect until I die.

Table of Contents

List of Tables

List of Figures

List of Abbreviations and Symbols

ρ	Density	[kg/m^3]
ρ_f	Fiber density	[kg/m^3]
ρ_o	Oil density	[kg/m^3]
$\Delta P/L$	Pressure drop per unit length	[atm/cm]
A_{CS}	Cross-section area of the sample	[cm^2]
$\dot{h}$	Rate of the meniscus height	[cm/s]
P_S	Suction pressure	[Pa]
ρ_{Bulk}	Sample's bulk density	[kg/m^3]
ΔP	Pressure difference across the interface	[Pa]
∇P	The gradient pressure	[Pa]
A	Area of cross-section where fluid flow	[cm^2]
CAs (θ)	Contact angle	°
F_G	Gravity force	[N]
F_H	Hydrostatic pressure	[N]
F_V	Viscous forces	[N]
F_Z	Vertical force	[N]
F_{Up}	Upward force	[N]
K	Permeability	[Darcy]
M	Mass	[kg]
m_f	Mass of fiber	[kg]
m_O	Mass of oil	[kg]
gm.gm^{-1}	Oil absorption capacity	
PET	Polyethylene terpthalate (Polyester)	

PP	Polypropylene	
PS	Polystyrene	
PU	Polyurethane	
PVC	Polyvinyle chloride	
Q	Volumetric flow rate	[cm^3/s]
r	Capillary tube radius	[cm^2]
RPM	Revolutions Per Minute	[1/s]
S	Oil Properties	
S_g	Saturation of gas	
S_n	Saturation of a particular fluid	
S_o	Saturation of oil	
S_w	Saturation of water	
ν	Darcy (volume averaged) velocity	[cm/s]
ν_z	Velocity in the z-direction	[cm/s]
V_{bulk}	Volume of bulk material	[cm^3]
V_g	Volume of gas	[cm^3]
V_n	Volume of a particular fluid	[cm^3]
V_o	Volume of oil	[cm^3]
V_p	Pore volume	[cm^3]
V_w	Volume of water	[cm^3]
η_{exp}	Mass absorption capacity	
μ	Fluid viscosity	[cP]
$\rho_{Sorbent}$	Material density in the sample	[kg/m^3]
ϕ	Porosity of the sorbents	

Chapter 1. Introduction

1.1 Motivation

Oil and its products are one of the great significant sources of energy in the modern industrial world. They are transported from the source of production to different users across the globe through oceans and inland waterways used for transport. During the exploration and transportation of oil from production sources to consumption locations entails high risks of accidental oil spills, which can cause severe damage to ecosystems and loss to human society. One of the most important events over the past decade was Deepwater Horizon oil spill, which there were approximately discharged 4.1 million barrels of oil and 2.1 million gallons of dispersants into the Gulf of Mexico in 2010 [1]. Moreover, the destruction of oil storage tanks in Kuwait became spilled several hundred million oil's gallons into the sea during the war in 1991 [2]. Recently, there are several industries which create enormous volumes of oil-contaminated water, for instance, mining, textiles, foods, petrochemicals, and metal/steel industries, which are becoming major pollutants all over the world, and they are a currently serious concerns to marine environments [3]. Learning from previous events enforce the organizations and researchers to develop a new strategy for oil spill disasters. This is challenging because consequences are conditional upon the particular geographic, ecological, societal, and temporal contexts.

Therefore, they have been addressing the need for over-optimistic expectations of the potential consequences of future oil spill disasters. Different response methods have been used in order to remove oil from the sea surface and to prevent the oil from contaminating the shoreline, such as physical, chemical, biological, and thermal treatments. These kinds of response methods have been used to minimize the amount of damage in the sea and to prevent the oils come into contact with the shoreline, which they will be mainly discussed in section 2.2.

Currently, oil/water separation is a significant area that has efficient method through using absorption technique for resolving the problem of oil/water pollution, owing to its low cost, facile operation, and low energy consumption, as shown in Figure 1.1 [3], [4]. Indeed, according to ISI Web of Science, a sharp increase in papers representing oil/water separation has recently occurred, as shown in Figure 1.2 [3]. Furthermore, the development of functional materials for effective treatment of oil/water pollution is crucial.

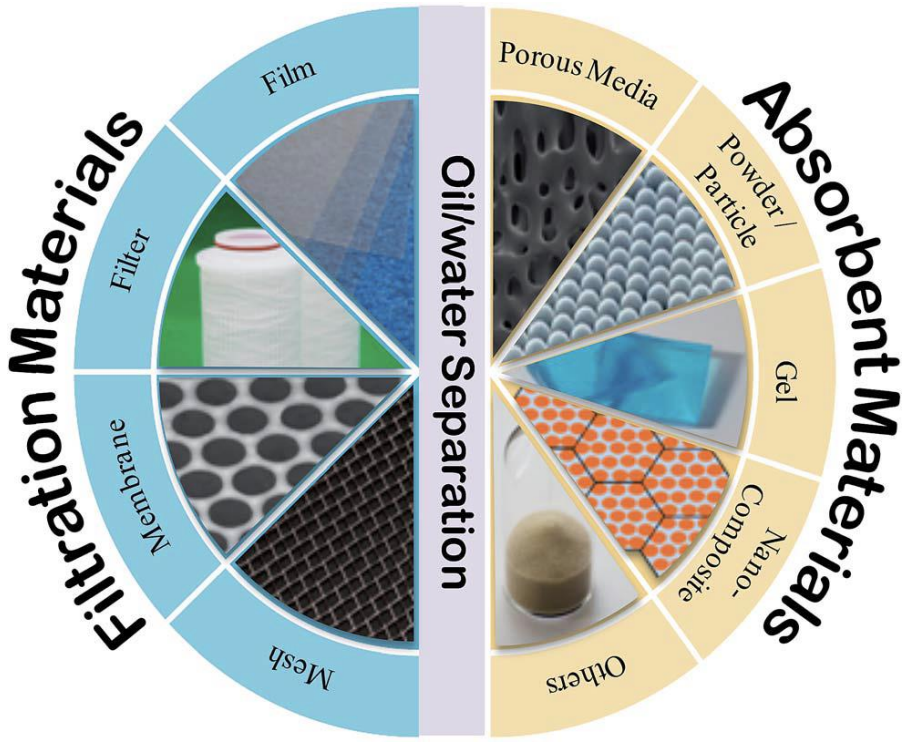

Figure 1.1 Typical materials used for oil/water separation [3]

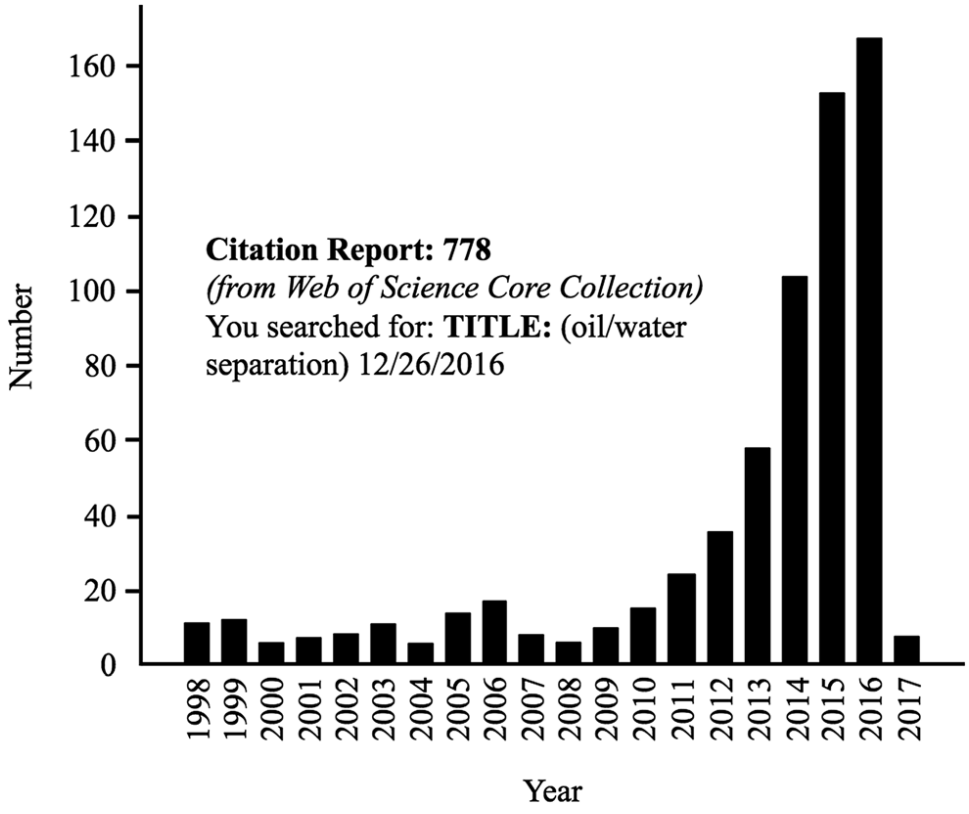

Figure 1.2 Number of articles of oil/water separation indexed in ISI Web of Science by the title of “oil/water separation” [3]

1.2 Objective of This Thesis

In this thesis, kapok, cotton, hemp, polyester, nylon, and glass fibers were used to build a porous medium and to study the efficiency for each fiber materials applying for oil or water absorption applications. The main objectives of this study are:

I. Test wettability of the fiber materials (sorbents).
II. Understand the mechanism behind the spontaneous imbibition of the fiber materials.
III. Test the reusability of the fiber materials.
IV. Combine the absorption capacities of sorbates into the sorbents derived by the use of experimental data and theoretical models.

The scopes of this study include

I. Perform spontaneous imbibition equipment with different hydrocarbons and evaluate the efficiency of sorbents.
II. Understand the character of hydrophilic and oleophilic for the fiber materials that would confirm by spontaneous imbibition.
III. Characterization of sorbates (hydrocarbons) and sorbents (fibers).
IV. Compare the performance of absorption capacity with a wide range of hydrocarbons into different sorbents.
V. Perform data analysis and evaluation of potential improvements to be used in the applications of oil-water separation.

Chapter 2. Literature Review

2.1 Clean-up of Oil-Polluted Water – An overview

Crude oil and its products are widely transported. The term oil used here means crude oil and its hydrocarbon products used as fuels and lubricants. In general, there is a high risk to the environment and marine life when oil is produced, transported, stored, and used. When an area pollutes with oil, the whole area becomes destroyed due to the oil's damaging characteristics [5]. Moreover, when oil comes into contact with objects, for example, beach, rocks, bird feathers or bathers hair, it is difficult to remove it [6]. The physical and chemical properties of oil can change gradually when the oil is spilled in water or on land [7]. Thus, oil settles on beaches and destroys organisms that live there. Furthermore, oil settles on ocean levels and moves around killing organisms that live in the bottom of the ocean, for instance, crabs, and threatens fish's hatcheries that live in coastal areas, which pollutes fish's flesh [8], [9]. Oil spill across the oceans and seas needs prompt attention, it should be removed as quickly as possible, due to their environmental and economic impacts, and the coating/adhering properties of these hydrocarbons [7], [8].

Finding effective decontamination and clean-up strategies are needed after a spill to assure the protection of the environment and human health. Therefore, one of the most effective approaches for cleaning up oil spills are sorption techniques. Sorption is the common term used for both absorption and adsorption. There are two mechanisms of sorption that a sorbent employs to sorb liquids. The absorption mechanism permits the liquids to penetrate into porous spaces of the material, while adsorption allows liquids to accumulate on their surfaces without the need for penetration into the pores of a material [10]. These terms are often confused with each other. Thus, this review will clarify the differences between them because of their relevance in porous media. The molecular diffusion of oil inside the structure of materials is often of negligible relevance compared to sorption.

2.1.1 Adsorption

Adsorption is defined as the physical process by which atoms, ions, or molecules of a liquid (adsorbate) become adhered to the solid’s surface (adsorbent). Adsorption occurs in three steps. Firstly, the adsorbate diffuses from the major body of the stream to the external

surface of the adsorbent particles, as shown in Figure 2.1. Secondly, the adsorbate moves in a relatively small area of the outer surface to the pores within each adsorbent particle. The bulk of adsorption usually occurs in these pores due to there is a considerable surface area. Lastly, the contaminant molecule becomes adhered to the surface in the pore. The adsorption on a surface is occurred because of binding the individual atoms, ions, or molecules of adsorbate and the adsorbent's surface. The adsorption process divided into physical and chemical adsorption. The physical adsorption occurs when the molecules of adsorbate and adsorbent become held to each other by Van der Waals force. When the electron density (high polarity) between adsorbate and adsorbent's surface becomes significant, then chemical adsorption will occur [11].

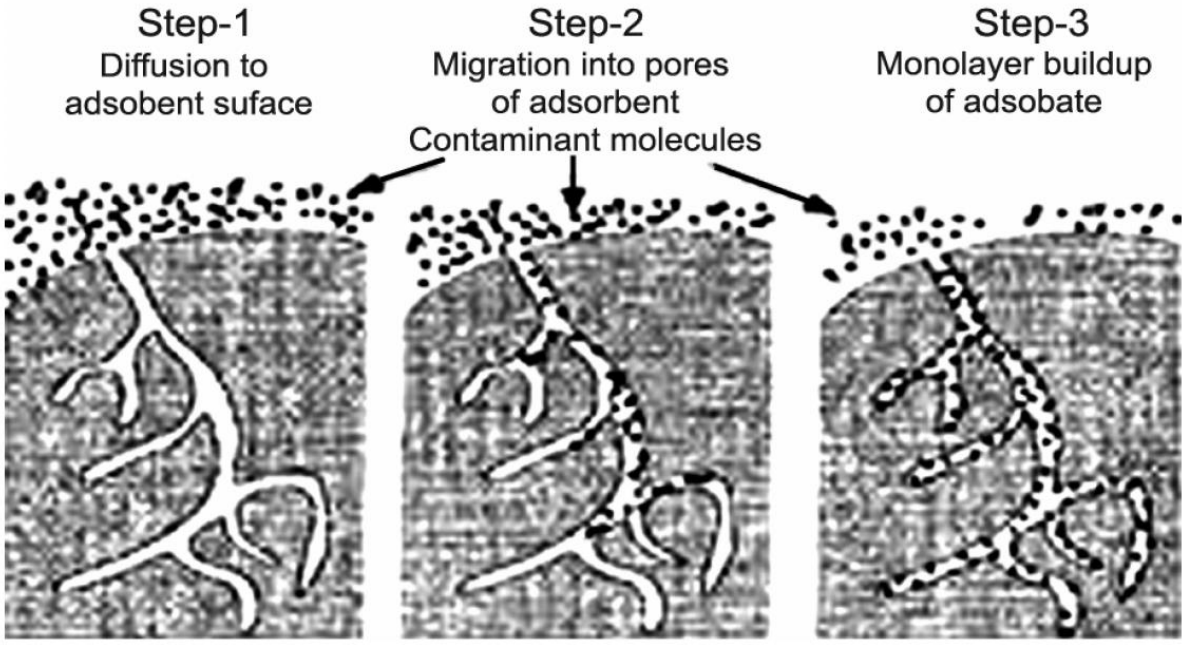

Figure 2.1 Mechanism of adsorption on surface and inside pores [11].

2.1.2 Absorption

Absorption is a process where one substance permeates another. Absorption is a phenomenon discriminated on the grounds of the method and the amount of transport of liquid into an absorbent. The main driving force for transporting the majority of the liquid into a material is employed by capillary pressure, which is discussed in great detail in section 2.7.1

The capillary force direct results from the intrinsic capacity for liquid attraction in the material and the overall driving force can significantly enhance by a secondary force, such as gravity or pressure.

2.2 Oil Decontamination Methods

Different techniques have been used for minimizing the impacts of oil spill on environmental and socioeconomic resources, and to reduce the time for recovery of affected resources by achieving an acceptable standard of cleanliness. Several methods have been used to eliminate oil from polluted water. These methods can be divided into four categories involving physical, chemical, biological, and thermal treatment.

2.2.1 Physical Methods

This method involves the physical separation of the oil spill from the contaminated environment. This method possesses three main techniques. Skimmers represent a type of mechanical equipment used to remove oil floating spills from the water surface. Many designs use skimming media, such as a conveyor belt, tube, or rope are placed to carry the floating oil and collect them for processing and recovery. Other skimmer technologies use suction to remove oil spill, while weir skimmers use gravity to gather skimmed oil into underwater storage tanks. Skimmers are generally effective in calm water, and suction skimmers are susceptible to clogging by floating debris.

Another physical technique is sorbent materials. They are a useful resource in response to the oil spill. Oil sorbents compose a wide range of organic, inorganic, and synthetic materials designed to recover oil in preference to water. The material to use depends on their composition, configuration, and intended applications in the response. This review considers the types of sorbents available and the effective way of these materials in section 2.3.

The hot water and high-pressure washing is a common technique used in shoreline clean-up [12]. In this technique, heaters are used to heat the water, which is then sprayed by hand with high-pressure wands or nozzles. The oil is then moved out to the water surface, which can be collected with skimmers or sorbents. But, the organisms have a high chance of being affected by the hot water in this technique.

2.2.2 Chemical Methods

Chemical treatment methods have been used for minimizing the environmental impacts resulting from oil spills. Chemical compounds are designed to assist in controlling and cleaning up oil contaminated the water. They have been employed to disperse the oil to treat shoreline areas from coating marsh and beach areas [13]. Spraying dispersants were used at extremely deep depths for the first time in USA history as well as they applied almost two million gallons of dispersants to break up the oil during the Deepwater Horizon oil spill [14]. However, this kind of treatment method used with varying degrees of success for mitigating the environmental effects [15].

A typical commercial dispersant contains solvents and surfactants. The solvents help to keep the chemicals mixed and dissolved into the oil while the surfactants facilitate the oil and water to mix easily. These dispersants contain molecules that one end is attracted to water and one end that is attracted to oil. As the dispersants are applied to an oil slick, these molecules attach to the oil leading to break up the oil slick into smaller oil droplets. These smaller droplets become mix into the water column to be eaten and further degraded by microbes and other organisms, as can be shown in Figure 2.2 .

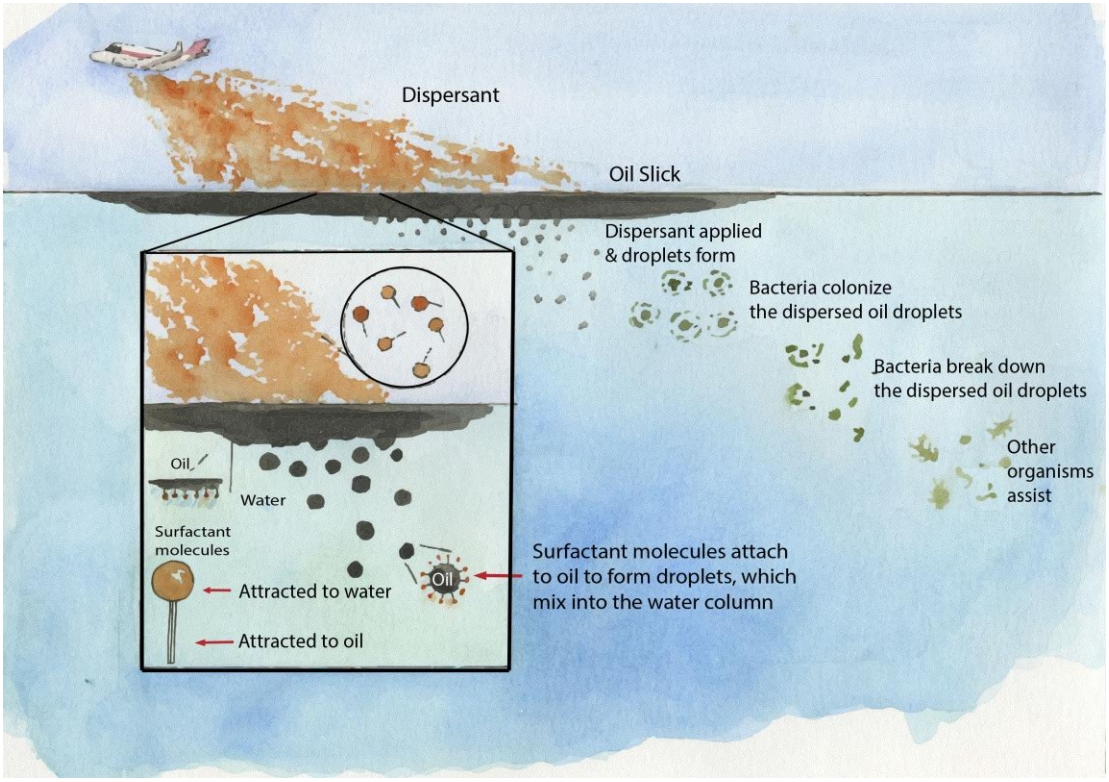

Figure 2.2 The strategy of dispersants [12].

2.2.3 Biological Methods

Bioremediation technologies have been used to degrade the oil spill in surface water. It involves the use of biological agents, which are biochemicals or microorganisms that enable an increase to the rate of natural biodegradation. According to the United States Environmental Protection Agency [12], microorganisms, such as bacteria, fungi, and yeast help to break down complex compounds into simpler products and slowly remove oil from the aquatic environment. But, this method can take years.

Moreover, bioremediation technologies can help biodegradation processes work faster. Fertilization and seeding are the two common bioremediation technologies that can be added to the contaminated environment. The fertilization can add nutrients, for example, phosphorus and nitrogen to stimulate the growth of microorganisms that are capable of biodegradation. In terms of seeding, it increases the population of microorganisms that can biodegrade the spilled oil.

2.2.4 Thermal Methods

Thermal treatment technologies possess an important role in the treatment of oil spills due to their ability to quickly and reliably meet cleanup standards. However, sustained high temperatures can damage the living organisms into the water and can obtain a lot of environmental concern.

2.3 Oil Sorbent Materials

The existence of sorbent materials in an oil spill areas aids in changing the liquid phase to the semi-solid phase [2]. The sorbents are used to recover liquids through the mechanism of absorption, and adsorption, or both. The absorbent is material imbibing and retaining the liquid causing the material to swell while adsorbent is coated by oils on its surface. When both mechanisms happen together, the sorbent structure tends to be useful in removing the oil spill. Combining both hydrophobicity and oleophilicity in making a sorbent material is needed in order for a sorbent to become useful for combating oil spills. Sorbents can be appropriately used for recovering small pools of oil unsuitable for other techniques.

The main purpose of creating a highly efficient porous material is to maximize the rate of absorbency so that it can be used in oil spill clean-up applications. Sorbents are attractive for oil spill clean-up applications due to the possibility of collecting and completely removing the oil from the spill site, and these sorbents, in some cases, can be recycled [16]. Booms can be used to physically corralled the oil for improved oil sorption and collection. A porous material requires some properties to be considered as a viable oil spill sorbent. These properties that are necessary for good absorbing materials are high uptake capacity, and hydrophobicity [16].

The sorbents must be hydrophobic and oleophilic, have a high rate of uptake and retention, and capable of releasing the oil that it has absorbed if is to be reused. The high uptake capacity assures that a large quantity of oil can be picked up relative to the weight of the sorbent material. The high rate of uptake implies the material absorbs the oil quickly. The retention over time signifies the oil does not leak from the sorbent material after it has picked up. Besides, the sorbents can ideally be recyclable and biodegradable. These sorbent materials can be divided into three categories including organic, mineral, and synthetic. Three natural (plant fibers) and three synthetic fibers were evaluated in this study. These sorbents will be discussed in section 2.3.1 and section 2.3.3.

2.3.1 Natural Organic Sorbents

The natural organic fibers can be divided into three categories: including animal fibers, mineral fibers, and plant fibers. The plant fibers can be classified according to their location in the plant as can be clearly seen in Figure 2.3. For instance, flax, hemp, jute, and ramie are extracted from the stem of the plant, and other fibers can be obtained from seeds, such as cotton and kapok, fruits (coconut, and pineapple), or the leaves of the plant (sisal and abaca).

Moreover, cattail pollen [17], [18], rice straw (Figure 2.4) [19]–[23], sugarcane bagasse [24], banana [25], pomelo peel [26], coconut coir [27], [28], oil palm waste [29], [30], nettle [31], jute [31], waste paper [32], [32]–[34], bamboo [35], human hair [36], chicken and avian feathers [37], are inexpensive and abundant materials used for oil spills. The natural organic sorbent exhibits unique hydrophobic–oleophilic characteristics, excellent buoyancy and high selectivity for various oils. They received more attention for cleaning up oil spills due to their low cost, abundancy, environmentally friendliness, and biodegradable materials. The natural

organic sorbents are capable to absorb 3 to 15 times for their weight of oil, but they tend to absorb both water and oil meaning that they may sink [13]. In this study, cotton, hemp, kapok fibers were used to build a porous medium and to study the efficiency for each fiber materials applying for oil spill clean-up applications.

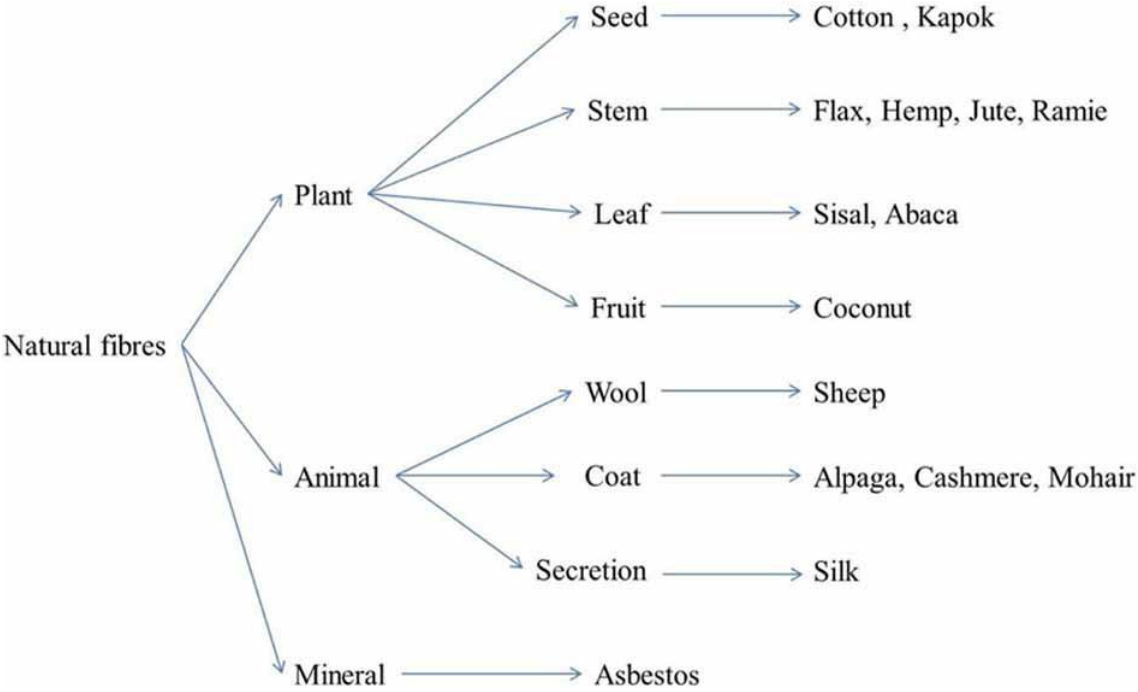

Figure 2.3 Classification of natural fibers [38].

Figure 2.4 Sorbent booms constructed from straw [12].

2.3.1.1 Cotton Fiber

Pure cotton is a well-known spongy, feathery stable fiber that can absorb both oil and water. It composes of cellulose (91%), water (7.85%), protoplasm pectin (0.55%), waxes, fatty substances (0.4%), and mineral salts (0.2%) [39]. It is mostly cellulose-based, environmentally friendly, degradable, low density, and inexpensive materials. Cotton fibers are produce in the flower of the plant. The cellulose holds the highest percentage of cotton's composition with a thicker lumen in the secondary wall leads the cotton fiber to be a hydrophilic material due to the hydroxyl groups on its structure. The wax layer on the primary wall in the cotton fiber contains a mixture of long-chain saturated fatty acids, alcohols, resins, and sterols that are responsible for attracting oil by non-polar mechanism [40].

Deschamps et al. [41] were studied the separation of oil (vegetable oil, mineral oil, fuel oil, and crude oil) contaminated water using raw and treated cotton fiber by acetylation. They found out both fibers were sorbed from 19 to 23 g/g and from 23 to 30 g/g respectively, and these fibers were also reused by simple squeezing up to 10 cycles. Moreover, they discovered that the sorption capacities in the tenth cycles of raw and treated cotton fibers were decreased in the range of 15-21 g/g and 11.5-12.5 g/g respectively. The sorption capacity of treated cotton fibers decreased compared to raw cotton fibers. They further confirmed that both fibers possessed higher lipophilic characteristics and greater stability in water overtime after the sorption experiments. Hussein et al. [42] were investigated a low-grade cotton fiber pad used for removing oil-polluted water. The sorption capacities ranged from 18.34 to 22.5 g/g, and both loose and pad cotton fiber showed excellent sorbent behavior for cleaning up oil spills. Peterson et al. [43] were also studied the oil sorption using cotton and polypropylene mats at room and frozen temperatures. They found out that cotton mats demonstrated the highest sorption capacity of 11.48 and 13.87 g/g compared to polypropylene, which showed sorption capacities of 9.82 and 11.29 g/g at two different temperatures. Due to their overall results, they concluded that cotton mats combined both absorption and adsorption mechanisms in the oil sorption, whereas polypropylene was based on the adsorption mechanism. Wang et al. [44] were used hydrophobic-modified cotton fiber with silica nanoparticles, and they found out that the sorption capacities of different oils were ranged from 36.7 to 62.6 g/g, as well as the modified cotton fiber was reused up to 80 cycles.

Wang et al. [45] were used carbon fibers with a hollow tubular structure derived from natural cotton. They were obtained a high sorption capacity due to the improved surface area and hydrophobicity in the range of 32-77 g/g with different oils involving vegetable and crude oil. They were further confirmed that the reusability of the hollow fiber. After the five cycles of reusability, the sorption capacity was showed 9% for the hollow fiber compared to 27% for untreated cotton fibers. Carmody et al. [46] found out a surface area of 8.2 m/g and demonstrated limited sorption sites on the surface of the raw cotton fiber. Hence, the high sorption capacities described in different literature above tend to be related to several factors including interactions between the oil and the wax present in the primary walls of the cotton fiber, uptake throughout interfiber capillaries between fiber bundles and internal lumen storage, fibers molecular arrangement, and fiber surface morphologies.

2.3.1.2 Hemp Fiber

Hemp was likely the first plant cultivated and manufactured in textile applications [47], [48]. It is fast-growing and cannot require demanding as to climate, soil quality, herbicides, pesticides, fungicides, fertilizer, and nutrients [47]. Also, it restores nutrients to the soil and deeply rooting that can provide a good disease break and help to maintain the soil structure [49]. It was rapidly grown all over the world until, in the 1930s, it was prohibited by most Western countries because of the high manufacturing in drug-related problems [47], [48]. Hemp fibers are typically longer and stronger than other fibers because they are bast fibers. It holds similar chemical composition to flax fiber, better moisture resistance, high tenacity at approximately 20%, and low elongation compared to flax fiber [49]. The Hemp fibers generally contain cellulose lower than in cotton fibers and amount to approximately 67-78%, and the rest contain about 16-19% hemicelluloses, 0.8-2.5% pectic substances, 2.9-3.3% lignin, and 1–2% fat [50], [51]. Due to the low-cost and high availability of hemp fibers, they have received considerable attention of researchers in manufacturing them in textiles, composites, medicine, building, construction, automotive, and packaging applications [51], [52]. The hemp fiber tends to be as oleophilic material due to the wax content on its surface, and its application is limited in oil spill clean-up.

2.3.1.3 Kapok Fiber

Kapok tree produces a light known fiber tree in the world and is referred to as poor man's silk. The kapok fiber is an agricultural product that possesses high oil absorbency characteristics. It is notable for its lightweight that floats in the air, fluffy, non-allergic, non-toxic, and yellow fibers. It holds rich oiliness and is an inelastic material to be spun [11]. It holds a large lumen and has a low bulk density at nearly 290 kg/m^3 [38]. Also, it is used in manufacturing pillows, life preservers, sleeping bags, and insulation. The kapok fibers commonly contain 64% cellulose, 13% lignin, and 23% pentosane [16]. It is significantly considered as excellent buoyancy, good hydrophobic/oleophilic properties and does not get wet with water due to the large lumen and the wax content on the surface of the kapok fiber at 3% [11], [16], [53]-[60].

Several studies were used kapok fiber as a sorbent material for oil spill cleanup, and they were suggested that it has a good oil sorption potential [53], [56]. Lim and Huang [54] were evaluated the sorption capacities of both kapok and polypropylene fibers. They found out that the kapok's sorption at a packing density of 0.02 g/cm^3 was higher than polypropylene with adsorption capacities of 36, 43, and 45 g/g for diesel, hydraulic, and engine oil respectively. Abdullah et al. [16] demonstrated a high sorption capacity of 50.8 g/g with engine oil at low density and low contact angle of kapok fiber. Similarly, Ali et al. [55] reported sorption capacities of 19.35, 25.71, 60.51, and 49.94 g/g for diesel, crude oil, new engine oil, and used engine oil, respectively. In recent work, Cao et al. [56] found out a sorption capacity of 27.86 g/g for vegetable oil using a kapok fiber.

The various authors attributed high sorption capacities of the kapok fiber due to the high porosity, low cellulose content, largely shaped lumens, and good hydrophobicity of the kapok fiber [38]. Oils can be adsorbed on kapok fiber through the coverage wax on kapok's surface and the packing densities of the fiber assemblies [18], [54], while the absorption process through oil capillary movements inside the lumens [57]. The physical characteristics of oils involving viscosity, contact angle, and surface tension are other factors affecting the sorption capacities of the kapok fiber. In terms of reusability, the kapok fiber demonstrated high oil sorption capacities with 4-15 cycles of use [38], [45], [58], [59].

2.3.2 Inorganic Sorbents

Natural inorganic sorbents have a higher density than the organic sorbent [4]. It has been particularly interesting to develop a sorbent demonstrating a high absorption capacity and low cost for removing various pollutants contaminating water. Zeolite, vermiculite, and pumice are natural inorganic sorbents. Currently, zeolites have widely used in oil spill decontaminations. Research on synthetic zeolites confirmed their superior efficiency compared to the other sorbents, and they applied on a large scale to remove oil from water surfaces [7]. Some natural inorganic materials are relatively inexpensive and have significant potential for modification and enhancement of their absorption capabilities [61]. They can imbibe 4 to 20 times for their weight of oil compared to the first category [13].

2.3.3 Synthetic Sorbents

The synthetic organic sorbents include man-made materials based on polymers, such as polypropylene (PP), polyurethane (PU), polystyrene (PS), polyvinyl chloride (PVC), polyester (PET), and nylon fibers. The common synthetic sorbents can absorb as much as 70 times of their weight for oil compared to the previous two categories [13]. These materials are mostly designed as fibrous beds with pores for liquids to penetrate. There are several applications have been made for developing synthetic organic sorbents with low cost, and high oil absorption capacity, and great oil-water selectiveness [62]. They have hydrophobic/oleophilic characteristics, a large amount of oil/water absorption capacity, high buoyancy, and are abundant in large scale fabrication. For example, the development of commercial polypropylene (PP) fiber mats have excellent property and nearly 15 g/g oil absorption capacity. However, they remained as a considerable environmental challenge due to their poor degradation [62]. Polyester, nylon, and glass fibers were used in this study as sorbents.

2.3.3.1 Polyester Fiber

Polyester fiber is one of the main sorbents used in oil spill clean-up. It is further considered as porous material due to it holds small voids allowing to absorb the oil [63]. However, the natural fibers have high water sorption by using them in the sea water, and they are still underdeveloped [64]. Hence, the polyester fibers have small voids leading to absorb the liquids inside the voids of the sorbents and hold the oil after sorption [63], [64]. This

material generally has a high capacity of oil absorbency because it is made from oil feedstock, which is non-renewable and increasingly expensive resources [16], [61]-[66]. It has chief benefits of hydrophobicity, efficient and easy to design, and low density, which allows a significant amount to be carried without having to worry about weight [67].

After the oil spill in the Gulf of Mexico, various studies on functionalized polyester were made to achieve the wetting properties needed for the oil/water separation [68]. Zhang and Seeger [68] were used superhydrophobic and superoleophilic polyester material coated with silicone nanofilaments via a chemical vapor deposition method. They obtained that the silicone nanofilaments coated lead the oil to penetrate the fiber with an absorption capacity of 2.92 (g/g) for crude oil and demonstrated that the oil absorption capacity was significantly based on the absorbent material and the fabric size. Elhaj et al. [69] were studied nonwoven textile materials (NWM) with various components of cotton, viscose, polyester, polyacrylonitrile (PAN), polyamide, and polypropylene used for oil spill cleanup. They found out that a high content of PAN was the most effective absorbents of NWF's compositions and demonstrated NWF with different synthetic fibers was effective, environment-friendly, and economic absorbents used for cleaning up oil spills.

The fibrous materials produced from petroleum are highly effective via oil flow through oil spill cleanup. The bulk density, free volume, increased porosity, and the rate of oil sorption are the main factors controlled by oil products [64], [65], [70].

2.3.3.2 Glass Fiber

Glass fiber is a very versatile class of materials. It has a variety of shapes and forms. This fiber is produced using raw materials and can be available in almost unlimited quantities [71]. It possesses the distinct advantage of combining very high strength with low density and, most of all, a very reasonable cost. The glass fibers are highly sophisticated engineering material due to their resistance to chemical and thermal attack, as well as desirable fiber properties, such as hardness, transparency, stability, flexibility, stiffness [71], [72]. The physical and chemical resistance are the two factors to achieve consistency in the glass fiber for production capability and efficiency [73]. The reactions of acids, bases, and water are referred to as a percent weight loss in which the low amount of these actions leading the glass fiber to be more resistant and corrosive material [74]. The application of fiberglass is used in

several fields involving the transportation, recreation, marine, pipes, and construction industries, but it is slightly limited in the oil spill cleanup applications.

Various studies explored the glass fiber for oil spill cleanup applications [75]. Akagi et al. [76] used an equation to study the relationship between the pressure drop toward the bed and the oil uptake in the bed at steady-state condition to separate oil-water mixtures by the glass fiber bed. The mechanism for separation was coalescence. They found out that a good agreement between the measured and calculated values of the pressure drop for both steady-state and unsteady states and obtained a new correlation equation to estimate the separation efficiency of oil droplets through the glass fiber bed influenced by the flow rate, the fiber diameter, the bed length.

Robelein and Blass [77] studied the separation of small droplets from several aqueous-organic systems using fiber media as coalescence aids, such as stainless steel, glass, and PTFE-fiber media. They discovered that the organic-aqueous phase was dispersed into drops due to the variations of various factors containing the fiber thickness, depths, the fiber bed porosity, drop size, and volume flow. They concluded that all fibers were increased with decreased fiber size due to the decrease in viscosity of the continuous phase, fiber bed depth, and porosity of the fiber media. Shin and Chase [75] investigated the effect of fiber size for both polyamide nanofibers or microfibers mixed with glass fiber as a filter media for removing water-in-oil emulsion. They pointed out that the polyamide nanofibers mixed with glass fiber showed greater separation efficiency and high capillary pressure because the nanofibers contribution to increase number of pores between the glass fibers. In contrast, the polyamide microfibers combined with glass fiber exhibited a low filter efficiency.

Other studies were used the glass fiber as an assistant for filters for oil/water separation. Kulkarni et al. [78] were used fibrous coalescing filters constructed of hydrophilic micro-glass fibers and hydrophobic polypropylene or polyester fibers. They used deionized water dispersed in diesel fuel to study the effect of filter wettability. The wettability of the alternating layers was used the modified Washburn's equation in their work to investigate the lipophilic to hydrophilic (L/H) ratio. They found out that the effect of pressure drop for the glass media-PP was significantly increased compared to the glass–PET media due to the lower pressure drop for the glass media-PP leading to an increase in the (L/H) ratio. In terms of efficiency, they obtained that the best performance of the glass media-PP indicated by the L/H ratio at around

3-10, while the best performance of the glass–PET media occurred with the L/H ratio of about 25.

Moorthy [79] was studied liquid-liquid coalescence experiments with glass fiber filter. The surface fibers were coated with various silanes achieved a high-performance filter wettability. Magiera and Blass [80] were investigated the separation of liquid-liquid dispersion through the hydrophilic glass and hydrophobic Teflon fibers with stainless steel fiber media. They found out that the hydrophilic glass and stainless-steel fiber media showed a high separation efficiency, while the hydrophobic Teflon fibers with stainless steel fiber obtained a low performance of fiber-bed settler.

The glass fiber performance depends on fiber surface wetting properties, fiber size, fiber orientation, porosity, binder content, and filter bed length. Besides, the separation efficiency is influenced by fluid and emulsion characteristics, such as composition, density, viscosity, and droplet size [81]-[86]. The oil flow rate is another significant factor controlling the mechanism of capture and transport of droplets with the fibers [75], [78].

2.3.3.3 Nylon Fiber

Polyamide (nylon) fiber is a humanmade synthetic fiber and is one of the most popular fibers. It is referred to as a ubiquitous polymer due to its versatile properties [87]. The nylon fiber is a semi-crystalline polymer bearing oleophilic hydrocarbon chains combined by hydrophilic functional amide groups. It possesses advantages including very high tensile strength with strong filament to filament bonding resulting from hydrogen bonding between the polyamide chains, rapid wet in a wide range of liquids [88]. Moreover, the nylon fiber is a versatile family of thermoplastics that possess a broad range of properties ranging from relative flexibility to significant stiffness and toughness [87]. Other relevant features are its inert and resistant to chemical attack, thermal stability, lustrous appearance, and good processability [89]. It can be made into a hydrophobic material by properly treating it with long-chain perfluoroalkyl compounds to reduce its surface energy and increasing its surface roughness [90].

Nylon fibers were used as a sorbent boom in conjunction with other polymers containment and to remove oil contamination in Pensacola Bay during the Deep Horizon oil spill [91]. Ortega et al. [91] studied the utilization of nylon-based spunbond fabric bags for

removal of crude oil and gear lube oil. They reported that the nylon bags could effectively remove 99% of the oil-contaminated water. The oil sorption versus fabric mass obtained was more than 2500% and 1000% of gear lube oil and crude oil respectively. They found out that the low area mass density of nylon bags was sorbed up to 16 times with crude oil and more than 26 times with gear lube oil. However, there are still some doubts about the use of the nylon fiber as a sorbent for separating oil-in-water emulsions due to limited reports on the performance of nylon fiber used for separating oil-in-water emulsions [91].

Nylon fibers can be considered to be amphiphilic, which can act both as oleophilic and hydrophilic compared to other synthetic fiber materials [92]. There are still limited investigations on the performance of the nylon fiber as sorbent; contribution factors in this respect are fiber thickness, fiber orientation, void space, and the interfacial distance between the surface of the fiber and the oil [91]. Furthermore, it was reported that the oil separation efficiency was affected by viscosity, density, and surface tension of oil.

2.4 Properties of a Porous material

Porous materials are used in a diverse range of technology and in nature. There are some typical examples of porous material are widely used in everyday life, such as cemented sandstone, foam rubber, tissue papers, textiles, and filters. Common examples of technologies that depend on porous media are petroleum production and hydrology. A material or structure needs to have these two conditions in order to be considered a porous medium [93]:

1. It needs to have empty spaces/voids embedded in the solid, and these pores normally take hold of some fluid, such as air, water, oil or a mixture of different fluids.
2. It should be permeable to a variety of fluids.

Another condition is the velocity of the solid material with regard to the boundary system is zero, whereas the velocity of the fluid is able to flow within the porous system [19].

In geology, porous solid plays an important in understanding the formation, structure, and potential use of many substances [94]. It also plays significantly in controlling fluid storage in aquifers, oil and gas fields and geothermal systems, and the ability to estimate the

connectivity of the pore structure through geological formations [95]. Therefore, to better understand a particular physical characteristic of porous solid, it is necessary to fully identify its void properties involving internal geometry, size, connectivity, arrangements, pore origin, and the saturation of voids with liquids [96]-[99]. These various properties of porous solids are mainly discussed in section 2.14.

2.5 Sorbent Forms

Sorbents are marketed in various shapes and forms depending on their composition and their intended use. According to ITOPF (International Tanker Owners Pollution Federation) [12], there are four main forms of sorbents. Form 1 is constructed using continuous materials in which their length and width are much greater than their thickness, such as sheet, films, and pads. Form 2 is often enclosed in an outer fabric, mesh, or netting in which they have small holes to permeate oil and enhance the ease of use. This form includes a boom, sock, and pillow, but the boom is the most common method of controlling oil spills, and it is mainly focused in this study. Form 3 are bundles of loose fibers allowing the oils to be recovered through a combination of adhesion to a large surface area and cohesion within the oil itself, such as pom-poms and snares. Form 4 is loose particulate materials that tend to recover small spills of oil on land. Figure 2.5 shows the different sorbents use in addressing the oil spill, and Table 2.1 gives an overview of the commercial products of booms used for cleaning up oil and other petroleum-based spills.

Figure 2.5 Four forms of sorbents; a) Form 1, b) Form 2, c) Form 3, d) Form 4 [12].

Table 2.1 Commercial products of oil booms with different filler materials.

Item Reference	Filler Material	Size (D × L)	Sorption Capacity (L)	Supplier
SPC810-E	Polypropylene-Nylon	20 cm × 0.03 cm	316	BRADY
SPC816-E	Polypropylene-Nylon	20 cm × 0.05 cm	263	BRADY
35ZR66	Polypropylene	20 cm × 0.03 cm	Up to 246	CONDOR
BOM414	Polyester-Polypropylene	12 cm × 0.06 cm	Up to 181.6	New Pig
37WSB5	Polypropylene	12 cm × 0.03 cm	Up to 167	The Cary Company
EPCENPOB810	Polyethylene-Polypropylene	12 cm × 0.03 cm	Up to 151	ENPAC
Chemtex B5 Absorbent Booms	Polypropylene	12 cm × 0.03 cm	132.5	Global Industrial
BOM1201	Cotton-Polyester Blend	12 cm × 0.07 cm	Up to 127	New Pig
SPC510	Polypropylene-Nylon	13 cm × 0.03 cm	123	BRADY
SKM500	Hydrophobic Cellulose	8 cm × 0.01 cm	UP to 114	New Pig
BOM1200	Cotton-Polyester Blend	12 cm × 0.03 cm	Up to 103	New Pig
SPC516	Polypropylene-Nylon	13 cm × 0.05 cm	101	BRADY
BOM600	Hydrophobic Cellulose and Copolymer Proprietary Blend	12 cm × 0.03 cm	Up to 91	New Pig
P-208	Polyester-Polypropylene	8 cm × 0.02 cm	Up to 59	3M
SORSF10BOOM	Natural Fiber-Cellulose	10 cm × 0.03 cm	Up to 23	Spill Fix
ULT5234	Polyethylene	10 cm × 0.0015 cm	Up to 23	ULTRATECH

2.6 Oil/Water Separation Using Meshes

There has been an across-the-board increase of using meshes with superwettability that has been entailing researchers to find a way to separate oils from water. The oil/water separation using meshes are suitable candidates leading them to have widespread use of practical applications because of their simplicity and low-cost.

Several methods of surface functionalization have been designed to achieve the function of the oil/water separation mesh. These oil/water separation meshes have been functionalized using various methods and materials involving inorganics, organics, self-assembling monolayers (SAMs), and bio-inspired materials.

2.6.1 Inorganic Materials

One of the broadest types of inorganic surface functionalized used is the growth of nanostructured copper oxides like CuO or Cu(OH)2 onto mesh surfaces [3]. Hence, there are many papers have reported on the growth of nanostructured copper oxides onto the mesh surface. For example, according to Liu et al. have described briefly a nanostruc-tured CuO-covered Cu surface formed through etching with potassium peroxydisulfate [3], [100]. Therefore, they found out that this surface exhibit a water-selective mesh, and it has more than 99.999% separation efficiency and can be used up to 60 times.

2.6.2 Organic Materials

Polymers have been applied widely to functionalize metal meshes to fulfill the wetting properties needed for the oil/water separation. Many papers have been used organic materials as a porous substrate for the creation of oil/water separation devices. One of these papers has reported the creation of the porous substrate from a polymer film, which is a polyethylene film authored by Zhao et al. [101]. This polyethylene film was firstly treated with sandpaper to increase roughness and then make holes were made by using needles to create voids. This resulting method yielded suitable oil/water separation meshes.

2.6.3 Self-Assembling Monolayers (SAMs)

Self-assembling monolayers (SAMs) have been used generally to functionalize metal meshes to fulfill the wetting properties needed for the oil/water separation. These chemical material are usually exhibited a hydrophobic oil-selective mesh [3]. For in-stance, stainless steel meshes were modified by using stearic acid [3], [102], [103], and Cu meshes by using thiols, such as dodecanethiol [3], [104]-[106].

2.6.4 Bio-Inspired Materials

Many papers have been derived much of inspiration from nature, and have reproduced some materials and structures naturally. One example of this was taken from marine life according to Cao et al. demonstrating the functionalization of stainless steel meshes from dopamine. They found out that dopamine can properly adhere to the metal mesh, and their surface functionalization exhibited a hydrophobic surface leading to remove oil from oil/water mixtures [107].

2.7 The Theory of Mesh for Oil/Water Separation

Commonly, woven metal wire meshes have been used as substrates with different chemicals to create a simple oil/water separation device. To create a mesh capable to separate oil/water mixtures, the contact angle (CAs, θ) need to be smaller than 90º [3]. This small (θ) resists the flow of one liquid whereas permitting the passage of the other [3]. Hence, this small contact angle (θ) resists the flow of one liquid whereas permitting the passage of the other [3]. Hence, this resistance is measured as a pressure called the intrusion/capillary pressure, see Figure 2.6

When a capillary tube is immersed in a large open vessel containing fluid, such as liquid, the combination of liquid's surface tension and wettability (contact angle) will cause the liquid to rise to a certain height. The liquid continues rising inside the tube until the force acting upward become balanced by the weight of the liquid. Thus, the upward force (F_{Up}) can be determined by the force per unit length (interfacial tension) times the circumference, which can be calculated from this below equation.

$$F_{Up}(\text{Surface tension and contact angle}) = P_{nw}\, A = 2\pi r\, \gamma_{lv} \cos(\theta) \quad (2.1)$$

Where P_{nw} is the non-wetting pressure, A is the capillary tube area, γ_{lv} is the interfacial tension of liquid and vapor, r is the capillary tube radius, and θ is the contact angle.

The upward force is counteracted by the weight of the water, which is a downward force equal to the density and volume of the water, as shown in equation 2.2.

$$F_{Down}(\text{Weight of water}) = P_w\, A = m_g\, g = V_w\, \rho_w\, g = \pi r^2 h\, \rho_w\, g \quad (2.2)$$

Where P_w is the wetting pressure, m_g is mass of water, g is acceleration gravity, V_w is the volume of water, ρ_w is the density of water.

After balancing between the upward force and the downward force, the equation becomes:

$$h = \frac{2\gamma_{lv}\cos(\theta)}{r\, \rho_w g} \quad (2.3)$$

Where, h is the steady-state height is given by the meniscus, which is the curvature in the upper surface of a liquid close to the surface of the wall tube, therefore; the capillary pull is balanced by the hydrostatic force of the liquid column.

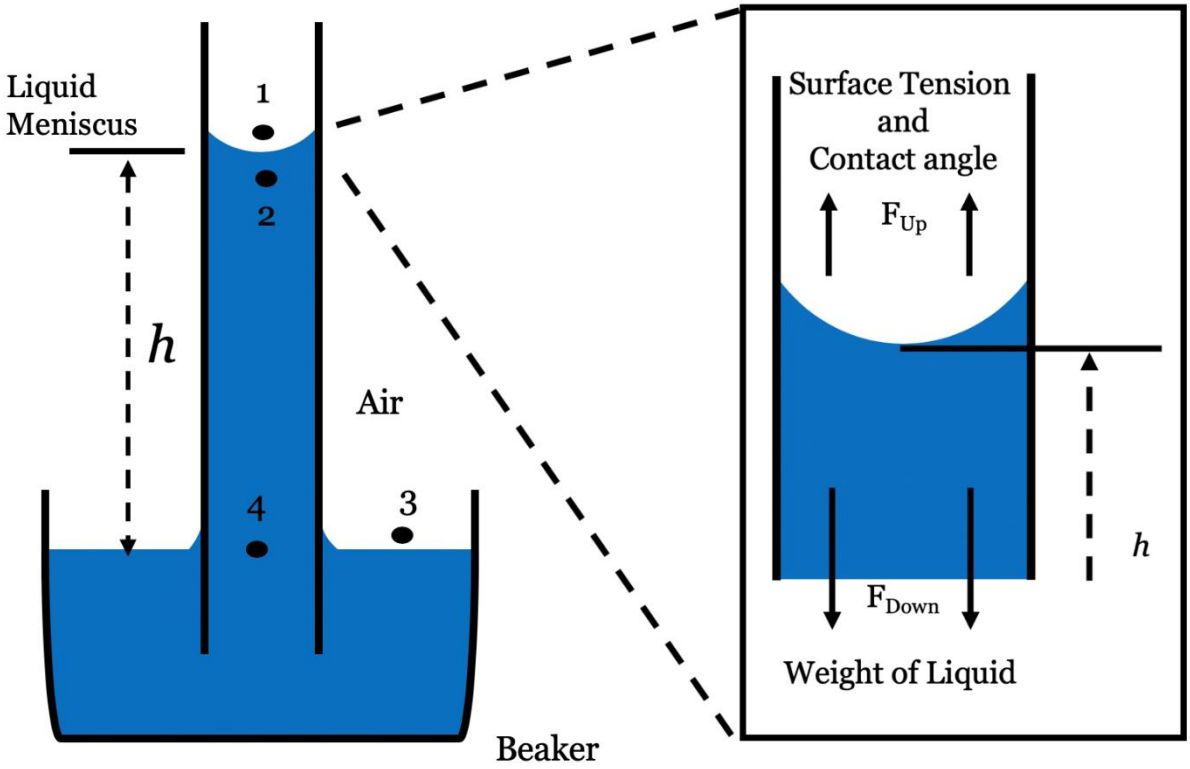

Figure 2.6 Capillary tube immersed in a wetting fluid reservoir

2.7.1 Capillary Pressure

Capillary pressure spontaneously occurs in a pores medium due to the presence of two immiscible fluids in the pores space. The capillary pressure is as a result of the interfacial tension existing at the interface separating two immiscible fluids. The interfacial tension itself is caused by the imbalance in the molecular forces of attraction experienced by the molecules. The intermolecular forces within the fluids cause a tendency in liquids to resist separation, which is referred to cohesive forces. Hence, when two fluids have weak electrostatic forces, they can combine forming a single fluid, which is referred to as miscible fluid. Whereas immiscible fluids have strong electrostatic forces between molecules inside the fluids leading them to resist the combination between the fluids. When a fluid tends to spread across the surface of solid material is referred to as adhesive forces.

As two immiscible fluids are in contact in a capillary tube, a discontinuity in pressure exists between the two fluids, which ultimately depend on the curvature of the interface separating the fluids. This difference existing across the interface is referred to as the capillary

pressure. In porous media, the capillary pressure is the difference between the pressure in the non-wetting phase and the pressure in the wetting phase. It can be written as referring to the above diagram:

$$P_C = P_1 - P_2 \tag{2.4}$$

The pressure at point 2 within the capillary tube is equal to the pressure at point 4 minus the hydrostatic pressure of the liquid:

$$P_2 = P_4 - \rho_l gh \tag{2.5}$$

and the same pressure as that at point 1 becomes:

$$P_1 = P_3 - \rho_v gh \tag{2.6}$$

After subtracting the above two equations and knowing that P_3 and P_4 have the same results, the equation becomes:

$$P_C = \rho_l gh - \rho_v gh = (\rho_l - \rho_v)gh \tag{2.7}$$

Therefore, assuming the density of air is negligible and using the expression for h in the above equation 2.3 leads to having this below equation:

$$P_C = \frac{2\gamma_{lv}\cos(\theta)}{r_C} \tag{2.8}$$

Where, γ_{lv} is the interfacial tension of liquid and vapor (N/m), θ is the contact angle of one phase submerged in the other, and r_C is the capillary radius (pore size) (m).

From the above equation, the inverse relationship between pore diameter and pressure is called the Washburn equation due to E. L. Washburn who described the capillary flow in a porous material in a bundle of capillaries tubes [108]. The tubes in this study are considered to have uniform diameter and length leading to consider the fluid flow in a single capillary tube.

Moreover, it can observe that a high resistance of oil penetrating through a potential mesh can move from a hydrophilic mesh with a high contact angle (θ) of oil in water, and with small mesh size, and vice versa. There is a considerable proportion of reported meshes formed from the hydrophilic type to permit passage of water, which are referred to as water-selective meshes. While there are a smaller proportion of reported meshes can be from oleophilic type to permit the passage of oils, which are referred to as oil-selective meshes. It can be able to create an oil/water separation mesh, which can make a switch between water-selective and oil-selective together [109].

Furthermore, there are advantages and disadvantages to meshes. The meshes effectively separate a larger volume of oil-contaminated water in a given time (flux) because they have a limited pore diameter, which can be in the order of 50 μm [3]. The meshes can only separate droplets, which these droplets have large size than mesh's size. Moreover, there are other advantages of using meshes, such as its simplicity and low cost, in addition; it has low pressure leading a liquid drive through it. However, there are disadvantages of using meshes. One of them is need to control the pressure in meshes to enable the passage of the liquid phase.

2.7 Permeability

Permeability is a property of the porous material to transmit fluids. The permeability is also defined as the measurement of how easily a fluid flows through porous media. In 1856, Henry Darcy (commonly known as Darcy) developed a fluid flow equation that has since fitted as the standard mathematical tools for porous media flow. Darcy's law is given as follows:

$$Q = \frac{K\,A}{\mu}\frac{\Delta P}{L} \tag{2.9}$$

Where, K is the permeability coefficient (Darcy), μ is the viscosity of flowing fluid (cP), A is the area of cross-section where fluid flows (cm^2), $\frac{\Delta P}{L}$ is the pressure drop per unit length in the flow direction (atm/cm), Q is the volumetric flow rate (cm^3/s). A porous material has permeability equal to 1 (Darcy) when a pressure difference of 1 (atm) will create a flow rate of 1 (cm^3 /s) of a fluid with 1 (cP) viscosity within a cube having side 1 (cm) in length.

$$1 \text{ darcy} = \frac{1 \left(\frac{\text{cm}^3}{\text{s}}\right) 1 \text{ (cP)}}{1 \text{ (cm}^2\text{)} \ 1 \left(\frac{\text{atm}}{\text{cm}}\right)} = 0.987 \ \mu\text{m}^2$$

One Darcy is a comparatively high permeability as the permeability of most porous materials are less than one.

2.8 Porosity

Porosity is one of the main macroscopic parameters to analyze a pore structure. It is defined as the ratio of the pore (void) volume to the total bulk volume of the media, and is expressed as a fraction or percent. There are many of the void spaces in a porous material that are interconnected, while some of the pore spaces are completely isolated. This leads to two well-defined types of porosity: effective porosity and absolute porosity. The effective porosity is defined as the percentage volume of interconnected voids/pores to the bulk volume of solid media. Whereas the absolute porosity is referred to the proportion volume of isolated voids/pores to the bulk volume of solid material.

Many experimental methods have been used to calculate the porosity. The efficient method in this study is the density method. This method mainly depends on knowing the sample's bulk density (ρ_{bulk}) and the material density in the material (ρ_{material}). Following that the bulk density can be calculated because the mass and the volume of the porous sample are known. Since the material density is known, the porosity can be calculated by using this equation:

$$\phi = 1 - \left(\frac{\rho_{\text{bulk}}}{\rho_{\text{material}}}\right) \tag{2.10}$$

2.9 Fluid Properties

Fluid properties are the physical characteristics of fluids that can change their flow. In this study, the crucially important fluid properties are density, viscosity and interfacial tension.

2.9.1 Oil Density

Density, ρ, is defined as mass per unit volume, and it has the SI-unit of kg/m^3. The order of increasing oil sorption capacity is associated with packing density [16]. Thus, the higher amount of effective space can increase the oil sorption capacity that is achievable at high packing density. Therefore, it is important to study the effect of packing density on the saturation time with different oil densities. Methods are described in detail for determining the oil, and it is mainly described in section 4.2.1.

2.9.2 Oil Viscosity

Viscosity is the main factor in influencing sorption rate of the fiber materials. The sorption capacity of the sorbents can be influenced by the oil density and viscosity [16]. With low viscosity of the oil, the sorption rate of fibers become increase compared to the higher viscosity of oil leading slightly to reduce the sorption rate of fiber materials. The significant reduction of oil flow is mainly due to the high oil viscosity resulting in longer saturation time. The rate of oil penetration into a capillary movement is inversely proportional to the oil viscosity [16]. Therefore, different viscosity is regarded as significant in studying the effect of the spilled oil, and it would entail sorbents with different porous medium properties. The viscosity measurements are performed with a rotating viscometer that is described in section 4.2.2.

2.9.3 Surface and Interfacial Tension

The property of the interface of two immiscible fluids referred to as surface and interfacial tension. When there are two liquids, such as oil and water, it is referred to as an interfacial tension. Whereas both phases are different, for example, gas and liquid, it is referred to as surface tension.

The interfacial tension causes the tendency of a liquid to exhibit a minimum free surface when it is in contact with an immiscible fluid. In other words, the molecules tend to attract among each other by the electrostatic forces in all directions in the liquid as shown in Figure 2.7 (a). But, in terms of the interface between two liquids, the molecules of one liquid cause the tendency to attract simply in its own direction leading to reduce the liquid surface as shown in Figure 2.7 (b).

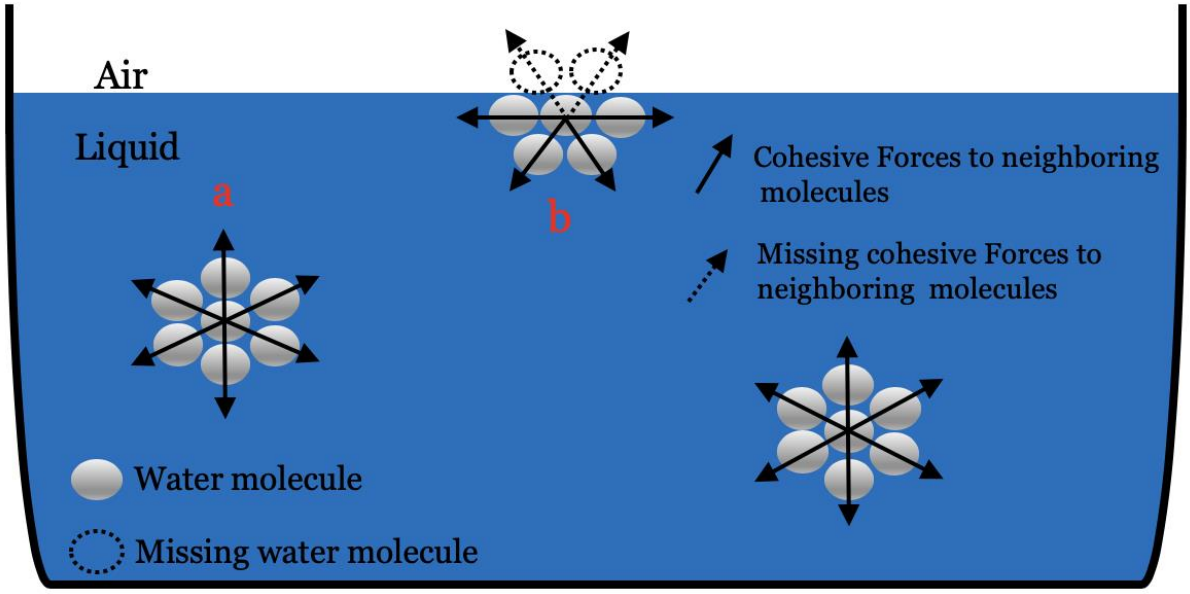

Figure 2.7 a) Interaction between molecules in the fluid; b) Interaction between molecules at the interface [110].

The Young-Laplace has described the discontinuity in pressure across the interface between two immiscible fluids. The discontinuity in pressure over an interface is referred to as capillary pressure, which is described in section 2.10.

2.10 Wettability

The recent progress of oil/water separation based on sorbent materials, such as porous materials possessing surface superwetting properties. The surface wettability is defined as an innate property of a solid material and determines the final wetting/dewetting properties when a liquid comes into contact with the material [3]. There is a direct impact against the wetting/dewetting behaviors of probe liquids on solid surfaces resulting from the surface chemistry and geometric morphology of solid surfaces [63], [97]. The superwettability has two types of material, that is, superhydrophobicity (low water affinity)/superoleophilicity (high oil affinity) showing oil-removing properties. The oil/water separation through the use of a superhydrophobic/superoleophilic stainless steel mesh, was easy to allow oil to penetrate the mesh, was first exhibited by Jaings's group in 2004 [111].

One of the most common properties for removing oil from water is hydrophobicity [112]. To possessing a high efficiency for oil-polluted water, it requires highly hydrophobic sorbents compared to low-hydrophobic sorbents [34], [53], [113]. Due to the low cost of the sorbents, it needs large amounts for cleaning up the oil spill. For this purpose, finding eco-environment friendly, cost-effective, and recyclable materials, with superhydrophobic properties, high efficiency, and high flux rates, allowing them to purify large volumes of oil/water components (containing emulsions) are needed [3].

Wettability is a surface phenomenon in which two immiscible fluids come into contact with a solid surface. The wettability illustrates the interactions between fluid and fiber materials, which describes the ability of the fluid to adhere to the surface of the fiber materials. The wetting degree of solids by liquids is usually measured by the contact angle that a liquid-liquid interface makes with a solid.

When a fluid drop on a plane solid surface, it will lead to taking various shapes. The particular shape, either flat or shaped like a pearl, is basically based on the wettability of the considered solid. Figure 2.8 describes the properties of wettability.

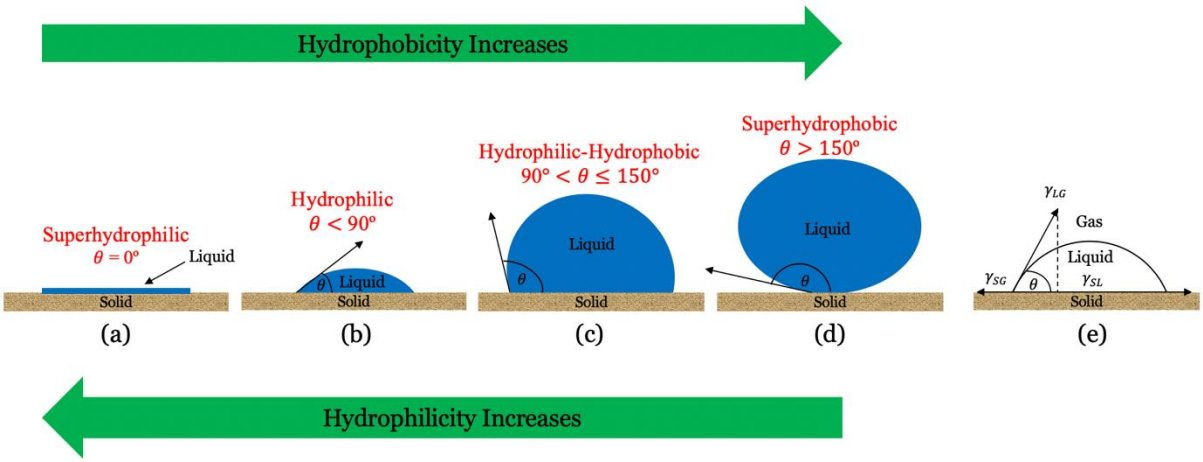

Figure 2.8 The difference between wetting and non-wetting fluid

The qualitative measurement that can measure the wettability of fiber materials is the contact angle. In terms of a superhydrophilicity, the contact angle with water tends to be near 0° (Figure 2.8 (a)), but when the contact angle tends to be smaller than 90° (Figure 2.8 (b)) or between 90° and 150° (Figure 2.8 (c)), it will refer to as hydrophilicity or hydrophilicity-hydrophobicity respectively. As the contact angle leads to be larger than 150° (Figure 2.8 (d)),

it is said to be superhydrophobic. Thomas Young has been described the contact angle as a consequence of the static equilibrium between a drop of liquid and a flat of a solid surface. When a liquid drop on a solid surface, a particular shape will occur due to the interfacial tensions. The relation between the contact angle, θ, and the interfacial tension can be derived from Figure 2.8 (e), and the relation is as follows:

$$\cos\theta = \frac{\gamma_{SG} - \gamma_{SL}}{\gamma_{LV}} \tag{2.11}$$

$$\gamma_{SL} + \gamma_{LV}\cos\theta = \gamma_{SG} \tag{2.12}$$

Where,

γ_{SG} is the interfacial tension between liquid and gas,

γ_{SL} and γ_{LV} are the interfacial tension between solid and liquid and solid and gas.

2.11 Spontaneous Imbibition

Imbibition has been playing an important role in numerous activities. The use of cloth or paper towels to dry dishes or clean up spilled liquid, and the transfer of ink or paint into paper are common examples of the imbibition process. The spontaneous invasion of wetting phase into a porous medium becomes an extremely widespread interest due to its presence in a wide range of practical applications, such as petroleum engineering, filtration, and contaminant cleanup.

The mechanism by which a wetting fluid is driven into a porous medium by capillary action is referred to as spontaneous imbibition. But, if the nonwetting fluid displaces the wetting is said to be of drainage mechanism. The imbibition mechanism is driven by surface energy through the action of capillary pressure [114]. Capillary pressure is proportional to the product of interfacial tension and the curvature of the interface. During the imbibition, the magnitude of the curvature relies on surface forces (cohesive and adhesive forces) in combination with pore geometry. In other words, when the curvature becomes concave and the pore size allows the interface to advance, the resulting displacement is spontaneous. Due to the dynamic forces that result from the spontaneous motion of the interface, the contact angle at the three phases line of contact and interface shape can be affected.

In spontaneous imbibition, the invader (oil) will displace the defender (air). The physical properties of fluids, the viscosities of the invader and defender, their densities, and the interfacial tensions are the common factors of controlling the spontaneous displacement mechanism. It can also depend on the saturation of the defender and its distribution inside the porous medium. Imbibition phenomena in tubes have a uniform cross-section area in this study, therefore; Washburn's equation is an appropriate instrument for the study of the obtained results, which is mainly discussed in section 2.12. This equation assumes that the porous media is a bundle of parallel capillary tubes that have uniform diameters.

2.12 Single Phase Flow Models

There are traditional models that have been applied on porous media. These models have been used to analyze the imbibition in the porous material. They include capillary, porous continuum, discrete, and statistical models. This study will be mainly discussing the first two models in great detail. First, it will discuss the capillary model known as the Lucas-Washburn model, which describes the capillary flow in a porous material as a bundle of capillaries tubes. Second, it will discuss the porous continuum model called Darcy-based model, which describes liquid transport through the porous material.

2.12.1 Lucas-Washburn Model

The advancement of mathematical models for fluid imbibition in porous media has become a relevant area of research [115]. For almost a century, spontaneous imbibition in homogenous porous media has been a topic of great significance for scientists and engineers due to its inherent complexity and practical importance in many technological applications [116]. Previous research on the imbibition process was taken a close interest in studying the relation between the imbibition rate and time, as well as the relation between the imbibition rate and porous medium characteristics.

Lucas [117] and Washburn [108] studied the relation between the imbibition rate and time thus creating a linear relationship between the imbibition rate and square root of time. In general, the Lucas-Washburn equation neglected the inertial and gravitational energies in many imbibition applications. Szekely et al. [118] neglected the inertial and gravity forces and

modified a differential equation for the imbibition rate, but they obtained a nonlinear ordinary differential equation. Soriano et al. [119] ignored the gravity force and used a model porous medium with experiments on spontaneous imbibition of a viscous fluid, and they found out that the Lucas-Washburn's law was a satisfactory fit with the average position of the interface.

Several papers investigated the relationship between the imbibition rate and porous medium characteristics. Xue et al. [120] investigated aqueous electrolyte imbibition in nanoporous gold and reported that the fluid flow can reversibly switch on and off during electric potential control of the solid-liquid interfacial tension. Also, they found out that Lucas-Washburn's law often worked with the special imbibition processes. Miranda et al. [121] studied the effects of the spontaneous imbibition interface as a function of time and paper orientation between ink and paper. They observed that the dynamic of the rough interface was dependent on paper orientation and showed the ink-paper interface did not moved due to the Lucas-Washburn Model. In terms of fiber orientation, Chawstiakm [122], Fowkes [123], William et al. [124], and Hodgson and Berg [125] were studied the imbibition rate along the fibers. You-Lo-Hsieh [126] were recently studied liquid wetting and its relation with fiber morphology and chemistry. Schuchardt and Berg [127] experimentally investigated the swelling phenomenon and built assumption on the modified Washburn equation that the pore radius of the porous medium can be linearly decreased with time. They found out a good comparison between the experimental data and the theoretical model.

Other studies on imbibition experiments are evaluated the absorption efficiency and liquid transport in porous media. Russel and Mao [128] used a method and equipment to study the in-plane anisotropic liquid absorption in nonwoven fabrics. Miller [129] experimentally studied the effect of gravity force on upward imbibition. Jeong [130] was used Stokes approximation to study the slip boundary condition on a porous wall. Furthermore, Lockington and Parlange [131] theoretically estimated water absorption in porous materials related to sorptivity. Gane et al. [132] were studied the theoretical and experimental data of the absorption rate and volume dependency through the complexity of porous networks.

Several studies attempted to perform horizontal spontaneous imbibition tests [133]. Until now, few experiments have been reported in horizontal directions for avoiding the effect of gravity on spontaneous imbibition mechanism [133], [134]. The experimental method based on the capillary rise has been used for porous media characterization. Amongst them,

estimation of height penetration and mass gain of wetting liquids in time are widely used. Therefore, Washburn's equation is an appropriate instrument for the study of the results obtained from the imbibition experiment. This model assumes that the porous media is a bundle of vertical capillary tubes that have uniform diameters, as shown in Figure 2.6. The Lucas-Washburn model further assumes a complete saturation with the wetted front [134].

However, Lucas-Washburn model depends on the momentum balance beside the moving meniscus, and the balance of the capillary force with the viscous force allows to analytical results. The complete balance design of forces besides moving the meniscus includes the capillary suction force is balanced with the inertial, viscous, and gravity forces. The inertial forces can be neglected in the model, while both gravity and viscous forces are needed to result in a non-linear ordinary differential equation. Previous studies have explored adaptions of the Washburn's equation to capillary-driven flow in sorbents. This study reviews the fundamentals of the Lucas-Washburn model and its modification for porous media to develop an understanding of implications associated with applying the model to flow in the sorbents.

2.12.1.1 Assumptions

The main shortcomings of the assumptions are applied in the derivation of the Lucas-Washburn model. It is reviewed in this study as follows:

i. Flow is only for a one-dimensional phase and cannot be performed to model for two or three-dimensional phases.
ii. The flow in capillaries is continuous, fully developed, steady, and laminar during the length of the capillary.
iii. The capillaries are cylindrical and of a uniform radius.
iv. The liquid flow in the capillary is incompressible with a constant of viscosity and contact angle.
v. There is no a tortuosity factor.

2.12.1.2 Mathematical Theory

Figure 2.6 depicts the schematic cylindrical syringe. The fluid flow is filled pore space of the sorbent and is modeled to occupy prominent place into a single capillary tube. The

average flow velocity of the fluid meniscus is represented as a control volume analysis. It is more convenient to apply here the mass conservation principle to a defined volume in pore space. It can be written as:

$$\frac{dM}{dt}\Big)_{System} = 0 = \frac{\partial}{\partial t}\int_{CV} \rho \, dV + \int_{CS} \rho \, \vec{v} \, . \, \overrightarrow{dA} \tag{2.13}$$

Since M is the mass, υ is the velocity, V is the volume, ρ is the density, and A is the cross-sectional area. As the liquid flows in the capillaries, the height in the control volume increased, and the outlet velocity is zero, as can be seen in the below equation:

$$\frac{d}{dt}\int_0^h \rho\pi r^2 \, dz - \rho\upsilon_z \, (\pi r^2) = 0 \tag{2.14}$$

where υ_z is the velocity in the z-direction, which is referred to as the rate of the meniscus height and is denoted as $\dot{h}$.

Using the momentum balance on the CV for the integral form of the z-direction that becomes as:

$$\sum F_z = F_H + F_V + F_G = \frac{d}{dt}\int_{CV} \rho\upsilon_z \, dV + \int_{CS} \rho\upsilon_z \, \vec{\upsilon} \, . \, \overrightarrow{dA} \tag{2.15}$$

Understanding the equilibrium height of a liquid in a single capillary cannot represent the speed at which the liquid flows into the capillary. As the driving force, the vertical force, F_z is balanced with the forces as hydrostatic pressure (F_H), viscous force (F_V), and gravity force (F_G), the equation is substituted with all forces and combined them with the right hand in equation 2.15 to become as:

$$P_C = \frac{8\mu h\dot{h}}{r^2} + \rho gh + \rho\frac{d(h\dot{h})}{dt} \tag{2.16}$$

According to the assumptions of the Lucas-Washburn model, the inertial force is negligible, which the below equation becomes as:

$$P_C \ln\left|\frac{P_C}{P_C - \rho gh}\right| - \rho gh = \frac{\rho^2 g^2 r^2}{8\mu} \, . \, t \tag{2.17}$$

As can be seen from the equation 2.17, the height can be used in this study as a function of time to fit the experimental data. Therefore, the mass is experimentally measured from the imbibition equipment, while the height (t) can be calculated from the below equation:

$$h(t) = \frac{\text{Oil Mass Absorbed}(t)}{A_{CS}\, \phi\, \rho_{oil}} \tag{2.18}$$

Since h is the height of the sorbents, ϕ is the porosity of the sorbents, and A_{CS} is the cross-section area of the sample. The fittings of the Lucas-Washburn model with the experimental data are mainly discussed in section 7.1.1.

2.12.2 Darcy-based Model

The process of fluid flow through porous media becomes of great interest to a broad range of engineers and scientists, as well as politicians and economics due to its practical importance in the groundwater flows and a variety of tertiary oil recovery processes [135]. The one-dimensional empiricism determined by Darcy in 1856, and it served as a starting point for various practical applications [136]. During a very long period of time, this law has been experimentally used in its global form. However, it was not considered in either a local differential form or a theoretical basis. J. Boussinesq [137] found a differential expression in the analysis of the fluid flow in aquifers resulting in an analogy with heat transfer in a continuum. There was an extension work for the relationship to non-homogeneous media between the flow rate and heat gradient. It was formally derived a one-dimensional flow with this law resulted from the Stokes equation for a flow parallel to a regular array of infinite parallel cylinders was according to Emersleben [138] in 1925. Muskat and Botset in 1931 [139] derived a dimensional analysis for a compressible flow that the pressure difference was known to replace with the differential square pressures.

Over the past century, substantial research in the literature proposed modifications to investigate, and improve Darcy's law for its application to more complicated transport processes. This law has become a constant challenge for theoreticians. Masoodi and Pillai [140] were theoretically studied the wicking fluid into a composite paper formed from cellulose and superabsorbent fibers. They proposed an adaptation of a new theoretical

approach with Darcy's law coupled with a modified continuity equation to investigate the effects of fluid absorption by the fibers, to describe the fiber swelling, and to estimate the porous structure by applying several permeability models. They found out that a good comparison between theoretical and experimental data and obtained the best performance of the proposed wicking model by assuming the volume of liquid absorbed into the fibers equal to the volumetric expansion, as well as a well performance of the permeability models by coupling them with the proposed wicking model. They indicated the new Darcy's law-based approach can be extended into two- and three-dimension wicking flows due to its versatility, while the Washburn model can only apply to one-dimensional flows. Mendez et al. [141] implemented Darcy's law using COMSOL to model fluid flow behavior with paper strips in μPADs that were straight channels connected to a fan-shaped section, and the fluid flows were controlled to study the effects of downstream geometry on upstream flows in the paper. They concluded that a quasi-steady flow can be performed in the fan portion of the paper without using an absorbent pad. Elizalde et al. [142] were used three-dimensional lattice-Boltzmann simulations to study the fluid flow through large random fiber webs and to compare the results with previous experimental, analytical, and numerical data for the materials. They reported that the simulated results were found to be correlated well with the experimental data thus confirming that the permeability was exponentially dependent on the porosity in a large porosity range. Therefore, the Darcy's law has been shown to be a reliable approach in its ability to study the fluid flow through different types and geometries of porous materials with proper assumptions or approximations to predict the pore size or permeability.

Understanding the fluid flows and transport processes in porous media are of utmost importance for industrial applications. Due to the random heterogeneous materials, the predictions of the effective transport properties play a significant role in the fluid flow of sorbents. Different techniques are used in modeling the fluid dynamics in porous media at various scales. Several studies of complicated pore structure and geometry of the porous media tend to depend on the assumptions of a representative volume element (RVE) [143]. The REV is the smallest volume at which large fluctuations of measured quantities, such as porosity and permeability that can be yield a value representative of the whole porous media. The fluid flow through porous media can be resolved by discrete numerical methods, which is used the momentum and continuity equations. In this study, it is considered a steady, single-phase fluid flow in the sorbents with an explicit description of

a spatially disordered macrostructure. The liquid flow is considered as incompressible with constant viscosity. Thus, the equation becomes as:

$$\nabla . v = 0 \tag{2.19}$$

$$v = -\frac{K}{\mu} . \nabla P \tag{2.20}$$

Where, v is the Darcy (volume averaged) velocity, ∇P is the pressure gradient driving the flow, μ is the fluid viscosity, and K is the permeability.

2.12.2.1 Mathematical Theory

The Darcy model is used to describe a pressure-driven flow through porous media. In this model, the main goal is to predict the change of height h of the liquid (oil or water) for a given sorbent (porous fiber media) as a function of time t, that is h = f(t). The momentum balance and continuity equation are used on the front liquid applying the volume-averaged approach, which can be shown in equations 2.19 and 2.20.

For a vertical capillary, the rising height in equation 2.20 is limited by the hydrostatic pressure:

$$P = p + \rho gh \tag{2.21}$$

For single-phase flow, the Darcy and continuity equation tends to be:

$$v = -\frac{k}{\mu}\frac{dP}{dh} \tag{2.22}$$

$$\frac{dv}{dh} = 0 \tag{2.23}$$

Combining the above equation and then integrating the equation by using the boundary conditions as $P = P\,atm$ at $h = 0$ and $P = (P_{atm} - P_s) + \rho gh$ at $h = h_f$ due to the h_f changes with time allowing the equation to be:

$$\frac{dh_f}{dt} = \frac{K}{\phi\mu}\left(\frac{P_s}{h_f} - \rho g\right) \tag{2.24}$$

Integrating equation 2.24 as the time started at t = 0 and the h_f becomes zero in which the final form equation is:

$$P_s \ln\left|\frac{P_s}{P_s - \rho g h_f}\right| - \rho g h_f = \frac{\rho^2 g^2 K}{\phi\mu} \tag{2.25}$$

Since P_s is the suction pressure deriving the liquid flows vertically upwards into the sorbents.

2.13 Approaches for Multi-Phase Flow in a Porous Medium

In addition to the flow of oil in sorbents, there are other topics related to the field of flow and transport in porous media ranging from storage of carbon dioxide in deep geological formations, the methane released by abandoned coal mines to paper manufacturing, polymer electrode membrane in the fuel cell, and fluid flow processes in the human body [150], [151], and also make use of similar theory.

There are conceptual similarities between single-phase and multi-phase flow which are modeled using equations similar to Darcy's law [144]. For multi-phase flow, the situations are conceptually more complicated [143], while the single-phase flow is the main focus on this thesis and discussed in more detail in section 2.12. The presence of a second phase may hinder the flow of the first phase when it is dependent on its distribution in the porous network. However, modeling multi-phase flow becomes a considerable technical challenge for theoreticians [145]. Using a phenomenological extension of Darcy's law is the most description for macro-scale two-phase flow in porous media. The extension of this law is to introduce the saturation-dependent parameters involving relative permeability and capillary pressure.

In each constituent phase, the capillary pressure is defined by the interfacial tension, micropore geometry, and surface chemistry of the porous medium, while the relative permeability is identified with the volume flow rate for each fluid to its pressure gradient and can be used to predict by material characteristics, morphology, and saturation, which is mainly described in section 2.14. Several approaches have been applied to describe the multi-phase

flow in the porous media. Hassanizadeh and Gray [146] studied a rational thermodynamic approach. An approach based on averaging and non-thermodynamics was proposed by Marle [147] and Kalaydjian [148]. In contrast, Gray, Miller [149] and Bowen [150] assumed free energies that were dependent on the saturation gradient resulted in additional dynamic force with Darcy's law.

However, there are four well-known problems associated with this model involving fluid pressures, relative permeability, and saturation [151]. The driving forces included in Darcy's law terms and the effects of dynamic pressure are found to be a great case of transient flow, and the rate of interphase mass or heat transfer is dependent on the amount of interfacial area [152], [153]-[157]. Despite the obvious shortcomings, the extended multi-phase Darcy description has received more attention by researchers and engineers and is numerically applied for a broad range of materials and applications.

2.14 Notion of Pore Size

A discussion on the structure of porous media should directly involve the notion of pore size and the pore concept. The pores are the openings in solid surfaces, which are the gases, liquids, or even foreign microscopic particles can occupy. In the science of porous structure, the word pore is often used without a proper definition. There is not a unique definition for pore because they are highly useful in terms of pore models. Therefore, this concept is widely used in the area of porous media.

Pores come in a variety of sizes for addressing a wide range of applications. A set of standards proposed by IUPAC [97] for the pore size has defined pore size ranges based on different size widths. Pores with an internal width of less than 2 nm are referred to as micropores, and the pores have internal width between 2 nm and 50 nm are called mesopores, and those that have larger internal width than 50 nm are referred to as macropores [94], as can be shown in Figure 2.9 .

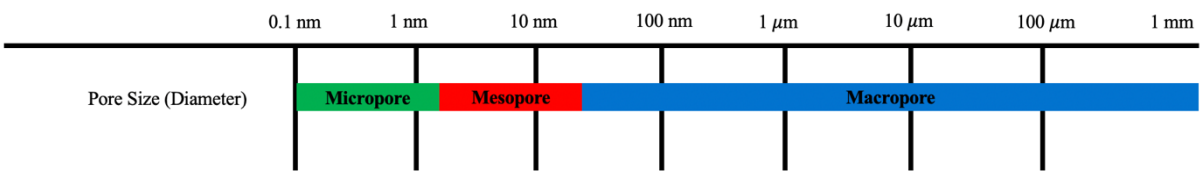

Figure 2.9 Pore sizes [94].

Pores can be defined by their accessibility to the surface of a material, as shown in Figure 2.10 The pores communicating directly with the external surface are named open pores, such as (b), (c), (d), (e) and (f). A blind pore (b and f) is accessible from the surface, but it does not travel completely from the upstream to the downstream surface due to it opens only at one end. A through pore (e) travels from the upstream surface to the downstream surface of a material. A closed pore (a) is inaccessible to its surfaces and is also product of insufficient evolution of gaseous substance. Moreover, the closed pore is not correlated with adsorption and permeability of molecules; however, it can be able to affect the mechanical properties of solid materials [158].

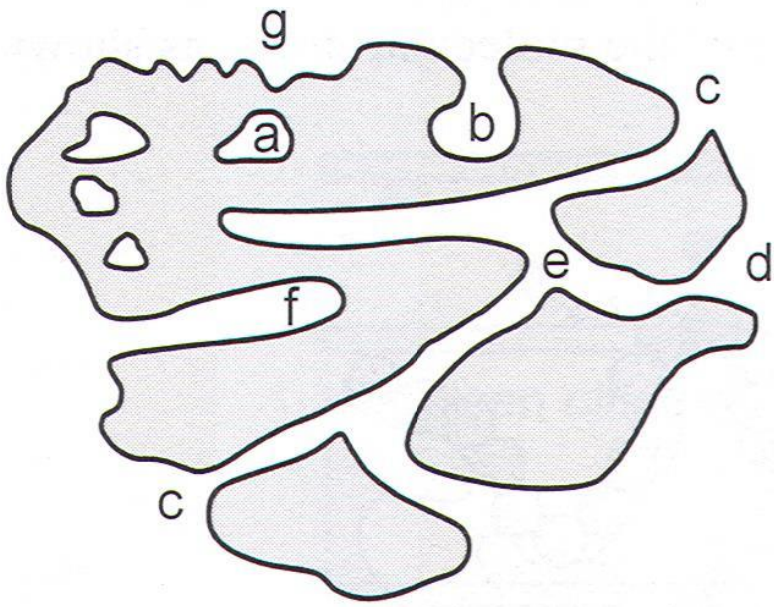

Figure 2.10 Schematic pores classification, according to their availability to surroundings (modified from IUPAC) a - closed pores, b, f - pores open only at one end, c, d, g – open pores, e - open at two ends (through) pores [97].

The pores space within the porous material become saturated with oil, gas, or water. Saturation is a fraction of pore space filled by a particular fluid, and it is expressed as follows:

$$S_n = \frac{V_n}{V_p} \qquad n = 1, \dots, m \tag{2.26}$$

Where, S_n is the saturation of a particular fluid, V_n is the volume of a particular fluid and V_p is the pore volume. The pore volume is the sum of all fluids (oil, water and gas) within the pore space as follows:

$$V_p = V_o + V_w + V_g \tag{2.27}$$

The sum of the saturation of all fluids present in the pore space is equal to one as follows:

$$S_o + S_w + S_g = 1 \tag{2.28}$$

Saturation is a factor that affects the wettability of the porous material and is important when it is related to the ability of the fluid flows through the porous material.

The study of the pore structure at both the microscopic and molecular scales is not the focus on this thesis. The sorption phenomena is described in this study by the macroscopic models due to the viscosity of the invader fluid (oil) that is higher than the defender fluid (air). Hence, this study will be mainly focused on how to use models that can explain macroscopic characteristics affected by the porous macrostructure.

Chapter 3. Materials

3.1 Materials Used in The Experiments

Six types of fibers were investigated. Kapok, cotton, hemp, polyester, nylon, and glass fibers were the materials used in this study, which they can be shown in Figure 3.1. Table 3.1 was summarized the commercial name and supplier for the six fibers.

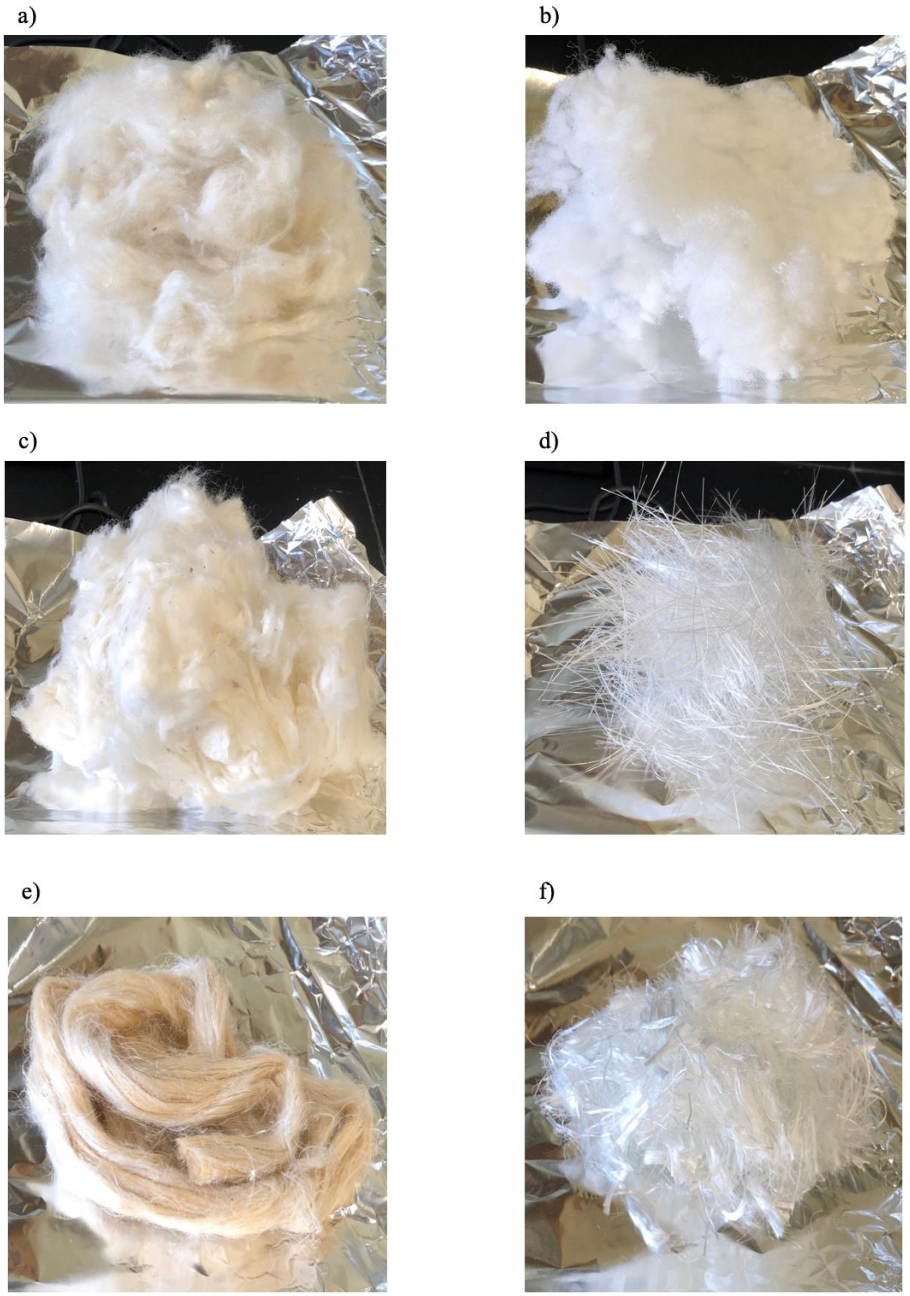

Figure 3.1 The materials used in this study; a) Kapok, b) Polyester, c) Cotton, d) Fiberglass, e) Hemp, and f) Nylon.

Table 3.1 Materials used in the experiments.

Fiber Type	Commercial Name	Supplier
Kapok	Bean Products	Chicago (USA)
Polyester	eLUXURY Company	Indiana (USA)
Cotton	Local Organic Farm	Texas (USA)
Fiberglass	Griffco Products	Michigan (USA)
Hemp	Living Dreams Company	Washington (USA)
Nylon	Local Store	Canada

3.2 Liquids Used in The Experiments

Water and 4 different hydrocarbons were used in this study. The liquids used are listed in Table 3.2 .

Table 3.2 Liquids used in the experiments.

Hydrocarbon Type	Commercial Name	Supplier
Gasoline	Local Gas Station	Canada
Diesel Fuel	Local Gas Station	Canada
Lubricant Motor Oil (Light)	Motomaster Diesel Motor Oil SAE 10W-30	Canadian Tire
Lubricant Motor Oil (Heavy)	Motomaster Diesel Motor Oil SAE 5W-40	Canadian Tire

Chapter 4. Methodology

The methodology is proposed to study the objectives of this thesis. It is important to study the motions of liquids inside the porous materials by using accurate measurements for the properties of the hydrocarbons. The most significant properties used in this study to physically characterize the hydrocarbons are viscosity and density.

4.1 Properties of the Sorbents

4.1.1 Density of the Fiber Materials

The porosity of the sorbents can be calculated by using the density method as it is discussed in detail in section 2.8. The porosity is calculated by equation 2.10. The bulk density of the fibers was calculated by knowing the volume of the sample holder and the mass of the fibers used to fill them at the maximum volume of the sample holder (graduated cylinder). The fiber materials density were taken from works of literature.

4.1.2 Surface Characteristics, Size, and Porosity of Fibers

Scanning electron microscope (JEOL 6610 SEM) was used to determine the morphology, surface porosity, and size of the fiber materials. All samples were stored in a dry and clean environment and were cut and coated with gold before using the SEM imaging.

4.2 Physical Data of Hydrocarbon Oils

4.2.1 Density

Densities of oils and water were calculated with the use of a graduated cylinder with a known volume at 100 mL. The mass of the oils were obtained by weighting the graduated cylinder before and after filling it with oils. The density, ρ, of the fluids were calculated as follows:

$$\rho_{Oil} = \frac{m_{Oil}}{V_{Oil}} \tag{4.1}$$

4.2.2 Viscosity

The apparatus used for measuring the viscosity of the oils and water was a rotating viscometer called Brookfield digital viscometer model DV-E. The measurement accuracy of the viscometer apparatus is $\pm$1%. The oils were poured into a glass beaker, and the oil viscosities were measured at room temperature. Yula-15E, LV-2 (62), and LV-4 (64) were the spindles used in the experiments. The speed of rotation was 100 rpm. Final step of the measurement was to wait for the viscosity measurement to stabilize.

4.3 Characterization of the Absorption Behavior

4.3.1 Sample Preparation

This experiment is based on the study of the absorption behavior by developing a sample holder. This sample holder was prepared using 30 mL graduated plastic syringes. It is made up of three parts: the tip, the barrel, and the plunger. The tip of the syringe is where a needle is attached, but, in this study, the tip end was cut open and joined to a steel wire mesh that possesses small perforations to allow the liquid to penetrate (the invader). The plunger rod was made small holes by drill machine to make the system is not airtight and leading the defender fluid (air) to escape during the imbibition process. The top end of the plunger is a piston-like device inside the barrel, while here it was made a small hole to fit a steel hook to attach to a load cell. The barrel is generally used for holding the liquid and visually measured the syringe's porous material contents. Particular amounts of mass of the fiber materials were weighed before placing them inside the syringe. The plunger was gently pushed to compress the fiber materials into the maximum volume of the syringe at 30 mL. The liquid can penetrate the fiber materials because of the capillary pressure, which they are assessed by the experimental setup, as can be shown schematically in Figure 4.1.

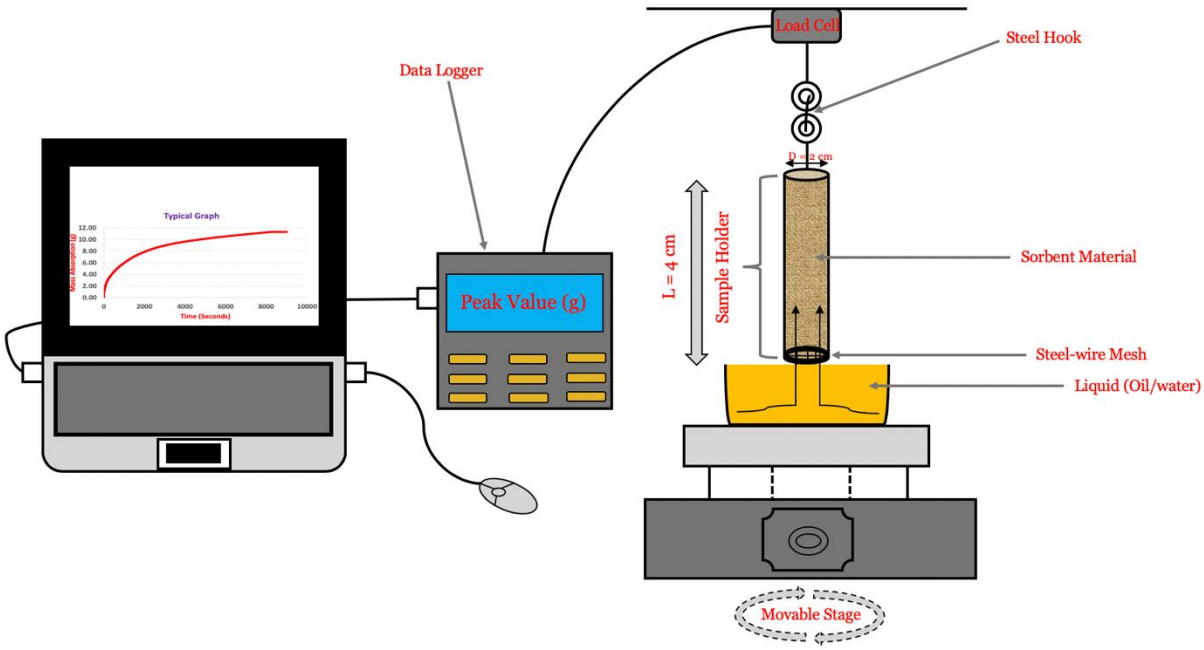

Figure 4.1 Schematic of the imbibition equipment.

4.3.2 First Trial: Testing the Uptake of Fibers by Imbibition Experiment

The sample holder containing the fiber materials were attached to a miniature load cell. This load cell is one of FUTEK's most popular models, the LSB200 S-Beam Jr with a resolution of 0.001 N. It was integrated to work with a data logger model IPM650. This FUTEK's IPM650 Panel Mount Display is a multi-purpose display compatible with strain and amplified sensors. This particular Panel Meter also has the capability of interacting with a computer through the USB link and can be used with the FUTEK SENSIT software.

There was a laboratory dish to place the hydrocarbon or water and a moving stage to locate them on it which the laboratory dish that filled with the hydrocarbon or water can be under the sample holder, as can be shown in Figure 4.2 The purpose of using the moving stage is to control the touch between the laboratory dish holding the hydrocarbon or water and the steel wire mesh below of the sample holder containing the fiber materials. As the moving stage is slowly raised to come into contact with the sample holder, the whole diameter of the steel mesh at the bottom of the sample holder should be touched so that the oil or water can come upward to all sides of the sample holder. When the sample holder becomes attach to the load cell, the load cell is set to read zero. The data logger was easily transferred the data to the computer and recorded mass data as a function of time.

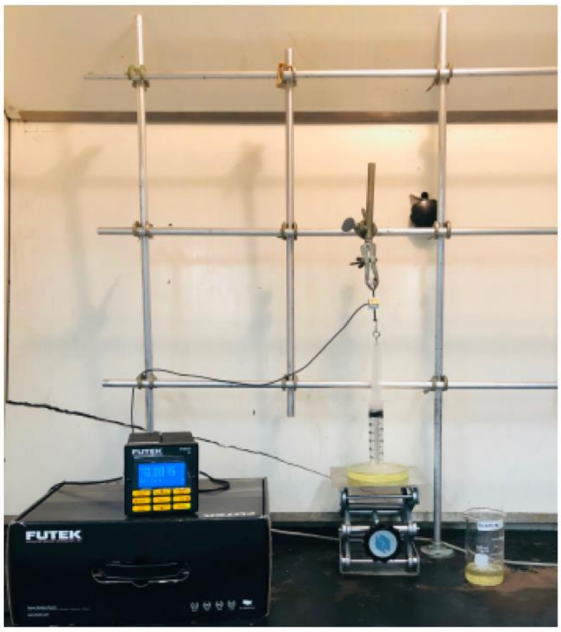

Figure 4.2 Experimental set-up of the imbibition equipment.

When the sample holder came in contact with the oil or water, the oil or water penetrated through the small perforations allow the mass of the sample holder to start increase due to the slowly imbibing oil or water. After a pre-set time interval, the FUTEK SENSIT software becomes read the mass automatically. The real-time graph served to indicate as the imbibition reaching a maximum amount of mass content for every six fiber materials that lead to completing the experiment. The time for each experiment considerably depends on the viscosities of the liquids that ranges from a few seconds to 8 hours.

There were some observations occurred on using the experiment. The moving stage is slowly reduced downwards from the sample holders after the imbibition reaching a maximum amount of mass content and this is due to surface tensions holding the oil. Each one of the fiber materials was measured three times with four different hydrocarbons, and the data from the four measurements were used to calculate an average mass.

4.4 Second Trial: Testing Reusability of Fibers with Oils

The reusability of the fiber materials was evaluated. After the fiber were used once, they were cleaned well from the oils and used a second time. In the clean-up method, the fibers were placed in a glass beaker and added a few drops of diluted commercial dishwashing liquid

as well as poured hot water into the samples. The samples were then left to soak in the detergent overnight, and the next day, they were removed from the solution and squeezed by hand with a constant force to remove the water-oil contained within. The samples were placed into a VWR 1400E vacuum oven to dry the samples and weighed again in the imbibition equipment to determine the effectiveness of the fiber materials. The cleaning processes was repeated three times for each fiber. Figure 4.3 shows the process of testing reusability of fibers.

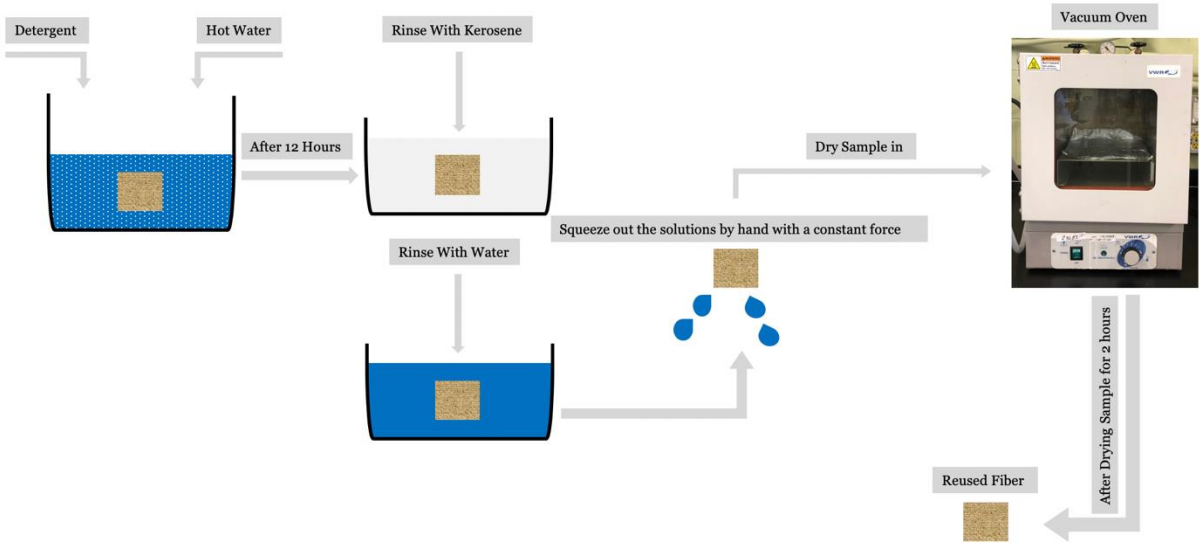

Figure 4.3 Schematic of testing reusability of fibers.

4.5 Calculations of Experimental Oil Absorption

The absorption capacity of the sorbents or mass absorbency is referred to as a mass of liquid absorbed per the mass of fiber used (sorbent). When the oil/water comes into contact with the fiber, the mass of the wetted fiber is only used to calculate the absorption capacity. Hence in this study, the absorption capacity is considered to as the amount of oil in grams of oil sorbed per a gram of the wetted fiber. There was an adequate quantity of dry fiber in all experiments to assure excess of fiber after equilibring was reached. The excess fiber was not included as fiber wet by oil. Therefore, the experimental oil absorption capacity $\eta_{exp.}$ of each sample was calculated as follows:

$$\text{Mass absorption capacity } \eta_{exp.} = \frac{\text{grams of liquid absorbed}}{\text{grams of wetted fiber}} \tag{4.2}$$

The oil absorbed is the amount of oil absorbed obtaining from the imbibition equipment and the wetted fiber is the amount of fiber entirely saturated with oil.

Moreover, this definition can be applied to different bulk densities for each different fibers with the same oils that they are compared. In this thesis, only one bulk density for each different fibers with different oils was evaluate.

It is important to study the volume of oil that has absorbed instead of the mass. Therefore, volumetric absorbency can be calculated as the rate of the volume of oil absorbed to the volume of the wetted fiber as follows:

$$\text{Volumetric Absorption } \% = \frac{\text{Volume ofliquid absorbed}}{\text{Volume of wetted fiber}} = \frac{{m_o}/{\rho_o}}{{m_f}/{\rho_f}} \tag{4.3}$$

Volumetric efficiency or wetting phase saturation of the sorbents are considered here to study the amount of saturation of the sorbents, which can be calculated by changing the absorbed mass into absorbed volume per the total pore volume of each sample. The equation is as follows:

$$\text{Wetting Phase Saturation (WPS) } \% = \frac{\text{mass of liquid absorbed}}{\rho_{liquid}\ \phi\ V_{bulk}} \tag{4.4}$$

Furthermore, it is important to study the rate of height for the sorbents. Therefore, the mass data was converted to height by considering a cylindrical geometry of the sorbent sample. The equation becomes as follows:

$$\text{Height (h)} = \frac{\text{mass of liquid}}{A_{CS}\ \phi\ \rho_{liquid}} \tag{4.5}$$

Chapter 5. Results

This chapter presents the experimental results. These experiments are based on the study of wettability and oil uptake by spontaneous imbibition of the six fibers with four hydrocarbon oil. The effect of different parameters on oil sorption capacity and sorbents characterizations are discussed in this part.

5.1 Wetting Characteristics of Sorbents

Kapok, cotton, hemp, polyester, nylon, and glass fibers are suitable candidates used in this study to separate oil/water mixtures. These porous materials possess large pore volume, flexibility, and commercial availability. The wetting characterization of the six fibers mainly depends on the contact angle and surface tension of water and four oils used in this study, which it presents in two parts. Although these six fibers have been investigated in the literature, there are no reports systematically comparing their performance for the hydrocarbons liquids and water as selected for this study. Moreover, the data in the literature is often made available under different experimental condition. This becomes a major barrier to select sorbents with best performance for applications in oil booms for example. The aim of this study is to enable a direct comparison among these six fibers. They were selected based on exceptional performance as previously reported separately by other authors.

5.1.1 Wetting Characteristics of Sorbents with Oil

To achieving a successful sorbent, the oil should wet the sorbent and therefore spread over its surface in preference to water. The contact angle and surface tension are significant parameters to determine the wetting ability of the surface in porous materials. Table 5.1 shows the values of contact angle and surface tensions for the four different hydrocarbon oils toward the kapok and polyester according to various works from other literature. In contrast to the other four fibers, they were found to be limited with the oils used in this study [16], [34], [53], [61]-[63]. All the four practical hydrocarbon oils are referred to as the wetting liquid for both kapok and polyester sorbents as $\theta<90\circ$.The nature of kapok has further high wax content at (3%) with high buoyancy leading the fiber to be superhydrophobic and oleophilic characteristics [18].

A liquid would wet a sorbent when its surface tension is lower than the critical surface tension. Therefore, for a sorbent to accomplish the required criteria, it should have a surface tension value is lower than in water and higher than in oil. Low surface tension implies that hydrocarbon oil penetrates both kapok and polyester porous structure and remain inside the pores of sorbents. Several natural and synthetic fibers hold suitable surface tension value except for the inorganic solids that do not meet the required value [12].

Table 5.1 Contact angle and surface tension of both kapok and polyester with oils.

Liquid	Contact Angle (°)	Surface Tension (mN/m)
	Kapok	
Gasoline	0 [16]	21.60 [16]
Diesel Fuel	0 [16]	25.84 [16]
Light Diesel Oil	24.9 [16]	31.67 [16]
Heavy Diesel Oil	24.9 [16]	31.67 [16]
	Polyester	
Gasoline	0 [159]	21.60 [16]
Diesel Fuel	0 [159]	25.84 [16]
Light Lubricant Oil	23 [159]	31.67 [16]
Heavy Lubricant Oil	23 [159]	31.67 [16]

5.1.2 Wetting Characteristics of Sorbents with Water

The term hydrophobicity is one of the main inherent sorbent characteristics to describe the high performance of the sorbents with the oil spill and to illustrate the attractive forces at the sorbents in the presence of water. The surface of the sorbent is one of the main determinants of the sorbents, and it can determine by two main factors containing contact angle and surface tension. The hydrophobicity of a sorbent is reported as the contact angle should have $\theta > 90^{\circ}$ to be classified the water as a nonwetting liquid [160], which is mainly mentioned in section 2.10.

Hence, the values of contact angle and surface tensions of the six fibers with water were obtained from different practical papers, which can be shown in Table 5.2 .

Table 5.2 Contact angle and surface tension of the six sorbents with water.

Fiber Type	Contact Angle (°)	Surface Tension of Water (mN/m)
	Water	
Kapok	136.2 [56]	72.48
Cotton	22.3 [161]	72.48
Hemp	26 [162]	72.48
Polyester	101 [159]	72.48
Fiberglass	34.54 [163]	72.48
Nylon	73 [88]	72.48

5.2 Characteristics of Sorbents

For a material to be suitable as an oil spill sorbent, it should have excellent innate characteristics including hydrophobicity/oleophilicity, high uptake, low-cost, non-toxic, easy to handle and be reusable. The sorbents were employed for creating highly efficient porous materials, and these porous materials require studying the physical properties to be considered viable sorbents for the oil spill.

5.2.1 Density and Porosity of Sorbents

One of the main goals of this study would be to discuss the importance of porosity, calculated by the bulk density, and the hydrocarbon characteristics on the sorption efficiency and kinetics of the sorption process. The porosity is not affected by the size of the fibers, but their sorting, packing and shape. Due to the complex sorting and shape of the fibers, the main factors affecting the porosity measurements are the arrangement of the fibers in the sample

holder and the amount (the packing). The volume of the holder is constant, and the amount of fiber can be easily changed, thus controlling the bulk density and porosity.

There is a close relationship between effective capillary diameter with a simply determined bulk density of the fiber samples. The bulk density can be determined as the mass of the fiber samples that fully occupied into a predetermined volume of the sample holder (30 mL). The unit for bulk density is g/cm^3. The sorbent density was obtained from data reported in the literature by other authors. Table 5.3 shows the bulk densities with the individual sorbent porosities calculated by equation 2.10.

Table 5.3 Specific gravity, bulk density, and porosity of six sorbents.

Sorbent Type	Specific Gravity (g/cm^3)	Bulk Density (g/cm^3)	Porosity
Kapok	1.320 [11]	0.0593	0.9550
Cotton	1.520 [11]	0.0647	0.9574
Polyester	1.380 [78]	0.0993	0.9280
Hemp	0.860 [164]	0.1030	0.8802
Nylon	1.130 [165]	0.1756	0.8445
Fiberglass	2.540 [163]	0.4955	0.8049

5.2.2 Surface, Fiber Diameter, and Voids between Fibers of Sorbents

The physical properties of raw kapok, cotton, hemp, polyester, nylon, and glass fibers were characterized based on morphology. The surface fibers morphologies were analyzed by Scanning Electron Microscope (SEM). The microphotographs of both raw kapok and polyester fibers are shown in Figure 5.1.

The unique surface structure of a sorbent can obtain more attraction to sorb, distribute, and trap the oil. By having considering the contact angles between the oil and water with a sorbent, other researchers quantified the relationship between roughness, curvature, and

contact angle [166]. Hence, rougher surfaces on the sorbents are associated with lower values of the contact angle due to the trapped air on surface pores.

The six fibers were completely showed different morphological structures. As can be seen from Figure 5.1 (a), the cotton fiber was exhibited as a twisted ribbon or tube. These twists are convolutions that tend to increase inter-fiber friction and to grow adequate strength for the cotton fiber [167]. The surface of cotton fiber was relatively rough and uneven. The raw kapok fiber has a hollow tubular/lumen structure and smooth surface area, as can be shown in Figure 5.1 (e). The smooth surface exhibit by the raw kapok fiber is observed due to the plant wax coverage on the surface. From Figure 5.1 (h), it can be seen that the surface of the hemp fiber is shown a smooth surface due to it is highly localized with the polysaccharides of lignin, pectin, and hemicellulose as can be confirmed with other studies [167].

In contrast, the polyester, nylon, and glass fibers were observed as straight, regular, and relatively smooth surfaces with circular structures, as can be shown in Figure 5.1 (k), (n), and (q) respectively. Furthermore, fiber diameters become an important in affecting oil retention. The porosity and pore size in the porous materials can mainly depend on the fiber diameter [168]. The sorbent is efficiently able to produce high pore spaces and can show better oil retention through having a lower fiber diameter between 0.9-10 micrometers [168], [169]. The fiber diameters in all SEM images were measured by using software Image J, and each fiber was selected with ten data points for measurement. The data from the ten measurements were used to calculate an average fiber diameter for each type of fiber, as can be shown in Table 5.4.

Table 5.4 Average fiber diameters of the six sorbents.

Fiber Type	Average Diameters (microns)	Standard Deviation
Cotton	14.13	0.16
Kapok	22.20	0.31
Hemp	35.03	0.46
Polyester	31.00	0.42
Fiberglass	26.84	0.37
Nylon	15.18	0.36

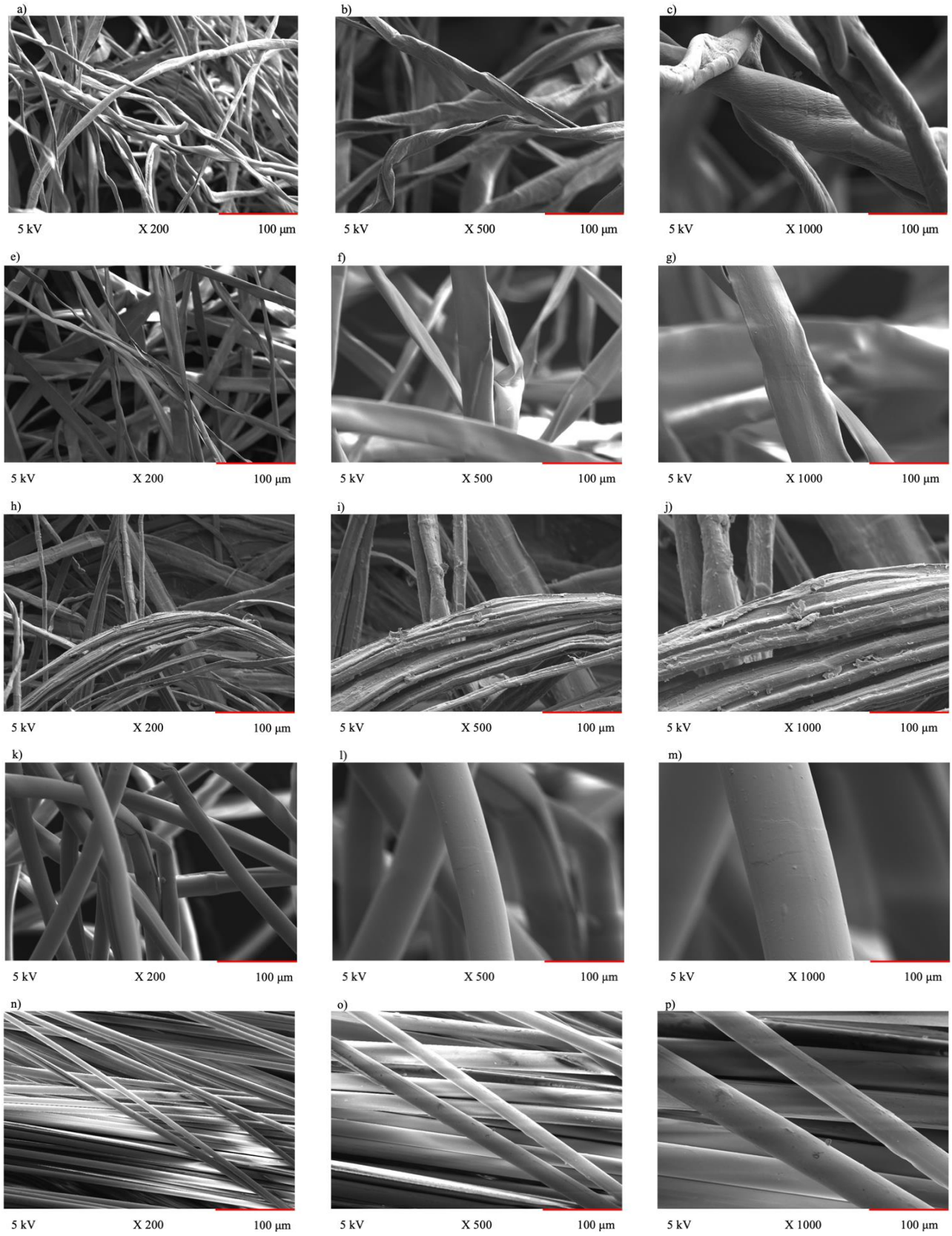
a)
5 kV X 200 100 µm
b)
5 kV X 500 100 µm
c)
5 kV X 1000 100 µm
e)
5 kV X 200 100 µm
f)
5 kV X 500 100 µm
g)
5 kV X 1000 100 µm
h)
5 kV X 200 100 µm
i)
5 kV X 500 100 µm
j)
5 kV X 1000 100 µm
k)
5 kV X 200 100 µm
l)
5 kV X 500 100 µm
m)
5 kV X 1000 100 µm
n)
5 kV X 200 100 µm
o)
5 kV X 500 100 µm
p)
5 kV X 1000 100 µm

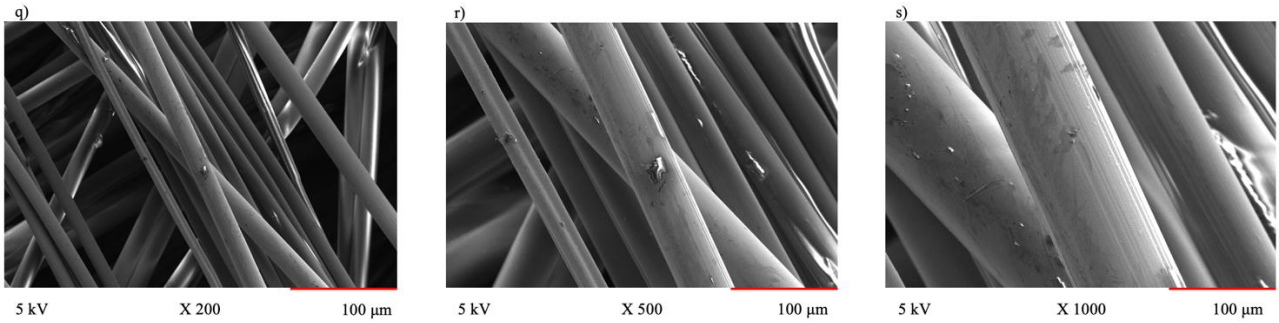

Figure 5.1 SEM micrographs of all six fibers; a) cotton, e) kapok, h) hemp, k) polyester, n)fiberglass, and q) nylon.

5.3 Characteristics of Liquids

The density and viscosity were measured for the liquids. The experimental procedures were illustrated in section 4.2.1 and section 4.2.2. Table 5.5 shows the values of the viscosities and densities of the liquids.

Table 5.5 Density and viscosity of oils and water.

Hydrocarbon Type	Density (kg/m^3)		Viscosity (mPa.s)	
	Average	Standard Deviation	Average	Standard Deviation
Water	1000	1.15	0.984	0.00
Gasoline	736.3	1.18	0.682	0.01
Diesel Fuel	817.3	1.65	1.578	0.01
Lubricant Oil (Light)	853.85	1.08	150.8	0.26
Lubricant Oil (Heavy)	875.1	1.65	157.8	0.66

5.4 The Spontaneous Imbibition Measurement

Sorption of a sorbate by sorbent is described as the non-wetting fluid (air) becomes displaced by the wetting fluid (hydrocarbon oil/water) resulting from the capillary forces. The sorption methods were studied by the spontaneous imbibition experiment. The spontaneous imbibition is a quantitative method. The preparation, setup, and procedure of the spontaneous imbibition test can be found in section 4.3.1

5.4.1 Sorption of Water in Sorbents

The capillary suction force is as a result of the interfacial tension existing at the interface separating two immiscible fluids. It will lead the liquid continues rising inside the tube until the force acting upward, resulted from surface tension and contact angle of liquid, becomes balanced by the force acting downward, came from the weight of the liquid. The saturated air in the voids of the sorbent samples becomes gradually displaced by the invading liquid. It briefly described in section 2.1. The load cell can precisely record the weight of the liquid imbibed at a present time interval. During the sorbent samples tend to reach the maximum amount of mass content, the time becomes to reach the steady-state, as can be shown in figure 5.2.

Hydrophobicity is a significant sorbent characteristic to describe the efficiency of oil sorption from the water surface. There are fundamental features to gain a superhydrophobic and superoleophilic sorbent involving the chemical constituent of the sorbent, the amount of wax content, the physical configuration of the fiber, the twists and the crimps, surface roughness, and porosity [16], [170]. Carbon (C), hydrogen (H), oxygen (O), and nitrogen (N) are the main components of the natural organic sorbents that all tend to form cellulose, hemicellulose, and lignocellulose [171]. Cellulose-based fibers can be effectively received more attraction to sorb water due to the hydroxyl groups (OH) located on their surface yield hydrophilicity, and they are limited in oil spill applications [172]. By obtaining a high wax content, the surface of a natural sorbent could become more hydrophobic [173], [174].

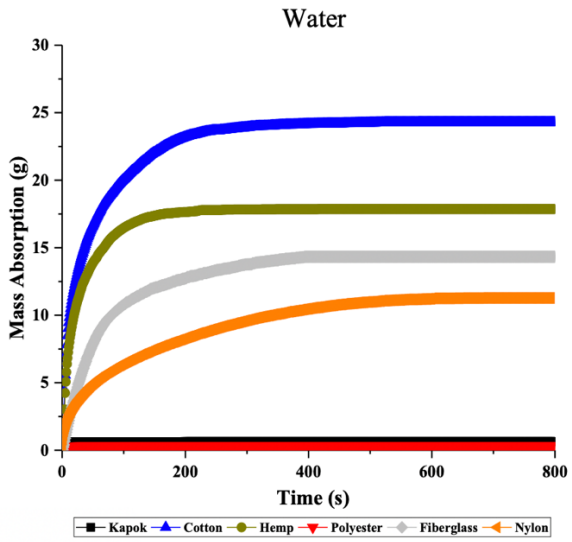

Figure 5.2 Water mass absorption for the six sorbents.

As the results indicate in Figure 5.2, cotton followed by hemp, fiberglass, and nylon had the highest water uptake compared to kapok and polyester. Besides high-water absorption for cotton and hemp fibers, it is noted that cellulose, hemicellulose, pectin, and lignin components have polar groups and thus are responsible for absorbing the water [38]. The kapok is significantly hydrophobic because of the wax content (3%) found on the fiber surface, which is higher than those to cotton and hemp fibers [18]. The fiberglass indicated a hydrophilic behavior due to its surface might be covered by a coated material, in contrast to the nylon fiber, the water molecules produce polar bonds with the hydrophilic functional amide groups in the nylon molecules. Meanwhile, the low water uptake of polyester are mainly due to their chemical components have non-polar groups, and hence the molecules are strong and stable and cannot break apart easily. The values of the first trial can be seen in Table 5.6 . The table below shows the saturated mass of the six samples toward the water.

Table 5.6 Mass and volume absorbed for the six samples with water.

Fiber Type	Mass Absorbed (g)	Volume Absorbed (cm^3)	Mass Absorbency (%) g oil absorbed/g wetted fiber
Kapok	0.63	3.47	3.05
Cotton	24.27	29.71	12.62
Polyester	0.33	0.36	9.03
Hemp	17.71	25.59	6.71
Nylon	11.27	21.59	2.97
Fiberglass	14.33	26.93	1.07

5.4.2 Sorption of Oils in Sorbents

All six fibers were absorbed the oils. The experimental curves are shown below for both kapok and polyester toward the four oils, whereas for the other four sorbents can be shown in Appendix A. The kapok, cotton and polyester samples exhibited a high value of oil absorption capacity compared to the other treatments. This behavior is attributed to the kapok, cotton and polyester samples because they have the highest value of porosity than the other treatments, as shown in Table 5.3. Table 5.3 illustrated the porosity of samples calculated by equation 2.10. Moreover, the hemp and fiberglass samples have a higher value of oil absorption capacity than the nylon sample. Another point is that nylon sample has the lowest value of both porosity and oil absorption capacities. It was further observed from the figures that the oil with higher viscosity, such as light and heavy diesel oils, tends to have lower oil mass absorption and can take a higher amount of time in penetrating through the fiber pores compared to gasoline and diesel fuel were quickly moved into the fiber interior pore.

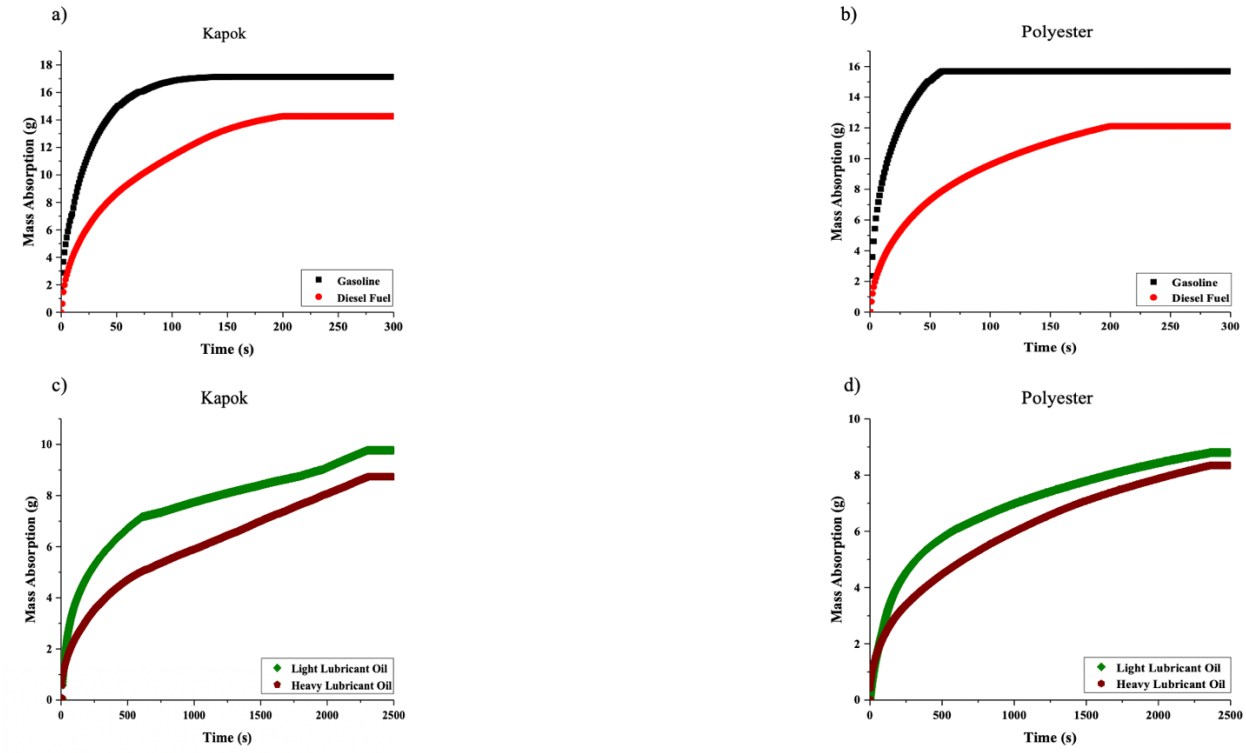

Figure 5.3 Oils mass absorption for both kapok and polyester.

Moreover, the kapok sample has a higher value of both porosity and oil absorption capacities compared to the other five samples. These values of the first trial can be clearly shown in Table 5.7 . The table below illustrates the saturated mass of the six samples with the four different oils.

Table 5.7 Mass and volume absorbed for the six sorbents with the oils.

Hydrocarbon Type	Mass Absorbed (g)	Volume Absorbed (cm^3)	Mass Absorbency (%) g oil absorbed/g wetted fiber
Kapok			
Gasoline	17.14	29.80	9.70
Diesel Fuel	14.27	23.62	10.19
Light Lubricant Oil	11.03	16.89	11.01
Heavy Lubricant Oil	9.15	13.38	11.53
Cotton			
Gasoline	16.04	29.26	8.47
Diesel Fuel	13.20	23.02	8.86
Light Lubricant Oil	9.29	15.72	9.13
Heavy Lubricant Oil	9.07	14.33	9.77
Polyester			
Gasoline	15.69	28.97	5.45
Diesel Fuel	12.12	21.27	5.74
Light Lubricant Oil	8.97	14.15	6.38
Heavy Lubricant Oil	8.18	12.48	6.60
Hemp			
Gasoline	14.02	28.76	4.73
Diesel Fuel	11.84	23.31	4.92
Light Lubricant Oil	8.21	15.75	5.05
Heavy Lubricant Oil	7.43	13.78	5.23
Nylon			
Gasoline	12.64	25.14	2.86
Diesel Fuel	11.45	16.04	3.05
Light Lubricant Oil	7.96	9.44	3.27
Heavy Lubricant Oil	7.09	7.49	3.77
Fiberglass			
Gasoline	11.58	22.89	1.02
Diesel Fuel	10.04	15.24	1.32
Light Lubricant Oil	7.37	8.11	1.83
Heavy Lubriacant Oil	6.94	6.99	2.00

It further compares the mass absorbency and the saturated mass of the six sorbents toward the different oils. With the increase in the saturated mass, the mass absorbency is

decreased, as explained in equation 4.2. As discussed earlier, the driving force ΔP is inversely proportional to the pore size. Therefore, the increase in the porosity of the fibers leads $\Delta P = \rho g h_f$ and the wetting front height to increase.

The values of saturated mass for different oils toward the six samples were calculated and converted into height easily reached by the oils obtained from equation 4.5. There was an increase in the wetting front height reached by the different oils due to the high porosity for the sorbents in the first trial, as can be shown in the below Figure 5.4 . It also shows that kapok has the highest height of the different oils compared to the other five sorbents.

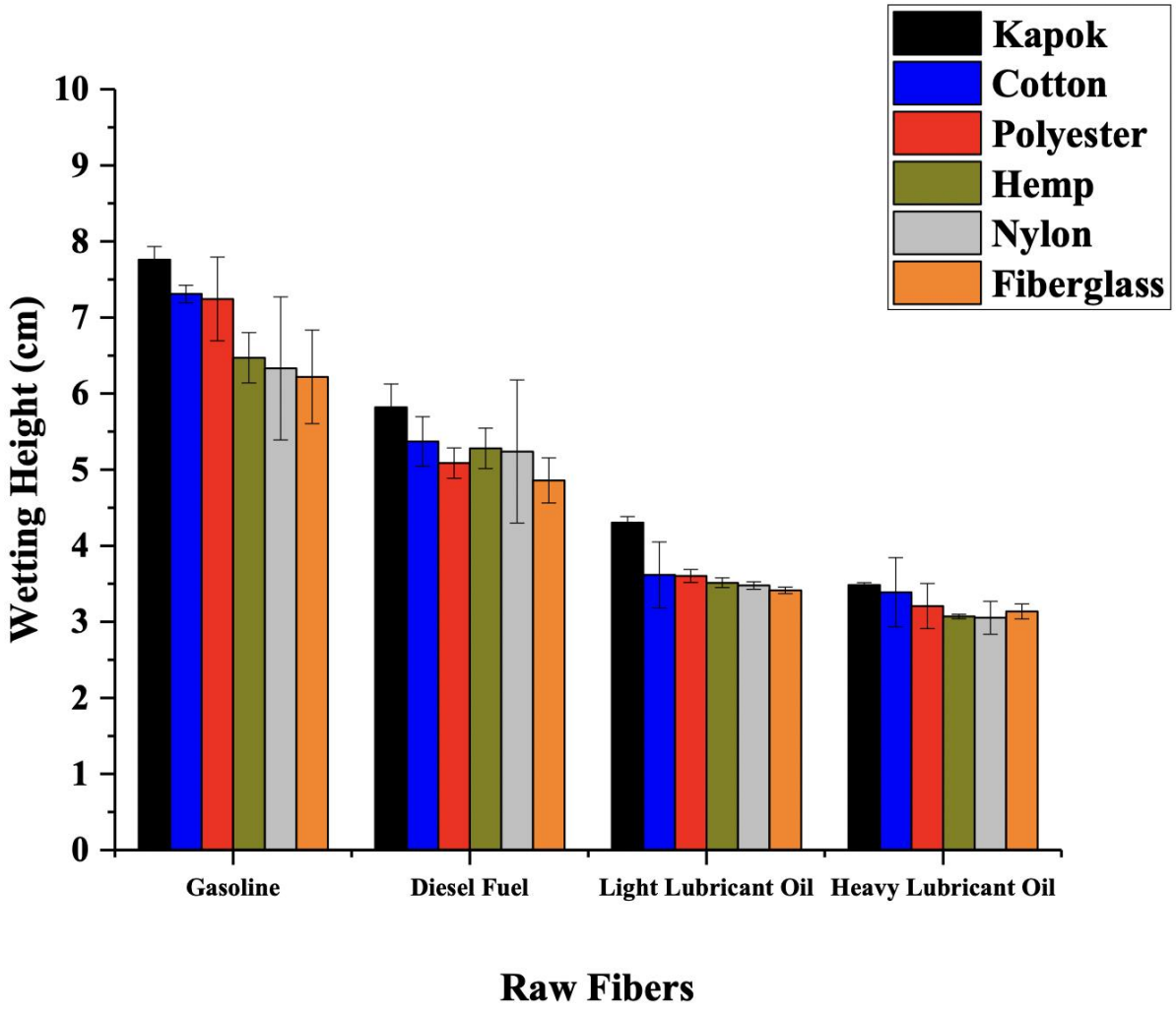

Figure 5.4 Wetting height of all six sorbents with the four oils.

Furthermore, the oil sorption capacity can be influenced by significant factors involving the surface area of the sorbent, pore size, shape and strength of fibers, viscosity, and oil type

[11]. Therefore, the increase in the volumetric absorbency results from the different values of the porosity and viscosity. By having a high oil viscosity, the pores might become obstructed and, hence, the oil sorption capacity decreases [11]. Figure 5.5 shows the comparison of the volumetric absorbency of the different oils via the six sorbents. The figure below illustrates that gasoline is the highest sorption compared to the other three oils. It was found from its low viscosity and density with the six samples compared to the other three hydrocarbons.

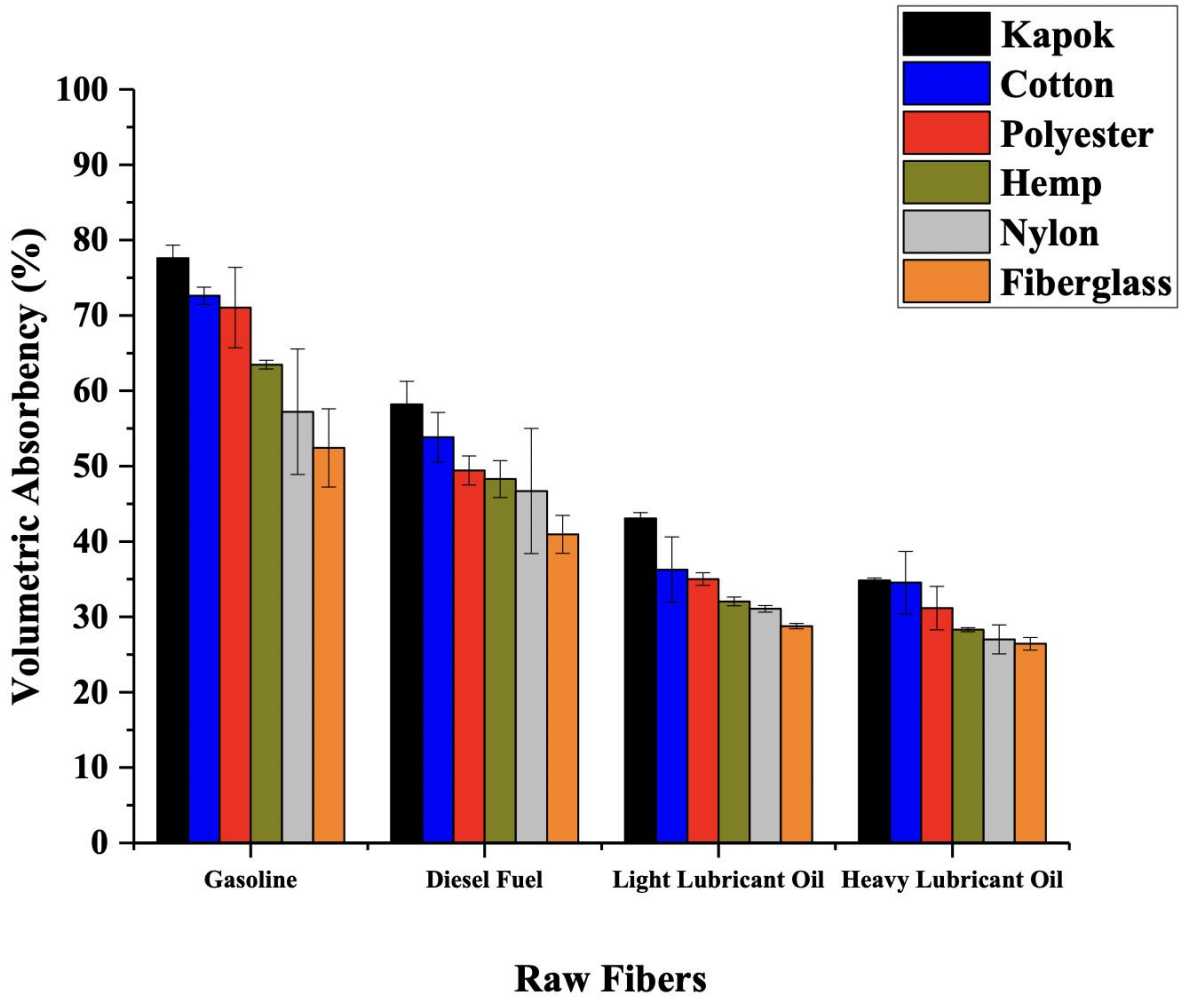

Figure 5.5 The comparison of volumetric absorbency for the six sorbents with the oils.

Chapter 6. Reusability of Sorbents

A reusability study was tested to investigate the fibers' stability under repeatable usage, to increase the environmental friendliness of these materials, and to decrease the cost of the methods in oil spill clean-up applications. The methodology of reusability for the sorbents with oil and water was discussed in more detail in section 4.4. According to the recyclability test results, there are distinct improvements in the absorption of both the oil/water capacity of the sorbents, which demonstrated stable reusability.

6.1 Hydrophobicity- Reusability

The goal of this study is to evaluate how the sorbents can be reused when the water is extracted. Hence, the methodology of recycling sorbents with water is mainly described in section 4.4. Figure 6.1 shows the absorbed water of the fiber samples after recycling them. The cotton, fiberglass, hemp, and nylon fibers showed the highest amount of water absorption capacity compared to the other samples. Table 6.1 shows the values of the saturated mass and volume for the six samples toward the water. It was observed that cotton followed by fiberglass, hemp, and nylon fibers imbibed in the water owing to their hydrophilic characters in the hydroxyl groups of the natural fibers, the possible coated material of the fiberglass, and the amide functional groups of the nylon fiber. In contrast, the buoyant nature of the kapok and polyester samples can be attributed to their superhydrophobic characters in the surface wax content of the kapok fiber and the petroleum-based components of the polyester fiber, which the fibers can repel water and float on the water surface.

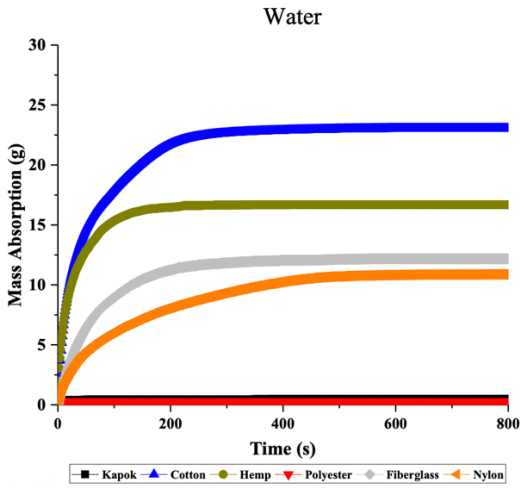

Figure 6.1 Mass absorption of the six sorbents with water in the reused method.

Table 6.1 Mass and volume absorbed for the six samples with water in the reused method.

Fiber Type	Mass Absorbed (g)	Volume Absorbed (cm^3)	Mass Absorbency
Kapok	0.50	2.54	3.31
Cotton	23.03	27.97	12.72
Polyester	0.29	0.31	9.18
Hemp	16.68	23.05	7.02
Nylon	10.87	19.93	3.10
Fiberglass	12.17	20.09	1.22

It was observed that the water mass absorption of all fibers was slightly decreased in the reusability method. The decrease results were due to the shape and strength of the fibers that were experimentally found to be influenced by compressing the fibers to extract the water and attempting to dry the fibers using the vacuum oven. There was another observation from using the spontaneous imbibition device that a material imbibed smaller than 1 g is referred to as a hydrophobic material in which both fibers in this study were sorbed below 1 g.

6.2 Oleophilicity- Reusability

The sorbent construction is one of the main factors in affecting the retention behavior of a sorbent [3], [11]. Therefore, a sorbent with high porosity can absorb more oil, but it has a weak oil retention capacity [3]-[11]. The amount of mass absorption for oils after recycling the fiber samples was lower than the succeeding sorption due to the retention of oil in the samples, as can be shown in Figure 6.2 . Likewise, owing to the retention of oil in the sorbent fibers, the mass absorption of the other four fibers was slightly decreased with progressing sorption times, as can be shown in Appendix B.

Moreover, the effect of fiber pore structure can significantly lead to affect oil movement and its retention properties [11]. Hence, the pores can be collapsed and obtained a lower oil capacity through the reduction in wet fiber strength and resiliency. This reduction is probably resulting from the mechanism of the reusability through the compression and dry processes. The slight changes further could be the small amount of diluted detergent used. All of these

factors represent direct challenges to quantitative prediction and interpretation of capillary liquid transport phenomena in fibrous materials [175].

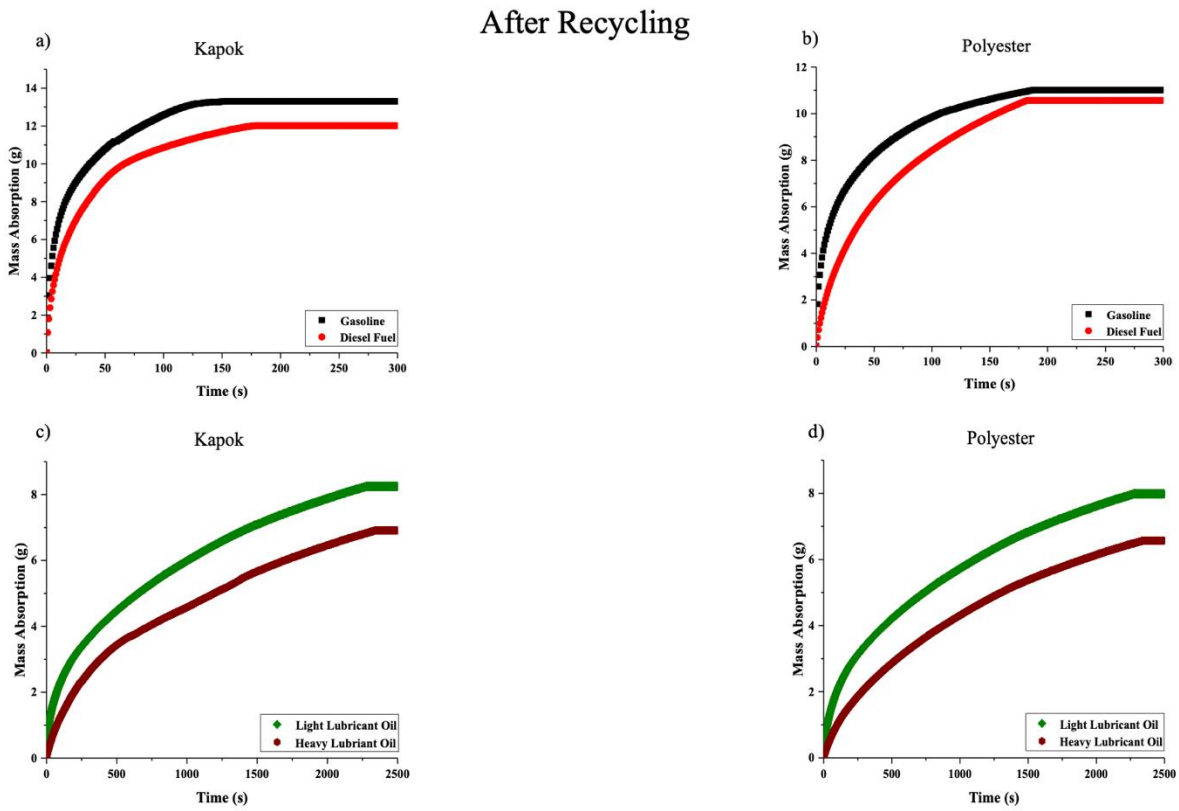

Figure 6.2 Mass absorption for both kapok and polyester with the oils in the reused method.

In terms of reusability, all fibers were slowly sorbed compared to the first trial due to the decreased porosity of the sorbents. Table 6.2 shows the mass and volume sorption of the sorbents with the hydrocarbon oils, which the kapok fiber was possessed high mass sorption than the other five fibers. The table below is also illustrated the reduction value in the mass absorbency of both sorbents with the oils.

Table 6.2 Mass and volume absorbed for the six samples with the oils in the reused method.

Hydrocarbon Type	Mass Absorbed (g)	Volume Absorbed (cm^3)	Mass Absorbency (%) g oil Absorbed/g wetted fiber
		Kapok	
Gasoline	13.30	26.48	8.47
Diesel Fuel	12.01	23.16	8.74
Light Diesel Oil	8.24	15.41	9.02
Heavy Diesel Oil	7.71	12.83	10.13
		Cotton	
Gasoline	12.53	26.03	7.39
Diesel Fuel	11.75	23.01	7.89
Light Diesel Oil	8.09	15.35	8.04
Heavy Diesel Oil	7.03	12.63	8.59
		Polyester	
Gasoline	11.01	26.34	4.21
Diesel Fuel	10.77	22.90	4.74
Light Diesel Oil	7.98	14.02	5.73
Heavy Diesel Oil	6.57	10.37	6.38
		Hemp	
Gasoline	10.93	26.10	4.06
Diesel Fuel	10.32	24.13	4.68
Light Diesel Oil	7.73	14.96	5.01
Heavy Diesel Oil	6.41	11.63	5.34
		Nylon	
Gasoline	10.81	22.54	2.73
Diesel Fuel	9.96	19.18	2.95
Light Diesel Oil	7.52	12.35	3.07
Heavy Diesel Oil	6.34	11.33	3.17
		Fiberglass	
Gasoline	10.41	21.73	0.96
Diesel Fuel	9.36	19.10	0.98
Light Diesel Oil	6.78	11.37	1.20
Heavy Diesel Oil	6.22	8.53	1.47

After recycling, the wetting front height of the sorbents is decreased with the oils. This is attribute to the reduction porosity of the sorbents in the second trial, as can be shown in

Figure 6.3 (a). The kapok fiber in the reusability method is slightly increased with the different oils compared to the other fibers. However, the volumetric absorbency is dramatically reduced due to the total pores volume of the sorbents after recycling is further reduced. The viscosity and density of the oils are resulted in controlling the highest sorption toward the sorbents. The figure below (b) shows the kapok fiber is the most sorption with the oils compared to the other five fibers.

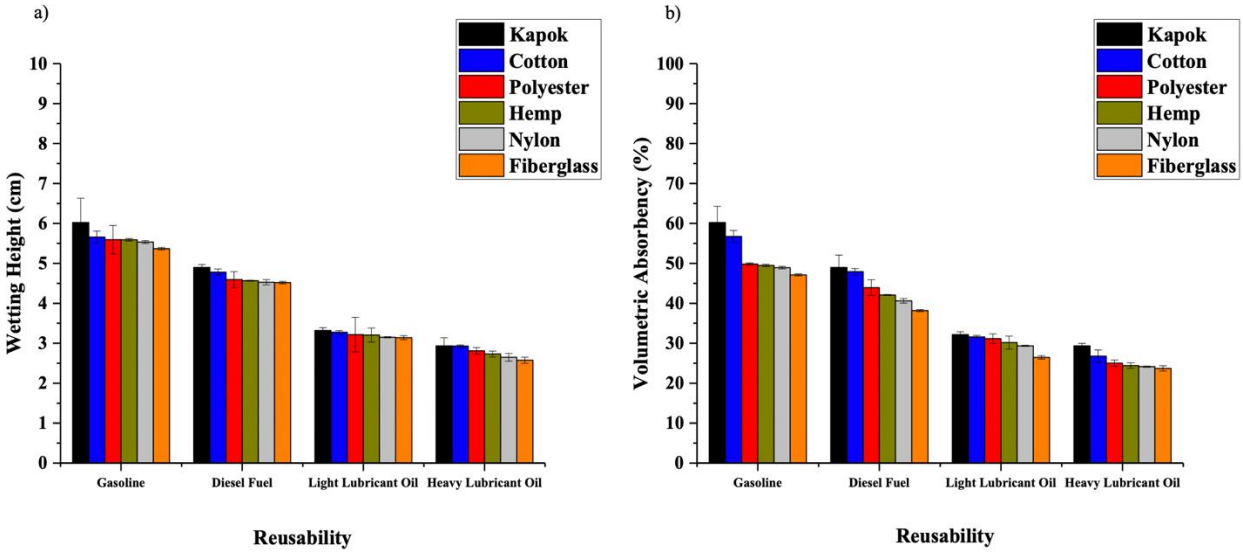

Figure 6.3 Wetting height (a) and volumetric absorbency (b) of the six sorbents with the oils in the reused method.

Furthermore, the chemical compatibility between oil and surface wax of the natural fibers tends to minimize the energy barrier of oils to penetrate the fiber pore structure. Other primary factors of the natural fibers in providing sufficient space for oil entrapment and the oil sorption and retention capacities include the tubular and hollow structure as well as the physical configuration involving the twist and the crimp and the size and strength of the fibers.

The oils remained trapped inside the kapok lumens after absorption in the first trial are likely to affect the oil absorption capacity of kapok in the subsequent cycles [16], [94]. In other words, the oil entrapment inside the hollow structure of the kapok fiber could be highly stable compared to the inter-fiber pores, which can be shown in Appendix G (Figure G.1). However, the other natural fibers used in this study were observed with different structures that could be obtained reasonable oil sorption and retention capacities.

The sorption efficiency was experimentally exhibited highly hydrophobic/oleophilic characteristics for both kapok and polyester, while the other four fibers were found to be hydrophilic/oleophilic characteristics. In the reusability method, the natural fibers can be reused to absorb more oils slightly, while the synthetic fibers in the next subsequent cycles can be absorbed the oils more than ten times due to their petroleum-based composition.

6.3 Saturated Pore Size

The identification of the pore size range that the materials are possessed, determination of the pore types, and estimation of the representative of an entire porous sample are the three main factors within a porous material for guidance on selecting the best method to perform successful pore size analysis. By using the imbibition experiment in this study, when oil or water is placed in contact with a large pore opening, the liquid is resulted in a constant or straight line graph due to the slow oil or water flow to occupy the fiber's large pore opening. Whereas the oil or water flow in a small pore opening, it was quickly penetrated the surface pores resulted in an increasing line graph, as can be shown in Figure 6.4. Both states were found out from the inverse relationship between pore diameter and pressure that is called Washburn's equation, as discussed in section 2.7.1.

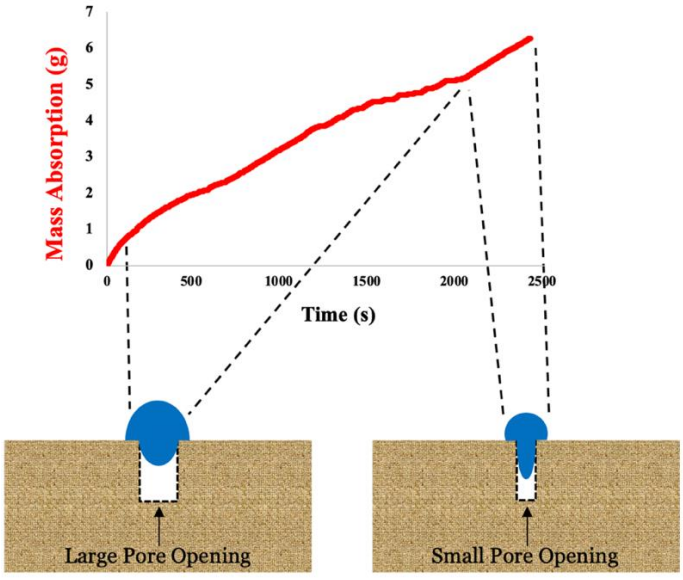

Figure 6.4 Illustration the relationship between the sizes of pore diameter and pressure corresponding to the spontaneous imbibition device's graph.

Chapter 7. Evaluation of Theoretical Models

7.1 Modelling Experimental Data

To study the oil absorption of sorbent, it can be considering the equilibrium condition of the capillary force and capillary kinetics of the liquids. In this chapter, the experimental sorption kinetics of kapok and polyester fibers were compared with the estimations of both the Lucas-Washburn and Darcy-based models due to the surface tension and contact angle of the four different oils were reasonable to obtain, while the other four fibers were found to be limited with the oils used in this study. These models are used to understand the fluid transport through the sorbents that mainly depend on the momentum balance and continuity equation corresponding to the imbibition rate.

7.1.1 Lucas-Washburn Model

The Lucas-Washburn model assumes the flow into a sorbent is a bundle of capillary tubes that have the same radius. The derivation of the model is explained in more detail in section 2.12.1 The analytical of the Lucas-Washburn model is often described the relation between the visible wetted front, h, and time [176]. There were two different approaches applied to the capillary rise for the sorbents. In the first approach, the mass increase as a consequence of the capillary rise in the sorbents is evaluated, while in the second approach, the experimental mass data was converted into wetted front height using equation 4.5. After the simplifications of the momentum balance neglecting the inertial effect, the final equation is lead to correlate the wetted front height with time. Equation 2.17 illustrated the relationship between the wetted front height and time that viscous and gravitational forces acting opposite to capillarity. Here, the model is validated against the experimental data that is predicted the wetted front height with time.

$$P_C \ln\left|\frac{P_C}{P_C - \rho gh}\right| - \rho gh = \frac{\rho^2 g^2 r^2}{8\mu} . t \tag{7.1}$$

The Lucas-Washburn model is a first-order non-linear equation, and the wetted front height can be shown in the following equation. Rearranging the above equation was performed

to make the wetted front height as the independent variable. The Young-Laplace equation is known as:

$$P_C = \rho g h = \frac{2\gamma \cos(\theta)}{r_C} \tag{7.2}$$

Thus, the equation becomes:

$$h = \frac{2\gamma \cos(\theta)}{r_C \rho g} = \frac{S}{r_C} \tag{7.3}$$

Because the contact angles and the liquid properties are known, these known numbers are denoted to as S. By combining equation 7.3 into equation 7.1 and bringing 't' to the left-hand side, the Lucas-Washburn equation is modified as:

$$t = \frac{16\mu\gamma \cos(\theta)}{g^2 \rho^2 r_C^3} \ln\left(\frac{S}{S - r_C h}\right) - \frac{8\mu}{g\rho r_C^2} h \tag{7.4}$$

From the above equation, r_C is referred to as the fitting parameter. By using the MATLAB function fminsearch, the least-square fitting was given between the modified Lucas-Washburn model and the experimental data to reduce the errors for both the observed times and modeled times. The MATLAB code can be shown in Appendix E. The fitting curves for both sorbents with all oils and water were not fit well. The gasoline curves of both sorbents for both raw and reused trials can be seen in Figure 7.1, while for the other three oils and water with both sorbents can be shown in Appendix C.

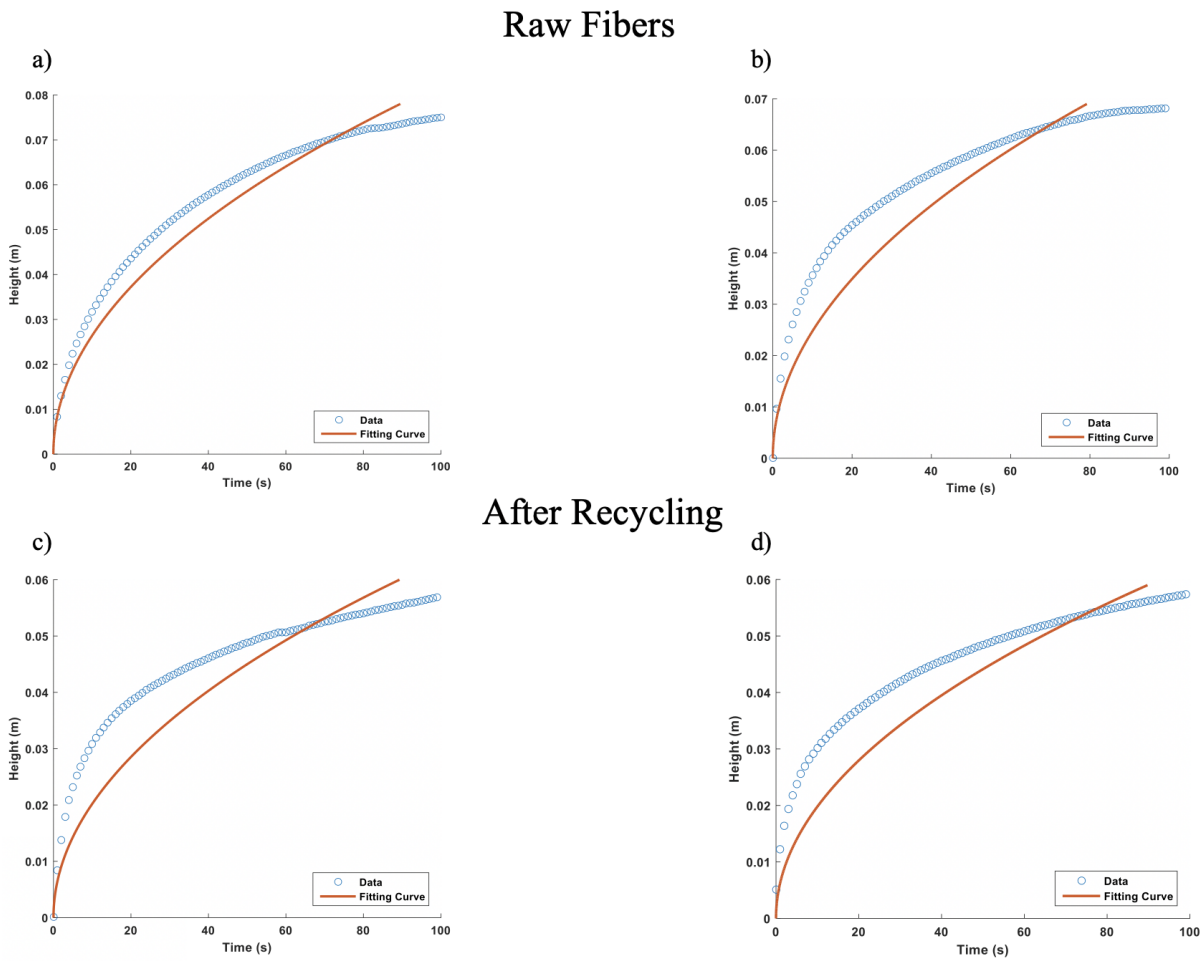

Figure 7.1 Lucas-Washburn model with gasoline a) and c) kapok and b) and d) polyester

Furthermore, the modified Lucas-Washburn model did not match with the experimental data due to the variation of contact angle as a function of the liquid used leading the fitted r_C, the effective capillary radius, not being correlated to the sorbents by using this model. This variation was observed from several researchers, and they have concluded that further studies are needed [134]. In contrast, Hamraoui and Nylander [177] briefly described a mechanism for comparing both the Lucas-Washburn model and the experimental data about the dynamics of capillary rise. In their analytical approach of applying the Lucas-Washburn equation, they considered the effects of surface tension, gravity, liquid viscosity, and neglecting the inertia force, as well as the contact angle of the liquid, was moving with the capillary walls of the porous material. Therefore, they found out that their analytical approach with both experimental data and the theoretical model was matched in which the contact angle was dynamic, and it was not a constant value.

7.1.2 Darcy-based Model

The Darcy model is further used to describe the fluid flow in the sorbents, as briefly described in section 2.12.2.1. For the one-dimensional fluid flow, the assumptions of both momentum and continuity equations are performed to the moving interface using the representative elementary volume approach, which is described in section 2.12.2. This model can be applied to 2-D and 3-D compared to the Lucas-Washburn model, which can be only performed on 1-D.

The permeability and capillary pressure are commonly the two main parameters used in the predictions for the porous structure. Equation 2.25 described the relationship between the meniscus height and time. In the equation, 't' was rewritten to be on the left-hand side in the form of:

$$t = \frac{\phi \mu P_c}{\rho^2 g^2 k} \ln \left| \frac{P_C}{P_C - \rho g h} \right| - \frac{\phi \mu h}{\rho g k} \tag{7.5}$$

Since both k and P_C were the fitting parameters, and the oil properties were known, fitting was performed by using the MATLAB fminsearch to fit the meniscus height against time. The MATLAB code can be shown in Appendix F. The experimental data of both kapok and polyester fibers with all oils and water were modeled with equation 7.5. Both sorbents with all oils showed good fitness, in contrast to water, the deviation line from the Darcy-based model did not agree well with the experimental data for both sorbents. In other words, both sorbents with water were resulted in a flat or straight-line graph that the predicted line cannot match with experimental data due to the physicochemical characteristics of both sorbents, as described briefly in section 5.4.1 and section 6.1. The fitting trends are shown below for the first and reused gasoline of both sorbents, whereas for the other three oils and water toward both sorbents with both methods can be shown in Appendix D.

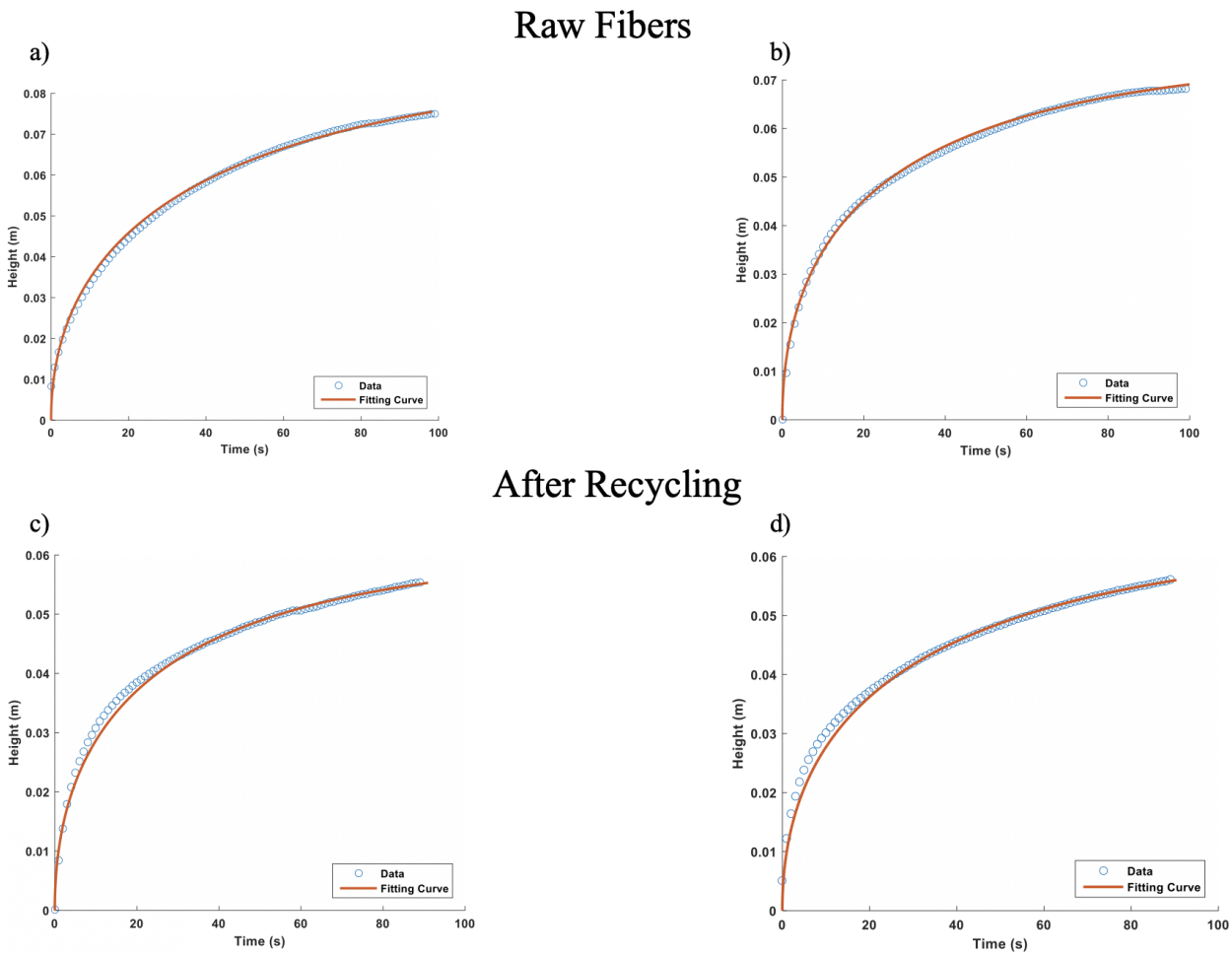

Figure 7.2 Darcy-based model with gasoline a) and c) kapok and b) and d) Polyester

As can be seen from using equation 7.5, all curves were proved a reasonably satisfactory fit with the experimental data. The two fitting parameters, P_C and K, were obtained for both sorbents with all oils by MATLAB. The fitting parameters for both sorbents with all oils were determined for both trials, which can be shown in the table below.

Table 7.1 The values of fitted parameters of both kapok and polyester and both methods with the oils

Hydrocarbon Type	Porosity ϕ	Viscosity (Pa.s)	Capillary Pressure (Pa)	Permeability (E^{-10} m^2)
		Kapok		
		Raw Fiber		
Gasoline	0.9550	0.0006	686	0.400
Diesel Fuel	0.9550	0.0015	674	0.706
Light Lubricant Oil	0.9550	0.1508	331	3.707
Heavy Lubricant Oil	0.9550	0.1578	330	3.721
		Reusability		
Gasoline	0.9550	0.0006	384	1.334
Diesel Fuel	0.9550	0.0015	353	1.874
Light Lubricant Oil	0.9550	0.1508	338	4.289
Heavy Lubricant Oil	0.9550	0.1578	319	5.197
		Polyester		
		Raw Fiber		

Gasoline	0.9280	0.0006	577	0.336
Diesel Fuel	0.9280	0.0015	543	1.051
Light Lubricant Oil	0.9280	0.1508	515	1.246
Heavy Lubricant Oil	0.9280	0.1578	456	2.334
		Reusability		
Gasoline	0.9280	0.0006	461	0.760
Diesel Fuel	0.9280	0.0015	401	1.505
Light Lubricant Oil	0.9280	0.1508	385	2.501
Heavy Lubricant Oil	0.9280	0.1578	353	2.921

As can be seen from the Darcy-based model, the P_C was regarded as a significant parameter in this study to predict the wetted front height for both sorbents against time. Hence, the capillary flows for both sorbents were in a bundle of vertically capillary tubes with the uniform diameter. The obtained capillary pressures and contact angles for both sorbents with the four oils were given to the Young-Laplace equation to find the effective capillary radius, r_C. In contrast to water with both sorbents, the effective capillary radius r_C, with both sorbents was found out to obtain a negative value by using equation 2.8 due to the contact angles of both sorbents with water have $\theta > 90^\circ$ to be classified as nonwetting sorbents with water. Hence, the effective capillary radius of both sorbents toward water cannot be related to using both models in this study. The capillary pressures and computed effective capillary radius results for both sorbents can be shown in Table 7.2 .

Table 7.2 Effective capillary radius and capillary pressure

Hydrocarbon Type	Surface Tension (mN/m)	Contact Angle (°)	Capillary Pressure (Pa)	Effective Capillary Radius (µm)
Kapok				
Raw Fiber				
Gasoline	21.60	0	686	62
Diesel Fuel	25.84	0	674	76
Light Lubricant Oil	31.67	24.9	331	173
Heavy Lubricant Oil	31.67	24.9	330	173
Reusability				
Gasoline	21.60	0	384	112
Diesel Fuel	25.84	0	353	146
Light Lubricant Oil	31.67	24.9	338	169
Heavy Lubricant Oil	31.67	24.9	319	179
Polyester				
Raw Fiber				
Gasoline	21.60	0	577	74
Diesel Fuel	25.84	0	543	95

Light Lubricant Oil	31.67	23	515	113
Heavy Lubricant Oil	31.67	23	456	127

Reusability

Gasoline	21.60	0	461	93
Diesel Fuel	25.84	0	401	128
Light Lubricant Oil	31.67	23	385	151
Heavy Lubricant Oil	31.67	23	353	165

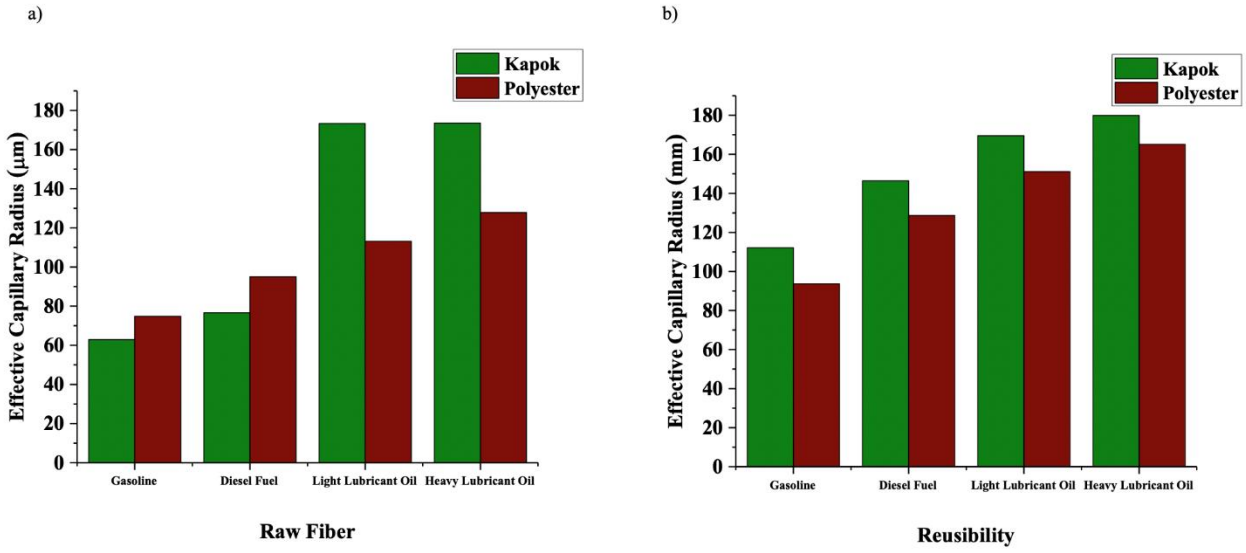

Figure 7.3 Effective capillary radius of both kapok and polyester with the oils a) raw fiber and b) reused method

Due to the high porosity of the kapok fiber that results from the small fiber diameter tends to have high oil sorption compared to the other five fibers. Moreover, by having a high capillary pressure that resulted from a high porosity, the effective capillary radius for both sorbents with the first trial tend to decrease, which both sorbents are referred to as suitable

sorbents for oil/water applications, as can be shown in Figure 7.3. The capillary pressure is a function of surface tension, capillary diameter, and contact angle between solid and liquid interfaces [16]. Hence, it plays a significant role in holding up the weight of oils within the random fiber structures and preventing the draining process.

The kapok fibers have a microtube with a hollow lumen structure. Abdullah et al. [16] were found a microtube structure of the kapok fiber with a huge hollow lumen and can be contributed to 77% of the fiber's volume. Hence, the oil droplets were absorbed on both the fiber surface due to the wax content (3%) and into the huge lumen of the fiber structure, providing to the exceptionally high oil sorption and retention capacity [18]. This significant microtube structure, the wax content, and the fiber diameter of the kapok fiber was further obtained by others [11], [16], [18], [54]. In contrast, in the reused trial, the capillary pressure for polyester fiber was higher than kapok fiber because of the porosity of kapok fiber was reduce in the reused trial. This was also due to possibility to the oils remained trapped inside the kapok lumens after absorption in the first trial leading to affect the oil absorption capacity of kapok in the subsequent cycles [16]. In other words, the oil entrapment inside the hollow structure of the kapok fiber could be highly stable compared to the inter-fiber pores.

Furthermore, the removal of wax content and the collapsed rigid and hollow structure of the kapok fiber could reduce the oil sorption capacity in the next subsequent leading to increase the kapok hydrophilicity. Abdullah et al. [16] were observed that the kapok fiber could be slightly increased the oil sorption capacity in the next subsequents due to the reduction of the meager amount of surface wax. They were also found that the presence of surface wax of the kapok fibers tend to cause the tubular structure to produce sufficient capillary pressure and can retain the absorbed oil.

Chapter 8. Conclusion and Future Works

8.1 Conclusion

In conclusion, oil spills through the exploration and transportation to different users have been a great concern to the oceans and inland waters, small or large. In the last decades, the oil spills are placed at high risk due to the toxicity of these compounds causing critical effects to the ocean flora and fauna, human health, and also economic losses. In this regard, the recent developments of oil/water separation technologies have been taking advantage of the special surface wettability of various sorbents. There is a great challenge in providing a clean environment from oil-contaminated water with the use of natural fiber-based oil sorbents compared to synthetic fibers. When the booms composed of the synthetic fibers are ineffective in rough seas, the natural fibers could be the best option for oil spill response due to their unique properties.

In this study, kapok, cotton, hemp, polyester, nylon, and glass fibers were used to compare their overall oil sorption characteristics and to find stable material for prolonged use. The sorption phenomena was evaluate by the spontaneous imbibition mechanism in which the invader (oil) is displaced the defender (air). The sorbents with the four oils were experimentally measured by the imbibition equipment as mass absorbed against time, and they were theoretically modeled to validate the experimental data as height against time. These models were discussed and assumed both sorbents with the oils in a bundle of vertical capillary tubes that have constant diameters. Applying these models on macroscale for both sorbents were discussed to study the main three parameters as capillary pressure, permeability, and effective capillary radius. Thus, the outcomes of this study could be summarized as:

- The oil absorption capacity on both raw and reusability methods was experimentally evaluated for the six fibers in which the sorbents are exhibited excellent hydrophobic/oleophilic characteristics. The effect of the oil sorption capacities of the sorbents was studied by the imbibition equipment (in a batch system). The sorption efficiency of the six sorbents with the four oils was discussed, and it was found out that the natural fibers can be used to slightly absorb more oils due to the reduction in the

physicochemical characteristics, whereas the synthetic fibers could pick up oil more than ten times because of their petroleum-based composition.

- Theoretical models such as Darcy based and Lucas-Washburn models were fitted with the experimental data for both kapok and polyester fiber, while the other four fibers were found the surface tension and contact angle to be limited with the four different oils used in this study. The comparison between theoretical predictions and experimental data of both sorbents with the four oils and water has shown unsatisfactory fitness with the combined Lucas-Washburn model due to the contact angle of liquids is varied as a function of times. Whereas the Darcy-based model has shown a satisfactory fitness with the experimental data for all oils, and it can be controlled through permeability and capillary pressure as fitting parameters, in contrast to water, it has shown an unwell fitness with both sorbents due to their straight line through the experimental data, and their contact angles have $\theta > 90^{\circ}$ to be found out their calculated effective capillary radius with water obtained negative values.

- Based on SEM analyses, kapok fiber was shown to be a microtube structure with hollow lumens. It can be highly absorbed the oil droplets in both on the fiber surface and into the lumen of the fiber contributing to the exceptionally high oil sorption and retention capacity due to three main factors: the hollow lumen network, inter-fiber distances, and liquid bridges between the fibers [16]. The cotton fiber was exhibited as a twisted tube with a relatively rough and uneven structure, while the hemp fiber was shown a smooth surface due to the fiber surface is localized with the polysaccharides of lignin, pectin. Hence, the natural fibers were shown to be naturally excellent material in oil sorptions due to their distinguished chemical and microstructural properties [173]. In contrast, the synthetic fibers were shown relatively smooth surfaces with circular structures and the petroleum-based composition of the synthetic fibers leading the oils to quickly penetrate the voids of the synthetic fibers.

8.2 Future Works

Further research are required to enhance the treatments of oil-polluted water, which can be on the following aspects:

- Sorption mechanism and theories of sorbents for oil/water separation were required for further developments. Finding super wetting materials such as kapok fiber with a hollow structure in which the oil can absorb in its core leading to increase its sorption can be a suitable candidate in selective oil/water separation. This work can use SEM to study the structure of the fiber before and after the sorption mechanism.

- Using pure oils for oil/water separation experiments are slightly different from the actual oil leakage accidents and industrial wastewater treatments. They are only appropriate to laboratory environments, and they do not match the actual oil-pollutants in oil leakage accidents and real-life industrial treatments.

- Further study can use a combination of two different methods of meshes that show antagonistic surface wetting properties, which allows having a continuous separation of massive volumes of oil/water mixture. This efficient method can be designed very cleverly to be useful for the treatment of oil-contaminated water. Dunderdale et al. [109] were used a combination of hydrophilic/hydrophobic polymer-brush to functionalizing stainless steel (SUS) mesh with antagonistic wetting properties to purify both the oil and water phases concurrently resulting in high flux rate and purity as shown in appendix H (Figure H.1).

- Using X-ray Computed Tomography (CT) is an advanced technique for visualizing interior features within a porous medium, and for predicting digital information on their 3-D geometries and properties of fluid flow like relative permeability much more satisfying. Another method that has received much attention recently is SEM. This sophisticated technology has been used to obtain pore size distribution effectively. Widiatmoko and Abdullah [178] were obtained the pore size distribution of porous materials by using Scanning electron microscope (SEM) images, and a program has written in Visual Basic to test the method, as can be shown in appendix H (Figure H.2).

References:

[1] S. E. Allan, B. W. Smith, and K. A. Anderson, “Impact of the Deepwater Horizon oil spill on bioavailable polycyclic aromatic hydrocarbons in gulf of Mexico coastal waters,” *Environmental Science & Technology*, vol. 46, no. 4, pp. 2033–2039, 2012.

[2] C. Hyung-Mln, and R. M. Cloud, “Natural sorbents in oil spill cleanup,” *Environmental Science & Technology*, vol. 26, no. 4, pp. 772–776, 1992.

[3] R. K. Gupta, G. J. Dunderdale, M. W. England, and A. Hozumi, “Oil/water separation techniques: a review of recent progresses and future directions,” *Journal of Materials Chemistry A*, vol. 5, no. 31, pp. 16025–16058, 2017.

[4] K. Zhu, Y. Y. Shang, P. Z. Sun, Z. Li, X. M. Li, J. Q. Wei, K. L. Wang, D. H. Wu, A. Y. Cao, and H. W. Zhu, “Oil spill cleanup from sea water by carbon nanotube sponges,” *Frontiers of Materials Science*, vol. 7, no. 2, pp. 170–176, 2013.

[5] J. O. Nwadiogbu, V. I. E. Ajiwe, and P. A. C. Okoye, “Removal of crude oil from aqueous medium by sorption on hydrophobic corncobs: Equilibrium and kinetic studies,” *Journal of Taibah University for Science*, vol. 10, no. 1, pp. 56–63, 2016.

[6] N. T. Duc, “Sorption studies of crude oil on acetylated sawdust,” *Vietnam Journal of Science and Technology*, vol. 54, no. 2A, p. 201, 2018.

[7] S. A. Sayed, and A. M. Zayed, “Investigation of the effectiveness of some adsorbent materials in oil spill clean-ups,” *Desalination*, vol. 194, no. 1–3, pp. 90–100, 2006.

[8] M. Hussein, A. A. Amer, and I. I. Sawsan, “Oil spill sorption using carbonized pith bagasse 1. Preparation and characterization of carbonized pith bagasse,” *Journal of Analytical and Applied Pyrolysis*, vol. 82, no. 2, pp. 205–211, 2008.

[9] O. T. Badejo, P. C. Nwilo, and F. I. Waterways, “Management of oil spill dispersal along

the nigerian coastal areas," *ISPRS Congress*, 2004.

[10] N. Al-Jammal, and T. Juzsakova, "Review on the effectiveness of adsorbent materials in oil spills clean up," *7th International Conference of ICEEE*, 2017.

[11] C. Praba Karana, R. S. Rengasamy, and D. Das, "Oil spill cleanup by structured fibre assembly," *Indian Journal of Fibre and Textile Research*, vol. 36, no. 2, pp. 190–200, 2011.

[12] ITOPF Ltd, "Use of sorbent materials in oil spill response," *Technical Information Paper*, 2012.

[13] A. K. Aboul-Gheit, F. H. Khalil, and T. Abdel-Moghny, "Adsorption of spilled oil from seawater by waste plastic," *Oil and Gas Science and Technology*, vol. 61, no. 2, pp. 259–268, 2006.

[14] L. J. Graham, C. Hale, E. Maung-douglass, S. Sempier, L. Swann, and M. Wilson "Chemical dispersants and their role in oil spill response," *Oil Spill Science: Sea Grant Programs of the Gulf of Mexico*, pp. 1-8, 2010.

[15] E. J. Struzeski, and R. T. Dewling, "Chemical treatment of oil spills," *2005 International Oil Spill Conference, IOSC 2005*, p. 1023, 2005.

[16] M. A. Abdullah, A. U. Rahmah, and Z. Man, "Physicochemical and sorption characteristics of Malaysian Ceiba pentandra (L.) Gaertn. as a natural oil sorbent," *Journal of Hazardous Materials*, vol. 177, no. 1–3, pp. 683–691, 2010.

[17] Y. Cui, G. Xu, and Y. Liu, "Oil sorption mechanism and capability of cattail fiber assembly," *Journal of Industrial Textiles*, vol. 43, no. 3, pp. 330–337, 2014.

[18] T. Dong, G. Xu, and F. Wang, "Oil spill cleanup by structured natural sorbents made from cattail fibers," *Industrial Crops and Products*, vol. 76, pp. 25–33, 2015.

[19] S. Ibrahim, I. Fatimah, H. M. Ang, and S. Wang, "Adsorption of anionic dyes in aqueous solution using chemically modified barley straw," *Water Science and Technology*, vol.

62, no. 5, pp. 1177–1182, 2010.

[20] N. A. T. M. Husseien, A.A. Amer, and Azza El-Maghraby, "Experimental Investigation of Thermal Modification Influence on Sorption Qualities of Barley Straw," *Journal Applied Sciences Research,* vol. 4, no. 6, pp. 652-657, 2008.

[21] Z. Wang, J. Li, J. P. Barford, K. Hellgradt, and G. Mckay, "A comparison of chemical treatment methods for the preparation of rice husk cellulosic fibers," *International Journal of Environmental & Agriculture Research*, vol. 2, no. 1, pp. 2454–1850, 2016.

[22] K. K. Kudaybergenov, E. K. Ongarbayev, and Z. A. Mansurov, "Petroleum sorption by thermally treated rice husks derived from agricultural byproducts," *Eurasian Chemico-Technological Journal*, vol. 15, no. 1, pp. 57–66, 2013.

[23] M. Husseien, A. A. Amer, A. El-Maghraby, and N. A. Taha, "Availability of barley straw application on oil spill clean up," *International Journal of Environmental Science and Technology,* vol. 6, no. 1, pp. 123–130, 2009.

[24] R. Behnood, B. Anvaripour, N. Jaafarzade, and H. Fard, "Application of natural sorbents in crude oil adsorption," *Iranian Journal Oil & Gas Science and Technology,* vol. 2, no. 4, pp. 1–11, 2013.

[25] G. Alaa El-Din, A. A. Amer, G. Malsh, and M. Hussein, "Study on the use of banana peels for oil spill removal," *Alexandria Engineering Journal*, vol. 57, no. 3, pp. 2061–2068, 2018.

[26] J. Zou, W. Chai, X. Liu, B. Li, X. Zhang, and T. Yin, "Magnetic pomelo peel as a new absorption material for oil-polluted water," *Desalination and Water Treatment*, vol. 57, no. 27, pp. 12536–12545, 2016.

[27] A. Osamor, and Z. Momoh, "An Evaluation of the Adsorptive Properties of Coconut Husk for Oil Spill Cleanup," *Institute of Research Engineers and Doctors*, pp. 33–37, 2015.

[28] N. A. Yusof, H. Mukhair, E. A. Malek, and F. Mohammad, “Esterified Coconut Coir by Fatty Acid Chloride as Biosorbent in Oil Spill Removal,” *BioResources*, vol. 10, no. 4, pp. 8025–8038, 2015.

[29] J. Idris, G. D. Eyu, A. M. Mansor, Z. Ahmad, and C. S. Chukwuekezie, “A preliminary study of biodegradable waste as sorbent material for oil-spill cleanup,” *The Scientific World Journal*, vol. 2014, 2014.

[30] S. M. Sidik, A. A. Jalil, S. Triwahyono, S. H. Adam, M. A. H. Satar, and B. H. Hameed, “Modified oil palm leaves adsorbent with enhanced hydrophobicity for crude oil removal,” *Chemical Engineering Journal*, vol. 203, pp. 9–18, 2012.

[31] S. Viju, G. Thilagavathi, B. Vignesh, and R. Brindha, “Oil sorption behavior of acetylated nettle fiber,” *Journal of the Textile Institute*, vol. 110, no. 10, pp. 1415–1423, 2019.

[32] S. Han, Q. Sun, H. Zheng, J. Li, and C. Jin, “Green and facile fabrication of carbon aerogels from cellulose-based waste newspaper for solving organic pollution,” *Carbohydrate Polymers*, vol. 136, pp. 95–100, 2016.

[33] H. Bi, X. Huang, X. Wu, X. Cao, C. Tan, Z. Yin, X. Lu, L. Sun, and H. Zhang, “Carbon microbelt aerogel prepared by waste paper: An efficient and recyclable sorbent for oils and organic solvents,” *Small*, vol. 10, no. 17, pp. 3544–3550, 2014.

[34] J. Feng, S. T. Nguyen, Z. Fan, and H. M. Duong, “Advanced fabrication and oil absorption properties of super-hydrophobic recycled cellulose aerogels,” *Chemical Engineering Journal*, vol. 270, pp. 168–175, 2015.

[35] A. O. Ifelebuegu, T. V. Anh Nguyen, P. Ukotije-Ikwut, and Z. Momoh “Liquid-phase sorption characteristics of human hair as a natural oil spill sorbent,” *Journal of Environmental Chemical Engineering*, vol. 3, no. 2, 2015.

[36] N. Adhithya, M. Goel, and A. Das, “Use of bamboo fiber in oil water separation,”

International Journal of Civil Engineering and Technology, vol. 8, no. 6, pp. 925–931, 2017.

[37] A. O. Ifelebuegu, J. E. Ukpebor, A. U. Ahukannah, E. O. Nnadi, and S. C. Theophilus, "Environmental effects of crude oil spill on the physicochemical and hydrobiological characteristics of the Nun River, Niger Delta," *Environmental Monitoring and Assessment*, vol. 189, no. 4, 2017.

[38] A. Célino, S. Fréour, F. Jacquemin, and P. Casari, "The hygroscopic behavior of plant fibers: A review," *Frontiers in Chemistry*, vol. 1, pp. 1–12, 2014.

[39] A. O. Ifelebuegu, and A. Johnson, "Nonconventional low-cost cellulose- and keratin-based biopolymeric sorbents for oil/water separation and spill cleanup: A review," *Critical Reviews in Environmental Science and Technology*, vol. 47, no. 11, pp. 964–1001, 2017.

[40]O. Carmody, R. Frost, Y. Xi, and S. Kokot, "Selected adsorbent materials for oil-spill cleanup," *Journal of Thermal Analysis and Calorimetry*, vol. 91, no. 3, pp. 809–816, 2008.

[41] G. Deschamps, H. Caruel, M.-E. Borredon, C. Bonnin, and C. Vignoles, "Oil Removal from Water by Selective Sorption on Hydrophobic Cotton Fibers. 1. Study of Sorption Properties and Comparison with Other Cotton Fiber-Based Sorbents," *Environmental Science & Technology*, vol. 37, no. 5, pp. 1013–1015, 2003.

[42] M. Hussein, A. A. Amer, and I. I. Sawsan, "Heavy oil spill cleanup using law grade raw cotton fibers: Trial for practical application," *Journal of Petroleum Technology and Alternative Fuels*, vol. 2, no.8, pp. 132–140, 2011.

[43] G. J. Peterson, S. G. Bajwa, and D. S. Bajwa, "Oil sorption of non-woven biological mats," *2016 American Society of Agricultural and Biological Engineers Annual International Meeting*, 2016.

[44] Z. Wang, J. P. Barford, C. W. Hui, and G. McKay, “Kinetic and equilibrium studies of hydrophilic and hydrophobic rice husk cellulosic fibers used as oil spill sorbents,” *Chemical Engineering Journal*, vol. 281, pp. 961–969, 2015.

[45] B. Wang, R. Karthikeyan, X. Y. Lu, J. Xuan, and M. K. H. Leung, “Hollow carbon fibers derived from natural cotton as effective sorbents for oil spill cleanup,” *Industrial and Engineering Chemistry Research*, vol. 52, no. 51, pp. 18251–18261, 2013.

[46] N. T. Hoai, N. N. Sang, and T. D. Hoang, “Oil Spill Cleanup using Stearic-acid-modified Natural Cotton,” *Journal of Materials and Environmental Science*, vol. 7, no. 7, pp. 2498–2504, 2016.

[47] J. Gale, “History of hemp,” *Textiles magazine*, vol. 23, no. 3, pp. 16–17, 1994.

[48] R. E. Schultes, “The Great Book of Hemp: The Complete Guide to the Environmental, Commercial and Medicinal Uses of the World’s Most Extraordinary Plant,” *Environmental Conservation*, vol. 23, no. 3, pp. 280–280, 1996.

[49] M. A. Fuqua, S. Huo, and C. A. Ulven, “Natural fiber reinforce composites,” *Polymer Reviews*, vol. 52, no. 3, pp. 259-320, 2012.

[50] A. Komuraiah, N. S. Kumar, and B. D. Prasad, “Chemical Composition of Natural Fibers and its Influence on their Mechanical Properties,” *Mechanics of Composite Materials*, vol. 50, no. 3, pp. 359–376, 2014.

[51] H. R. Kymäläinen, M. Koivula, R. Kuisma, A. M. Sjöberg, and A. Pehkonen, “Technologically indicative properties of straw fractions of flax, linseed (Linum usitatissimum L.) and fibre hemp (Cannabis sativa L.),” *Bioresource Technology*, vol. 94, no. 1, pp. 57–63, 2004.

[52] G. Buschle-Diller, C. Fanter, and F. Loth, “Structural Changes in Hemp Fibers as a Result of Enzymatic Hydrolysis with Mixed Enzyme Systems,” *Textile Research Journal*, vol. 69, no. 4, pp. 244–251, 1999.

[53] K. Hori, M. E. Flavier, S. Kuga, T. B. T. Lam, and K. Iiyama, “Excellent oil absorbent kapok [Ceiba pentandra (L.) Gaertn.] fiber: Fiber structure, chemical characteristics, and application,” *Journal of Wood Science*, vol. 46, no. 5, pp. 401–404, 2000.

[54] T. T. Lim, and X. Huang, “Evaluation of kapok (Ceiba pentandra (L.) Gaertn.) as a natural hollow hydrophobic-oleophilic fibrous sorbent for oil spill cleanup,” *Chemosphere*, vol. 66, no. 5, pp. 955–963, 2007.

[55] N. Ali, M. El-Harbawi, A. A. Jabal, and C. Y. Yin, “Characteristics and oil sorption effectiveness of kapok fibre, sugarcane bagasse and rice husks: Oil removal suitability matrix,” *Environmental Technology*, vol. 33, no. 4, pp. 481–486, 2012.

[56] S. Cao, T. Dong, G. Xu, and F. Wang, “Oil Spill Cleanup by Hydrophobic Natural Fibers,” *Journal of Natural Fibers*, vol. 14, no. 5, pp. 727-735, 2017.

[57] T. Dong, F. Wang, and G. Xu, “Sorption kinetics and mechanism of various oils into kapok assembly”, *Marine Pollution Bulletin*, vol. 91, no. 1, pp. 230–237, 2015.

[58] J. Wang, Y. Zheng, and A. Wang, “Investigation of acetylated kapok fibers on the sorption of oil in water,” *Journal of Environmental Sciences (China)*, vol. 25, no. 2, pp. 246–253, 2013.

[59] T. Dong, S. Cao, and G. Xu, “Highly efficient and recyclable depth filtrating system using structured kapok filters for oil removal and recovery from wastewater,” *Journal of Hazardous Materials*, vol. 321, pp. 859–867, 2017.

[60] S. Meiwu, X. Hong, and Y. Weidong, “The Fine Structure of the Kapok Fiber,” *Textile Research Journal*, vol. 80, no. 2, pp. 159–165, 2010.

[61] B. D. Cassie, A. B. D. Cassie, and S. Baxter, “Of porous surfaces,” *Transactions of the Faraday Society*, vol. 40, no. 5, pp. 546–551, 1944.

[62] A. Bayat, S. F. Aghamiri, A. Moheb, and G. R. Vakili-Nezhaad, “Oil spill cleanup from sea water by sorbent materials,” *Chemical Engineering and Technology*, vol. 28, no. 12,

pp. 1525–1528, 2005.

[63] C. J. Nederveen, “Absorption of liquid in highly porous nonwovens,” *Tappi Journal*, vol. 77, no. 12, pp. 174–180, 1994.

[64] M. Seddighi, and S. M. Hejazi, “Water-oil separation performance of technical textiles used for marine pollution disasters,” *Marine Pollution Bulletin*, vol. 96, no. 1-2, pp. 286–293, 2015.

[65] R. Asadpour, N. Sapari, Z. Tuan, H. Jusoh, A. Riahi, and O. Uka, “Application of sorbent materials in oil spill management: a review,” *Casp J Appl Sci Res*, vol. 2, no. 2, pp. 46–58, 2013.

[66] L. Feng, Z. Zhang, Z. Mai, Y. Ma, B. Liu, L. Jiang, and D. Zhu, “A super-hydrophobic and super-oleophilic coating mesh film for the separation of oil and water,” *Angewandte Chemie – International Edition*, vol. 43, no. 15, pp. 2012–2014, 2004.

[67] S. Wang, W. Qin, and Y. Dai, “Separation of oil phase from dilute oil/ water emulsion in confined space apparatus,” *Chinese Journal of Chemical Engineering*, vol, 20, no. 2, pp. 239–245, 2012.

[68] L. Zhang, Z. Zhang, and P. Wang, “Smart surfaces with switchable superoleophilicity and superoleophobicity in aqueous media: Toward controllable oil/water separation,” *NPG Asia Materials*, vol. 4, no. 2, 2012.

[69] M. Neznakomova, S. Boteva, L. Tzankov, and M. Elhag, “Non-woven Textile Materials from Waste Fibers for Cleanup of Waters Polluted with Petroleum and Oil Products,” *Earth Systems and Environment*, vol. 2, no. 2, pp. 413–420, 2018.

[70] E. E. Sirotkina, and L. Y. Novoselova, “Materials for adsorption purification of water from petroleum and oil products,” *Chemistry for Sustainable Development*, vol. 13, no. 3, pp. 359-375, 2005.

[71] F. T. Wallenberger, J. C. Watson, and H. Li, “Glass Fibers,” *ASM International*, vol. 21, pp. 27-34, 2001.

[72] F.T. Wallenberger, “Structural Silicate and Silica Glass Fibers,” *Advanced Inorganic Fibers*, Springer, Boston, MA, pp. 129–168, 2000.

[73] A. A. R. Amer, M. M. A. B. Abdullah, L. Y. Ming, and M. F. M. Tahir, “Performance and properties of glass fiber and its utilization in concrete-A review,” *AIP Publishing LLC*, vol. 2030, no. 1, pp. 020296, 2018.

[74] D. Hartman, and M. E. Greenwood, D. M. Miller, “High strength glass fibers,” *Agy*, pp. 1–11, 1996.

[75] C. Shin, and G. G. Chase, “Separation of water-in-oil emulsions using glass fiber media augmented with polymer nanofibers,” *Journal of Dispersion Science and Technology*, vol. 27, no. 4, pp. 517–522, 2006.

[76] Y. Akagi, K. Okada, T. Dote, and N. Yoshioka, “Separation of oil from oil-In-water mixture by glass fiber beds,” *Journal of Chemical Engineering of Japan*, vol. 21, no. 5, pp. 457–462, 1988.

[77] F. Rebelein, and E. Blass, “Separation of micro-dispersions in fibre-beds,” *Filtration and Separation*, vol. 27, no. 5, pp. 360–363, 1990.

[78] S. Kulkarni, U. Patel, and G. Chase, “Layered hydrophilic/hydrophobic fiber media for water-in-oil coalescence,” *Separation and Purification Technology*, vol. 85, pp. 157–164, 2012.

[79] K. Moorthy, “Effect of surface energy of fibers on coalescence filteration,” Electronic Thesis or Dissertation, *The University of Akron*, 2007.

[80] R. Magiera, and E. Blass, “Separation of liquid-liquid dispersions by flow through fibre beds,” *Filtration and Separation*, vol. 34, no. 4, pp. 369–376, 1997.

[81] S. S. Sareen, P. M. Rose, R. C. Gudesen, and R. C. Kintner, “Coalescence in fibrous beds,” *AIChE Journal*, vol. 12, no. 6, pp. 1045–1050, 1966.

[82] R. N. Hazlett, “Fibrous bed coalescence of water: Steps in the Coalescence Process,” *Industrial and Engineering Chemistry Fundamentals*, vol. 8, no. 4, pp. 625–632, 1969.

[83] H. Speth, A. Pfennig, M. Chatterjee, and H. Franken, “Coalescence of secondary dispersions in fiber beds,” *Separation and Purification Technology*, vol. 29, no. 2, pp. 113–119, 2002.

[84] R. M. Š. Sokolović, T. J. Vulić, and S. M. Sokolović, “Effect of bed length on steady-state coalescence of oil-in-water emulsion,” *Separation and Purification Technology*, vol. 56, no. 1, pp. 79–84, 2007.

[85] S. Basu, “A study on effect of wetting on mechanism of coalescence in a model coalesce,” *Journal of Colloid and Interface Science*, vol. 159, no. 1, pp. 68–76, 1993.

[86] C. Shin, G.G. Chase, and D.H. Renekar, “The effect of nanofibers on liquid-liquid coalescence filtration performance,” *AIChE Journal*, vol. 51, no. 12, pp. 3109–3113, 2005.

[87] P. K. Vagholkar, “Nylon (Chemistry, Properties and Uses),” *International Journal of Scientific Research*, vol. 5, pp. 4–7, 2016.

[88] R. A. Ortega, E. S. Carter, and A. E. Ortega, “Nylon 6,6 nonwoven fabric separates oil contaminates from oil-in-water emulsions,” *PLoS ONE*, vol. 11, no. 7, 2016.

[89] Nexant, “Nylon 6 and Nylon 6,6 Process Technology, Production Costs, Regional Supply/Demand Forecasts, and Economic Comparison of Alternative Production Routes,” Report Abstract, *The ChemSystems Process Evaluation/Research Planning (PERP) program*, 2009.

[90] J. Du, L. Zhang, J. Dong, Y. Li, C. Xu, and W. Gao, “Preparation of hydrophobic nylon fabric,” *Journal of Engineered Fibers and Fabrics*, vol. 11, no. 1, pp. 31–37, 2016.

[91] A. E. Ortega, J. T. Walker, W. W. Whitfield, and J. Bostwick, “Materials and methods for removing oil from bodies of water,” *U.S. Patent Application No. 12/787,987*, 2011.

[92] A. R. De Anda, L. A. Fillot, S. Rossi, D. Long, and P. Sotta, “Infleuence of the sorption of polar and non-polar solvents on the glass transition temperature of polyamide 6,6 amorphous phase,” *Polymer Engineering and Science*, vol. 51, no. 11, pp. 2129–2135, 2011.

[93] M. Singh, C. Singh, and D. Gangascharyulu,“Modelling for flow through unsaturated porous media with constant and variable density conditions using local thermal equilibrium Modeling for Flow through Unsaturated Porous Media with Constant and Variable Density Conditions using Local Thermal Equilibrium,” *International Conference on Advances in Emerging Technology*, 2016.

[94] B. D. Zdravkov, J. J. Čermák, M. Šefara, and J. Janků, “Pore classification in the characterization of porous materials: A perspective,” *Central European Journal of Chemistry*, vol. 5, no. 2, pp. 385-395, 2007.

[95] L. M. Anovitz, and D. R. Cole, “Characterization and analysis of porosity and pore structures,”, *Reviews in Mineralogy and Geochemistry*, vol. 80, no. 1, pp. 61–164, 2015.

[96] K. Kaneko, “Determination of pore size and pore size distribution. 1. Adsorbents and catalysts,” *Journal of Membrane Science*, vol. 96**,** pp. 59–89, 1994.

[97] International Union of Pure and Applied Chemistry Physical Chemistry Division Commission on Colloid and Surface Chemistry, Subcommittee on Characterization of Porous Solids: “Recommendations for the characterization of porous solids (TechnicalReport),” *Pure Appl. Chem.*,vol. 66, no. 8, pp. 1739–1758, 1994.

[98] S. P. Rigby, R. S. Fletcher, and S. N. Riley, “Characterisation of porous solids using integrated nitrogen sorption and mercury porosimetry,” *Chemical Engineering Science*, vol. 59, no. 1, pp. 41–51, 2004.

[99] C. L. Mangun, M. A. Daley, R. D. Braatz, and J. Economy, “Effect of pore size on adsorption of hydrocarbons in phenolic-based activated carbon fibers,” *Carbon*, vol. 36, no. 1-2, pp. 123–129, 1998.

[100] N. Liu, Y. Chen, F. Lu, Y. Cao, Z. Xue, K. Li, and L. Feng, “Straightforward Oxidation of a Copper Substrate Produces an Underwater Superoleophobic Mesh for Oil/Water Separation,” *ChemPhysChem*, vol. 14, no. 15, pp. 3489–3494, 2013.

[101] T. Zhao, D. Zhang, C. Yu, and L. Jiang, “Facile fabrication of a polyeyhylene mesh for oil/water separation in a complex environment,” *ACS Applied Materials & Interfaces*, vol. 8, no. 36, pp. 24186–24191, 2016.

[102] N. Liu, Y. Cao, X. Lin, Y. Chen, L. Feng, and Y. Wei, “A Facile Solvent-Manipulated Mesh for Reversible Oil / Water Separation,” *ACS Applied Materials & Interfaces*, vol. 6, no. 15, pp. 28–33, 2014.

[103] P. Yin, T. Yao, Y. Wu, L. Zheng, Y. Lin, W. Liu, H. Ju, J. Zhu, X. Hong, Z. Deng, G. Zhou, S. Wei, and Y. Li, “Single Cobalt Atoms with Precise N-Coordination as Superior Oxygen Reduction Reaction Catalysts,” *Angewandte Chemie - International Edition*, vol. 55, no. 36, pp. 10800–10805, 2016.

[104] B. Wang, and Z. Guo, “PH-responsive bidirectional oil-water separation material,” *Chemical Communications*, vol. 49, no. 82, pp. 9416–9418, 2013.

[105] L. Wang, K. Pan, L. Li, and B. Cao, “Surface hydrophilicity and structure of hydrophilic modified PVDF membrane by nonsolvent induced phase separation and their effect on oil/water separation performance,” *Industrial & Engineering Chemistry Research*, vol. 53, no. 15, pp. 6401-6408, 2014.

[106] S. Yanlong, Y. Wu, F. Xiaojuan, W. Yongsheng, and Y. Guoren, "Applied Surface Science Fabrication of superhydrophobic-superoleophilic copper mesh via thermal oxidation and its application in oil – water separation," *Applied Surface Science*, vol. 367, pp. 493–499, 2016.

[107] Y. Cao, X. Zhang, L. Tao, K. Li, Z. Xue, L. Feng, and Y. Wei, "Mussel-Inspired Chemistry and Michael Addition Reaction for Efficient Oil/Water Separation," *ACS Applied Materials & Interfaces*, vol. 5, no. 10, pp. 4438-4442, 2013.

[108] E. W. Washburn, "The dynamics of capillary flow," *Physical Review*, vol. 17, no. 3, pp. 273–283, 1921.

[109] G. J. Dunderdale, C. Urata, T. Sato, M. W. England, and A. Hozumi, "Continuous, High-Speed, and Efficient Oil/Water Separation using Meshes with Antagonistic Wetting Properties," *ACS Applied Materials & Interfaces*, vol. 7, no. 34, pp. 18915–18919, 2015.

[110] I. M. Hauner, A. Deblais, J. K. Beattie, H. Kellay, and D. Bonn, "The Dynamic Surface Tension of Water," *Journal of Physical Chemistry Letters*, vol. 8, no. 7, pp. 1599–1603, 2017.

[111] L. Feng, Z. Zhang, Z. Mai, Y. Ma, B. Liu, L. Jiang, D. Zhu, "A super-hydrophobic and super-oleophilic coating mesh film for the separation of oil and water," *Angewandte Chemie – International Edition*, vol. 43, no. 15, pp. 2012–2014, 2004.

[112] J. S. A. Cortez, B. I. Kharisov, T. E. S. Quezada, and T. C. H. García, "Micro- and nanoporous materials capable of absorbing solvents and oils reversibly: the state of the art," *Petroleum Science*, vol. 14, no. 1, pp. 84–104, 2017.

[113] Y. Yang, Z. Liu, J. Huang, and C. Wang, "Multifunctional, robust sponges by a simple adsorption - Combustion method", *Journal of Materials Chemistry A*, vol. 3, no. 11, pp. 5875–5881, 2015.

[114] N. R. Morrow, and G. Mason, "Recovery of oil by spontaneous imbibition," *Current Opinion in Colloid and Interface Science*, vol. 6, no. 4, pp. 321–337, 2001.

[115] J. Hyväluoma, P. Raiskinmäki, A. Jäsberg, A. Koponen, M. Kataja, and J. Timonen, "Simulation of liquid penetration in paper," *Physycal Review E – Statistical, Nonlinear, and Soft Matter Physics*, vol. 73, no. 3, 2006.

[116] J. M. Bell, and F. K. Cameron, "The flow of liquids through capillary spaces," *The Journal of Physical Chemistry*, vol. 10, no. 8, pp. 658-674, 1905.

[117] R. Lucas, "Rate of capillary ascension of liquids," *Kolloid Z*, vol. 23, no.15, pp. 15-22, 1918.

[118] J. Szekely, A. W. Neumann, and Y. K. Chuang, "The rate of capillary penetration and the applicability of the washburn equation," *Journal of Colloid and Interface Science*, vol. 35, no. 2, pp. 273–278, 1971.

[119] J. Soriano, A. Mercier, R. Planet, A. Hernández-Machado, M. A. Rodríguez, and J. Ortín, "Anomalous roughening of viscous fluid fronts in spontaneous imbibition," *Physical Review Letters*, vol. 95, no. 10, pp. 104501, 2005.

[120] Y. Xue, J. Markmann, H. Duan, J. Weissmüller, and P. Huber, "Switchable imbibition in nanoporous gold," *Nature Communications*, vol. 5, 2014.

[121] A. M. Miranda, I. L. Menezes-Sobrinho, and M. S. Couto, "Spontaneous imbibition experiment in newspaper sheets," *Physical Review Letters*, vol. 104, no. 8, 2010.

[122] S. Chwastiak, "A wicking method for measuring wetting properties of carbon yarns," *Journal of Colloid and Interface Science*, vol. 42, no. 2, pp. 298–309, 1973.

[123] F. M. Fowkes, "Role of Surface Active Agents in Wetting," *Journal of Physical Chemistry*, vol. 57, no. 1, pp. 98-103, 1953.

[124] J. G. Williams, C. E. M. Morris, and B. C. Ennis, "Liquid flow through aligned fiber beds," *Polymer Engineering & Science*, vol. 14, no. 6, pp 413-419, 1974.

[125] K. T. Hodgson, and J. C. Berg, "The effect of surfactants on wicking flow in fiber networks," *Journal of Colloid and Interface Science,* vol. 121, no. 1, pp. 22–31, 1988.

[126] Y. L. Hsieh, "Novel surface chemistry and geometric features of fibers: Regulation of liquid wetting and absorption," *Joint INDA-TAPPI Conference - INTC 2005: International Nonwovens Technical Conference*, pp. 369–374, 2005.

[127] D. Schuchadt, and J. Berg, "Liquid transport in composite cellulose-superabsorbent fiber networks," *Wood and Fiber Science,* vol. 23, no. 3, pp. 342–357, 1991.

[128] N. Mao, and S. J. Russell, "Capillary pressure and liquid wicking in three-dimensional nonwoven materials," *Journal of Applied Physics*, vol. 104, no. 3, 2008.

[129] B. Miller, "Critical evaluation of upward wicking tests," *International Nonwovens Journal*, vol. 9, no. 1, pp. 35–40, 2000.

[130] J. T. Jeong, "Slip boundary condition on an idealized porous wall," *Physics of Fluids*, vol. 13, no. 7, pp. 1884–1890, 2001.

[131] D. A. Lockington, and J. Y. Parlange, "Anomalous water absorption in porous materials," *Journal of Physics D: Applied Physics*, vol. 36, no. 6, pp. 760–767, 2003.

[132] P. A. C. Gane, C. J. Ridgway, and J. Schoelkopf, "Absorption Rate and Volume Dependency on the Complexity of Porous Network Structures," *Transport in Porous Media,* vol. 54, no. 1, pp. 79–106, 2004.

[133] K. Li, D. Zhang, H. Bian, C. Meng, and Y. Yang, "Criteria for applying the lucas-washburn law," *Scientific Reports*, vol. 5, pp. 14085, 2015.

[134] S. Ahadian, S. Moradian, F. Sharif, M. Amani Tehran, and M. Mohseni, "Prediction of time of capillary rise in porous media using Artificial Neural Network (ANN)," *Iranian Journal of Chemistry and Chemical Engineering,* vol. 26, no. 1, pp. 71–85, 2007.

[135] J. Niessner, S. Berg, and S. M. Hassanizadeh, “Comparison of Two-Phase Darcy’s Law with a Thermodynamically Consistent Approach,” *Transport in Porous Media*, vol. 88, no. 1, pp. 133–148, 2011.

[136] S. Whitaker, “Flow in porous media I: A theoretical derivation of Darcy’s law,” *Transport in Porous Media*, vol. 1, no. 1, pp. 3–25, 1986.

[137] J. Boussinesq, “Recherches théoriques sur l'écoulement des nappes d'eau infiltrées dans le sol et sur le débit des sources,” *Journal de Mathématiques Pures et Appliquées*, vol. *10*, pp. 5-78., 1904

[138] O. Emersleben, “Das Darcysche Filtergesetz,” *Physik. Z*, vol. *26*, pp. 601-610, 1925.

[139] M. Muskat, and H. G. Botset, “Flow of gas through porous materials,” *Physics*, vol. 1, no. 1, pp. 27-47, 1931.

[140] R. Masoodi, and K. M. Pillai, “Darcy’s Law-Based Model for Wicking in Paper-Like Swelling Porous Media,” *AIChE Journal*, vol. 56, no. 9, pp. 2257–2267, 2010.

[141] S. Mendez, E. M. Fenton, G. R. Gallegos, D. N. Petsev, S. S. Sibbett, H. A. Stone, Z. Yi, and G. P. Lopez, “Imbibition in Porous Membranes of Complex Shape: Quasi-Stationary Flow in Thin Rectangular Segments,” *Langmuir*, vol. 26, no. 2, pp. 1380–1385, 2010.

[142] E. Elizalde, R. Urteaga, and C. L. A. Berli, “Rational design of capillary-driven flows for paper-based microfluidics,” *Lab on a Chip*, vol. 15, no. 10, pp. 2173–2180, 2015.

[143] J. M. Huyghe, C. W. Oomens, and D. H. Van Campen, “Low Reynolds number steady state flow through a branching network of rigid vessels. II. A finite element mixture model,” *Biorheology*, vol. 26, no. 1, pp. 73–84, 1989.

[144] W. J. Vankan, J. M. Huyghe, J. D. Janssen, and A. Huson, “Poroelasticity of saturated solids with an application to blood perfusion,” *International Journal of Engineering Science*, vol. 34, no. 9, pp. 1019–1031, 1996.

[145] J. J. L. Higdon, “Multiphase flow in porous media,” *Journal of Fluid Mechanics*, vol. 730, pp. 1–4, 2013.

[146] J. C. Muccino, W. G. Gray, and L. A. Ferrand, “Toward an improved understanding of multiphase flow in porous media,” *Reviews of Geophysics*, vol. 36, no. 3, pp. 401–422, 1998.

[147] C. M. Marle, “On macroscopic equations governing multiphase flow with diffusion and chemical reactions in porous media,” *International Journal of Engineering Science*, vol. 20, no. 5, pp. 643–662, 1982.

[148] F. Kalaydjian, “A macroscopic description of multiphase flow in porous media involving spacetime evolution of fluid/fluid interface” *Transport in Porous Media*, vol. 2, no. 6, pp. 537–552, 1987.

[149] W. G. Gray, and C. T. Miller, “Thermodynamically constrained averaging theory approach for modeling flow and transport phenomena in porous medium systems: 1. Motivation and overview”, *Advances in Water Resources*, vol. 28, no. 2, pp. 161–180, 2005.

[150] R. M. Bowen, “Compressible porous media models by use of the theory of mixtures,” *International Journal of Engineering Science*, vol. 20, no. 6, pp. 697–735, 1982.

[151] J. E. Killough, “Reservoir simulation with history dependent saturation functions,” *Society of Petroleum Engineers AIM J*, vol. 16, no. 1, pp. 37-48, 1976.

[152] F. Stauffer, “Time dependence of the relations between capillary pressure, water content and conductivity during drainage of porous media,” *IAHR Symposium On scale effects in porous media, Thessaloniki, Greece*, vol. 29, pp. 3-35, 1978.

[153] M. Mirzaei, and D. B. Das, “Dynamic effects in capillary pressure-saturations relationships for two-phase flow in 3D porous media: Implications of micro-heterogeneities,” *Chemical Engineering Science*, vol. 62, no. 7, pp. 1927–1947, 2007.

[154] S. Manthey, S. M. Hassanizadeh, and R. Helmig, “Macro-scale dynamic effects in homogeneous and heterogeneous porous media,” *Transport in Porous Media*, vol. 58, no. 1-2, pp. 121–145, 2005.

[155] D. A. DiCarlo, “Modeling observed saturation overshoot with continuum additions to standard unsaturated theory,” *Advances in Water Resources*, vol. 28, no. 10, pp. 1021–1027, 2005.

[156] D. A. DiCarlo, “Experimental measurements of saturation overshoot on infiltration,” *Water Resources Research*, vol. 40, no. 4, 2004.

[157] S. Bottero, S. M. Hassanizadeh, P. J. Kleingeld, and A. Bezuijen, “Experimental study of dynamic capillary pressure effect in two-phase flow in porous media,” *Computational Methods in Water* Resources, pp. 18–22, 2006.

[158] M. Sefara, “Pore classification in the characterization of porous materials : A perspective,” vol. 5, no. 2, pp. 385–395, 2007.

[159] O. Ozkan, and H. Y. Erbil, “Interpreting contact angle results under air, water and oil for the same surfaces,” *Surface Topography: Metrology and Properties*, vol. 5 ,no. 2, pp. 024002, 2017.

[160] A. Patalano, F. Villalobos, P. Pena, E. Jauregui, C. Ozkan, and M. Ozkan, “Scaling sorbent materials for real oil-sorbing applications and environmental disasters,” *MRS Energy & Sustainability*, vol. 6, 2019.

[161] M. El Messiry, A. El Ouffy, and M. Issa, "Microcellulose particles for surface modification to enhance moisture management properties of polyester, and polyester/cotton blend fabrics," *Alexandria Engineering Journal*, vol. 54, no. 2, pp. 127-140, 2015.

[162] H. Chen, H. Cheng, Z. Jiang, D. Qin, Y. Yu, G. Tian, F. Lu, B. Fei, and G. Wang, "Contact angles of single bamboo fibers measured in different environments and compared with other plant fibers and bamboo strips," *BioResources*, vol. 8, no. 2, pp. 2827–2838, 2013.

[163] K. V. Van De Velde, and P. Kiekens, "Wettability and surface analysis of glass fibres," *Indian Journal of Fibre and Textile Research*, vol. 25, no. 1, pp. 8–13, 2000.

[164] S. Sair, A. Oushabi, A. Kammouni, O. Tanane, Y. Abboud, and A. El Bouari, "Mechanical and thermal conductivity properties of hemp fiber reinforced polyurethane composites," *Case Studies in Construction Materials*, vol. 8, pp. 203–212, 2018.

[165] R. Arrigo, N. T. Dintcheva, G. Nasillo, and E. Caponetti, "Polyamide/carbonaceous particles nanocomposites fibers: Morphology and performances," *Polymer Composites*, vol. 36, no.6, pp. 1020-1028, 2015.

[166] G. Jin, C. Torres-Verdín, and C. Lan, "Pore-level study of grain-shape effects on petrophysical properties of porous media," in *SPWLA 50th Annual Logging Symposium 2009*, 2009, pp. 1-13.

[167] J. W. S. Hearle, and J. T. Sparrow, "Mechanics of the extension of cotton fibers. I. Experimental studies of the effect of convolutions," *Journal of Applied Polymer Science*, vol. 24, no. 6, pp. 1465–1477, 1979.

[168] N. P. G. Suardana, Y. Piao, and J. K. Lim, "Mechanical properties of hemp fibers and hemp/pp composites: effects of chemical surface treatment," *Materials Physics and Mechanics*, vol. 11, no. 1, pp. 1-8, 2011.

[169] S. Soliman, S. Sant, J. W. Nichol, M. Khabiry, E. Traversa, and A. Khademhosseini, "Controlling the porosity of fibrous scaffolds by modulating the fiber diameter and packing density," *Journal of Biomedical Materials Research Part A*, vol. 96, no. 3, pp. 566-574, 2011.

[170] Q. F. Wei, R. R. Mather, A. F. Fotheringham, and R. D. Yang, "Evaluation of nonwoven polypropylene oil sorbents in marine oil-spill recovery," *Marine Pollution Bulletin*, vol. 46, no. 6, pp. 780–783, 2003.

[171] O. Hasanzadeh, "Collecting oil spill with natural sorbents from the sea surface," *New Technologies in Chemical and Petrochemical*, 1993.

[172] A. Aqsha, M. M. Tijani, B. Moghtaderi, and N. Mahinpey, "Catalytic pyrolysis of straw biomasses (wheat, flax, oat and barley) and the comparison of their product yields," *Journal of Analytical and Applied Pyrolysis*, vol. 125, pp. 201–208, 2017.

[173] E. Anuzyte, and V. Vaisis, "Natural oil sorbents modification methods for hydrophobicity improvement," *Energy Procedia*, vol. 147, pp. 295-300, 2018.

[174] H. M. Choi, H. J. Kwon, and J. P. Moreau, "Cotton Nonwovens as Oil Spill Cleanup Sorbents," *Textile Research* Journal, vol. 63, no. 4, pp. 211–218, 1993.

[175] J. Wang, Y. Zheng, A. Wang, "Effect of kapok fiber treated with various solvents on oil absorbency," *Industrial Crops and Products*, vol. 40, pp. 178–184, 2012.

[176] Y. lo Hsieh, "Liquid Transport in Fabric Structures," *Textile Research Journal*, vol. 65, no. 5, pp. 299–307, 1995.

[177] A. Hamraoui, and T. Nylander, "Analytical approach for the Lucas-Washburn equation," *Journal of Colloid and Interface Science*, vol. 250, pp. 415–421, 2002.

[178] E. Widiatmoko, and M. Abdullah, Khairurrijal, "A method to measure pore size distribution of porous materials using scanning electron microscopy images," *American Institute of Physics*, vol. 1284, no. 1, pp. 23–26, 2010.

Appendices

Appendix A

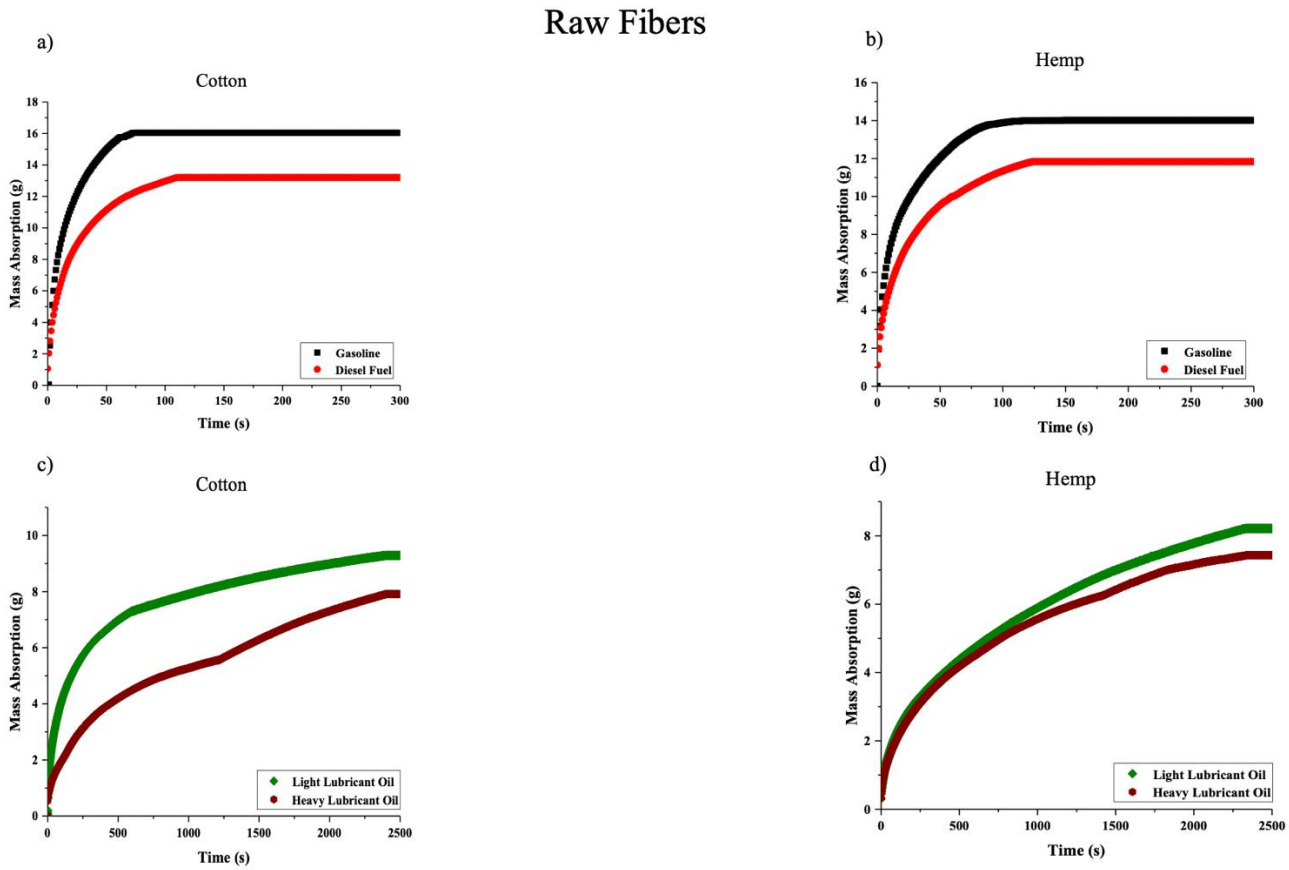

Figure A.1 Oil mass absorption for cotton and hemp in the first trial

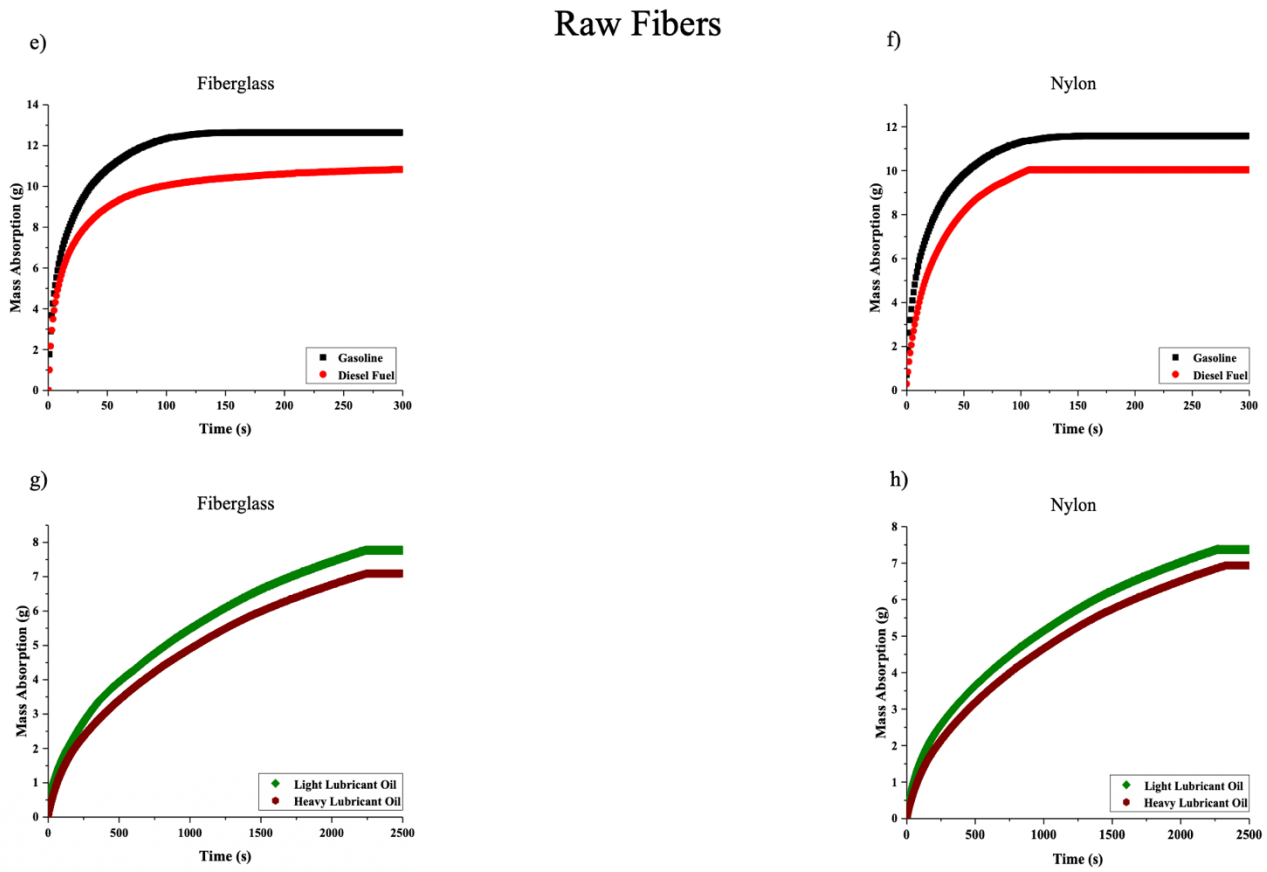

Figure A.2 Oil mass absorption for fiberglass and nylon in the first trial

Appendix B

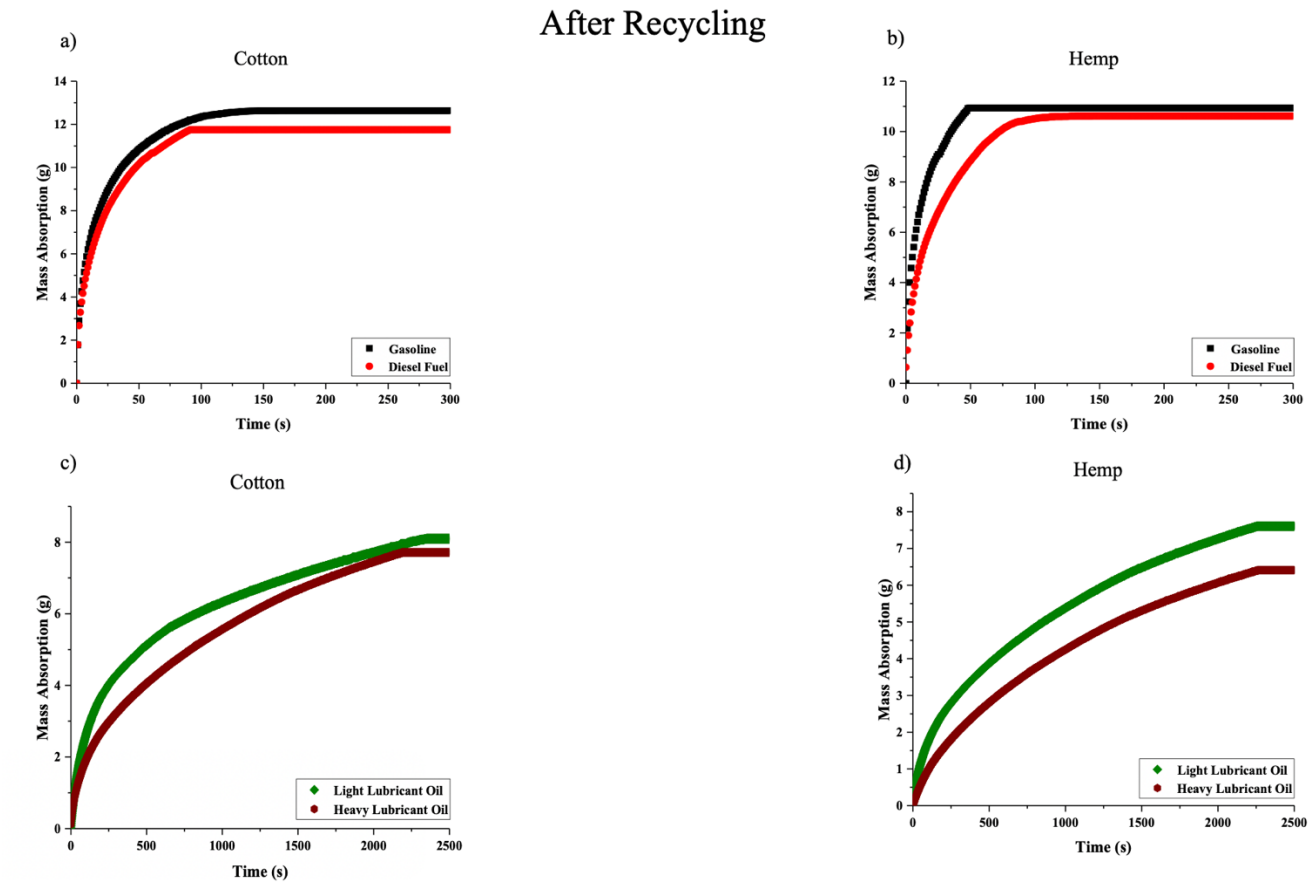

Figure B.1 Mass absorption of cotton and hemp with the oils in the reused method.

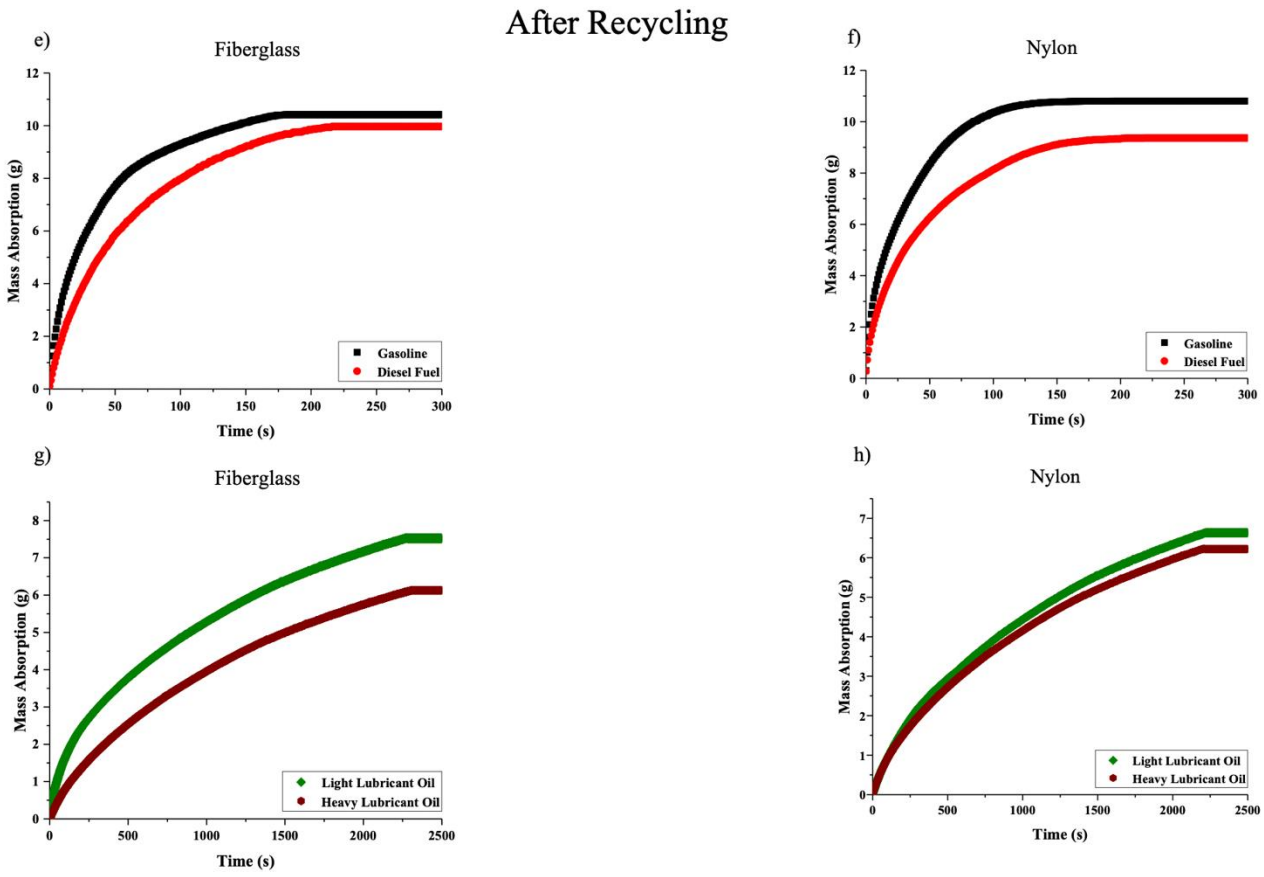

Figure B.2 Mass absorption of fiberglass and nylon with the oils in the reused method.

Appendix C

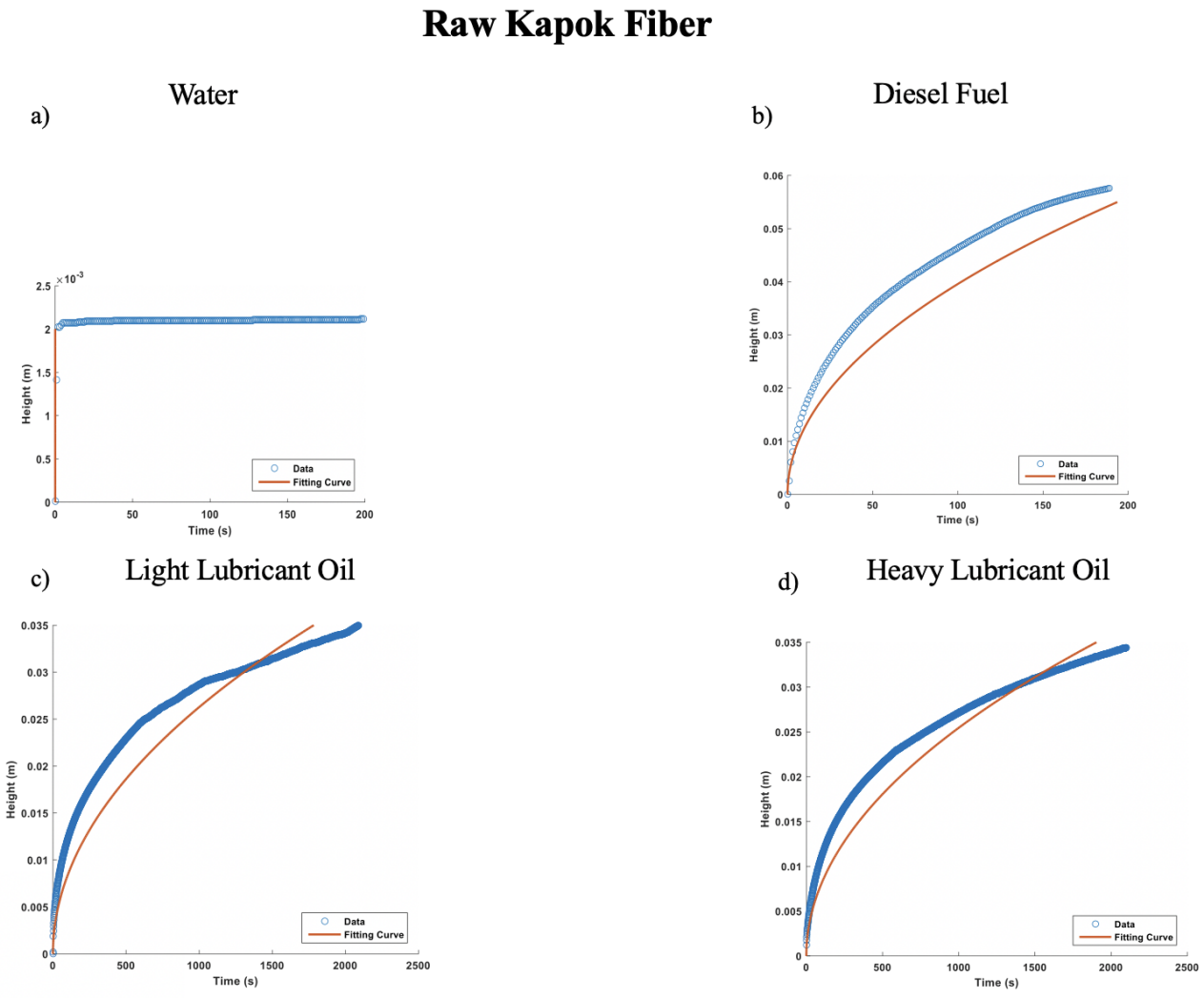

Figure C.1 Lucas-Washburn curves for kapok with water and different oils.

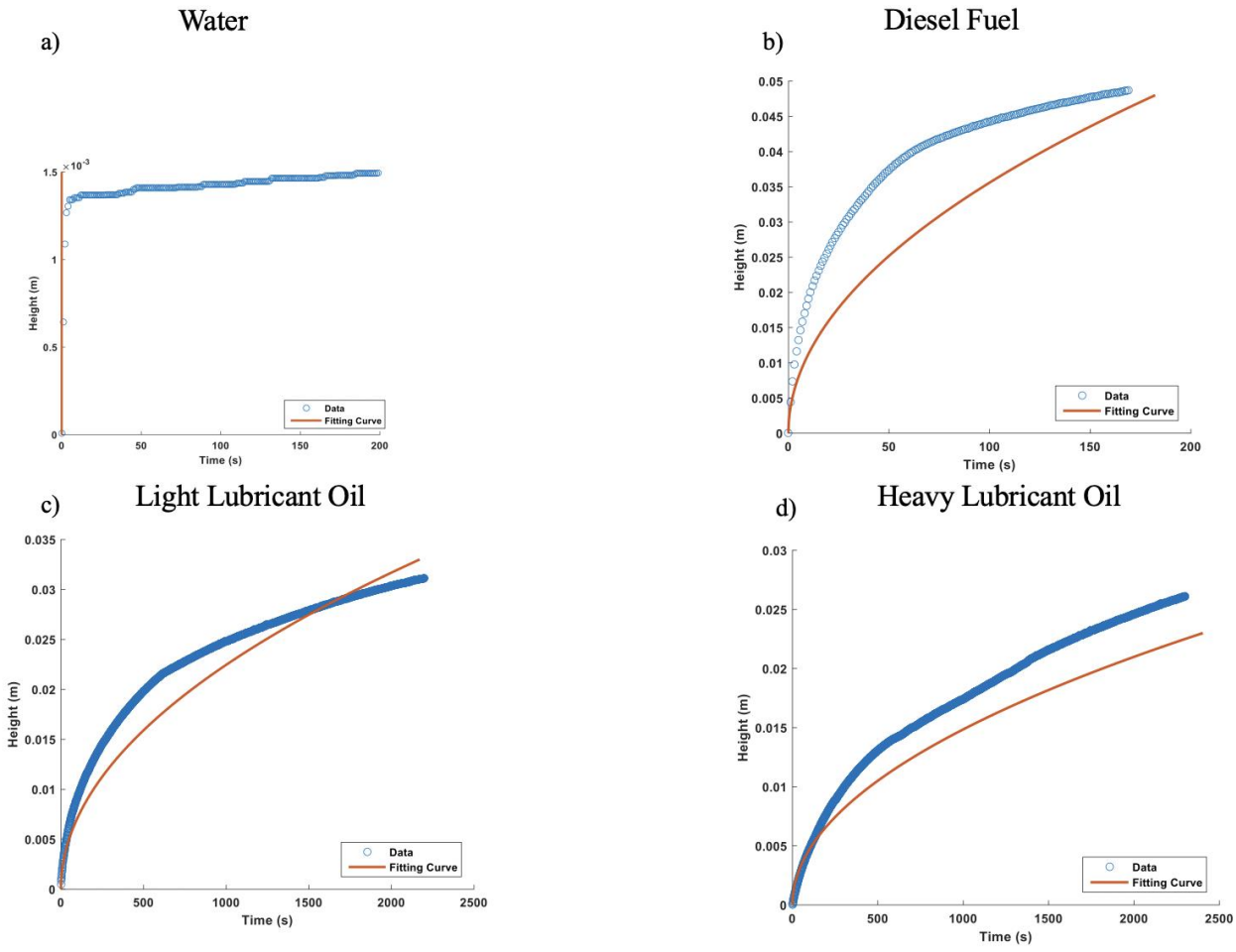

Figure C.2 Lucas-Washburn curves for kapok with water and different oils after recycling.

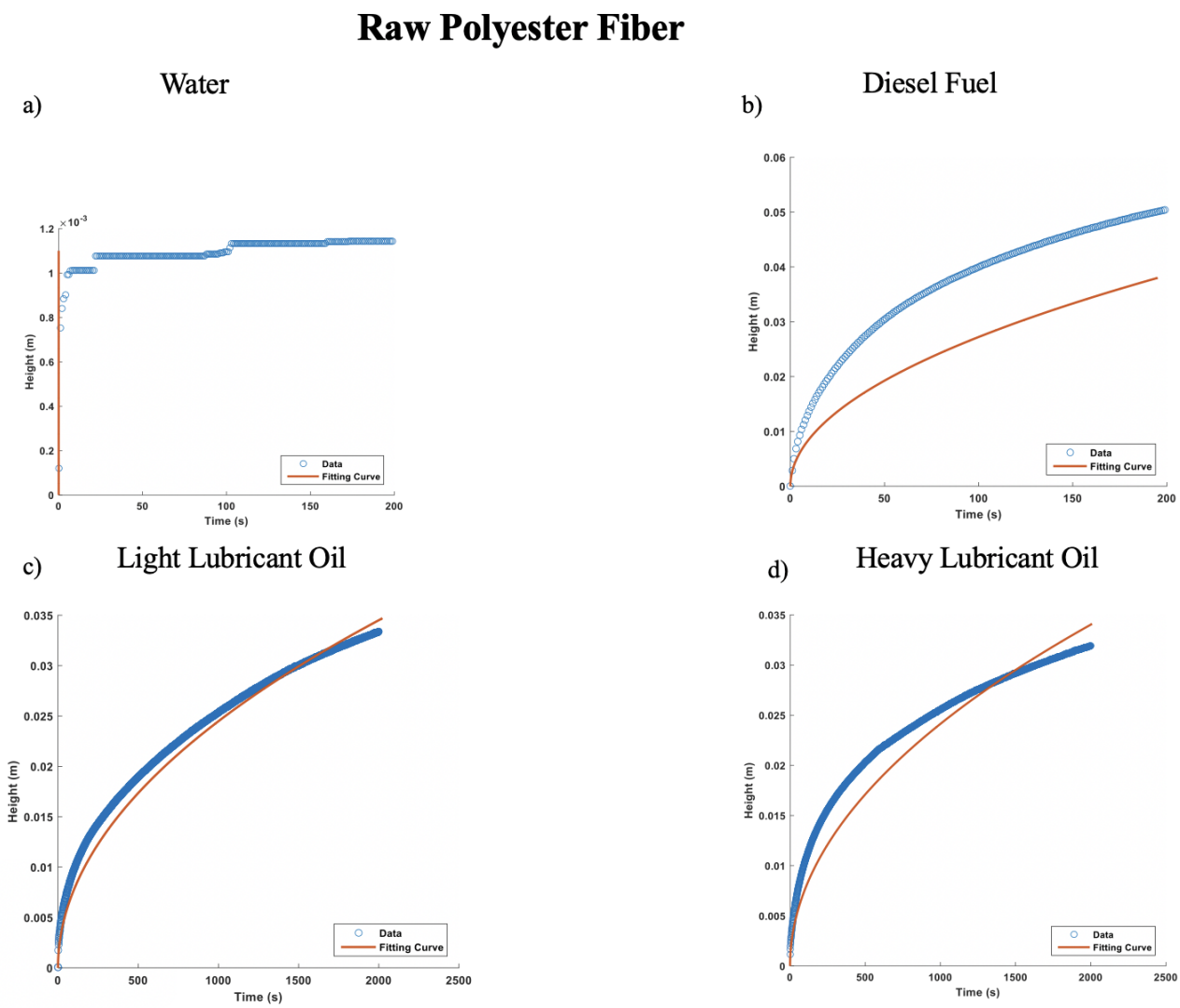

Figure C.3 Lucas-Washburn curves for polyester with water and different oils.

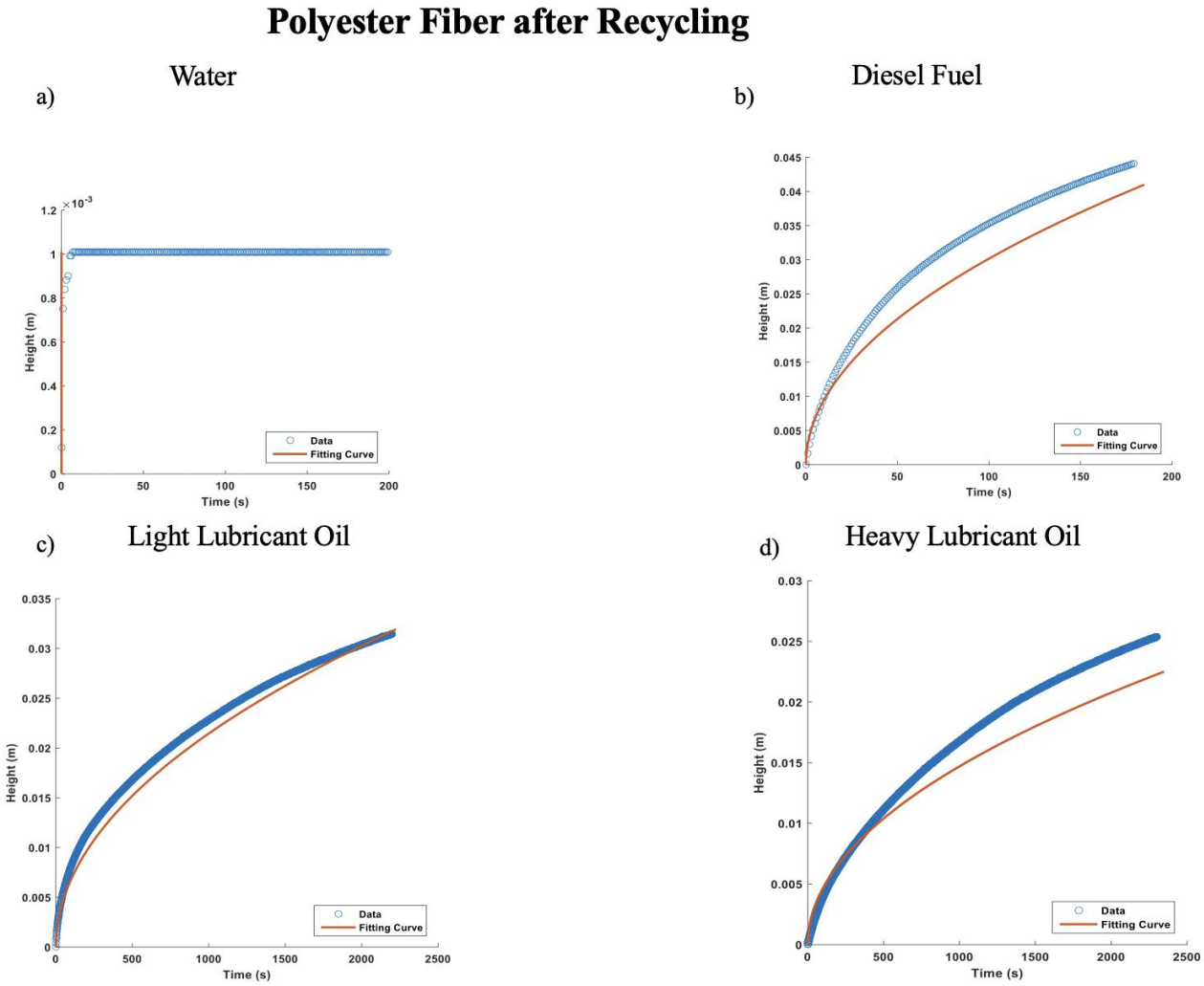

Figure C.4 Lucas-Washburn curves for polyester with different oils after recycling.

Appendix D

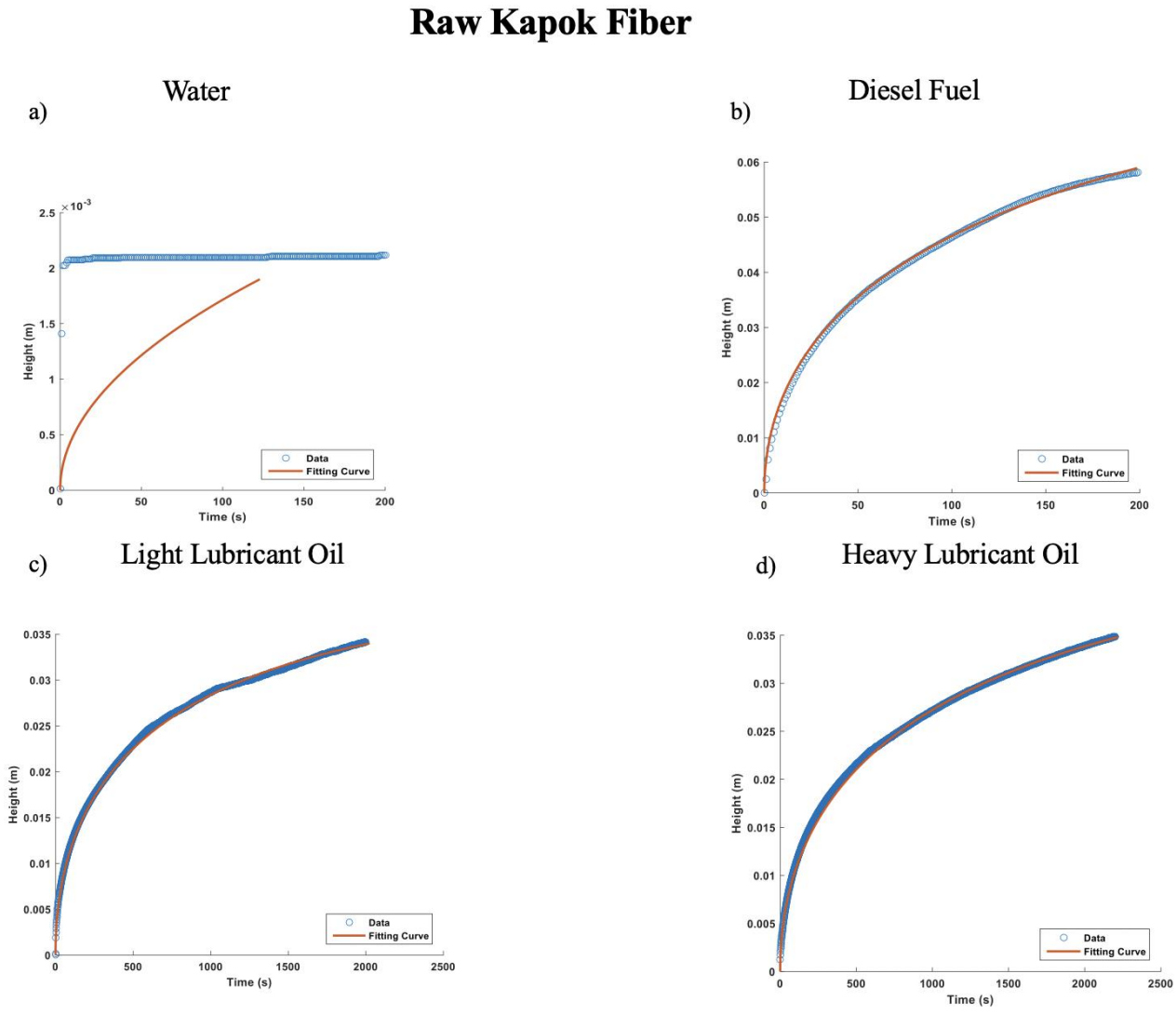

Figure D.1 Darcy-based law curves for kapok with water and different oils.

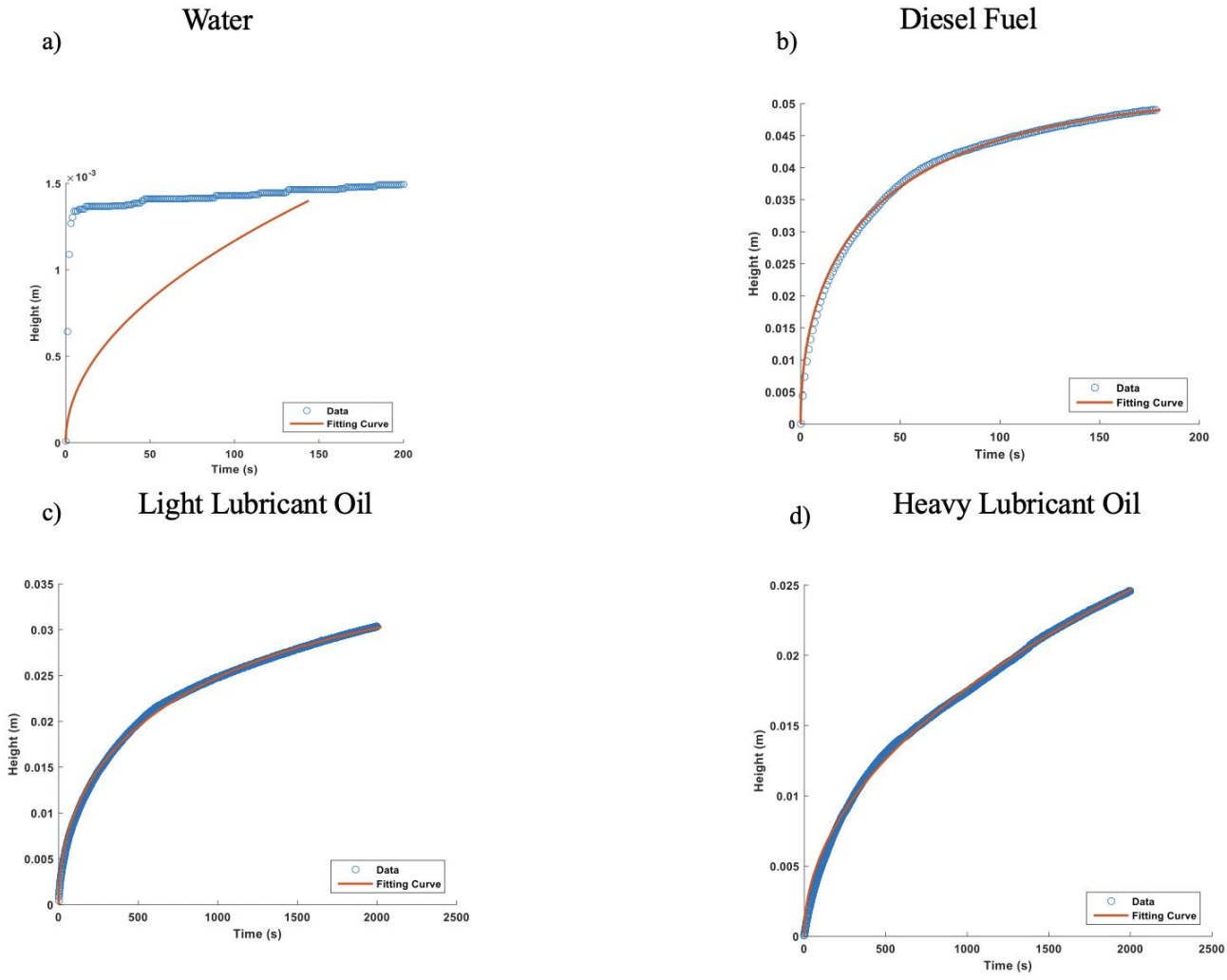

Figure D.2 Darcy-based law curves for kapok with water and different oils after recycling.

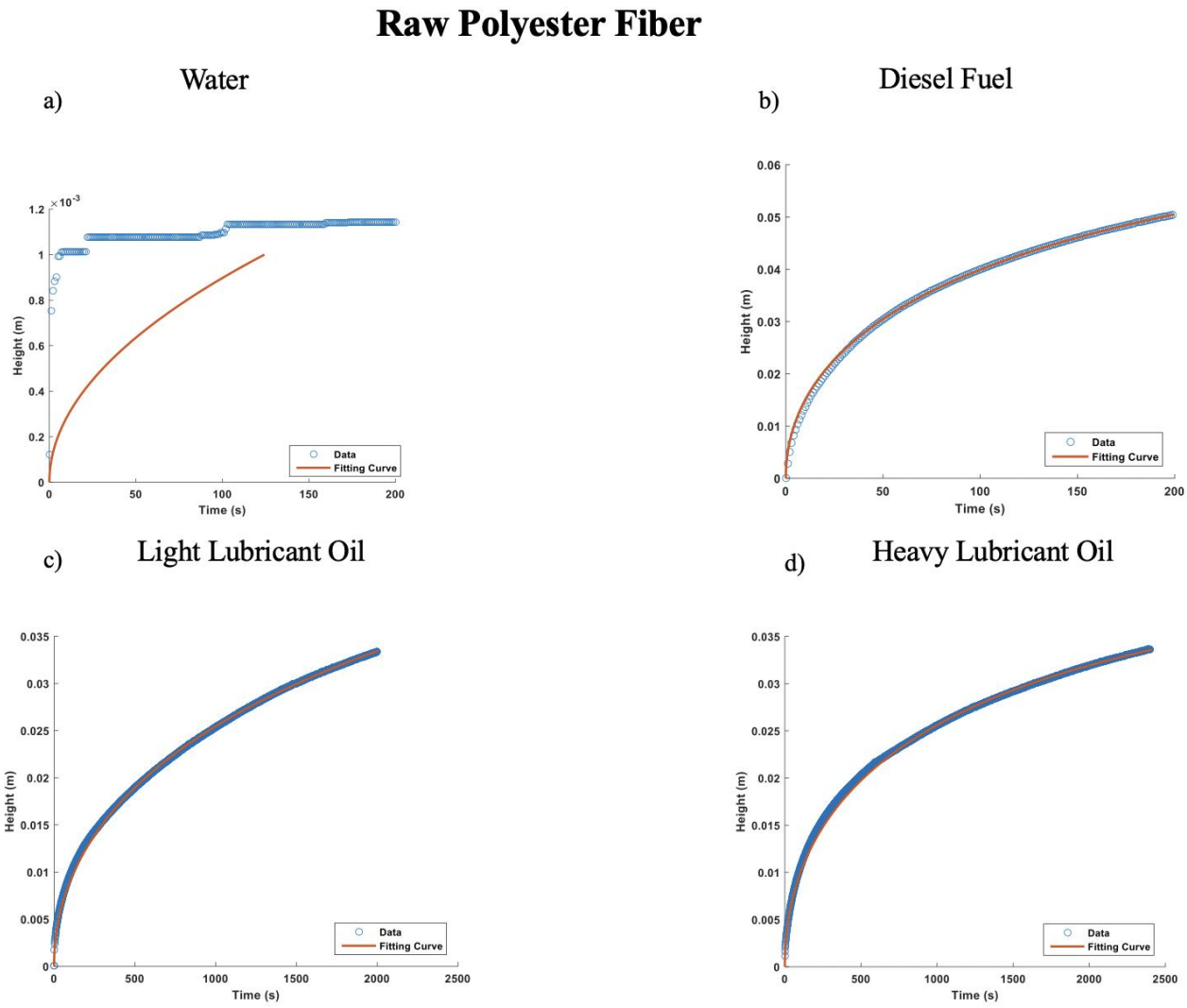

Figure D.3 Darcy-based law curves for polyester with water and different oils.

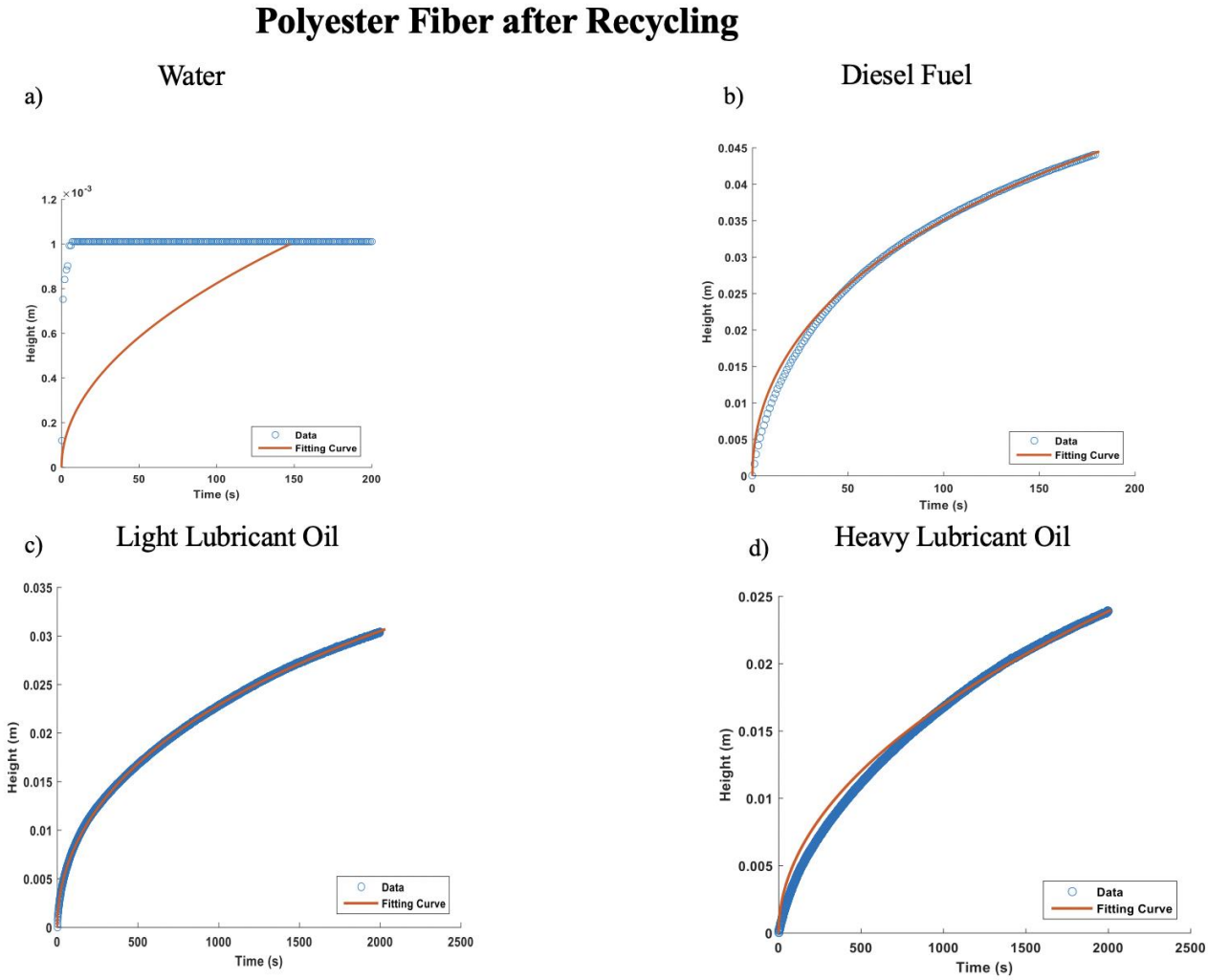

Figure D.4 Darcy-based law curves for polyester with water and different oils after recycling.

Appendix E

MATLAB Code for Lucas-Washburn model:

```
M = xlsread(Path);
tdata = M(:,1);
hfdata = M(:,2);
plot(tdata,hfdata)
%FUNCTION Fun = lsqcurvefit(@(x,hdata)
%Initial Guess:
a0 = 0.9e-6;eta = Oil Viscosity; gamma = Oil Surface Tension; theta = Oil Contact Angle; g
= Acceleration Gravity; rho = Oil Density; S = 2*gamma*cosd (theta)/rho/g; Rc = x;
A1 = 16*eta*gamma*cosd(theta)/(g^2)/(rho^2)/(Rc^3);A2 = log(beta./(beta - Rc*h)); A3 =
8*eta/g/rho/(Rc^2)*h; t = A1*A2 - A3; plot(t,h,'LineWidth',2); legend('data','Fitting Curve');
xlabel('Time (s)'); ylabel('Height (m)'); hold off;
```

Appendix F

MATLAB Code for Darcy-Based Model:

```
M = xlsread(Path);
tdata = M(:,1);
hfdata = M(:,2)
%FUNCTION Fun = lsqcurvefit(@(x,hdata) Darcy
(x,hdata),a0,hfdata(1:ndata),tdata(1:ndata));
%Initial Values:
a0 = [1.00 1000];
visc = Oil Viscosity; rho = Oil Density; g = Acceleration Gravity; phi = Porosity;
ps = bestx(2) %Suction Pressure; K = bestx(1) %Permeability;
A1 = 1e10*phi*visc/(rho^2)/(g^2)/K; A2 = ps*log(abs(ps./(ps-rho*g*h))); A3 = rho*g*h; t =
A1*(A2 - A3); plot(t,h,'LineWidth',2); legend('data','Fitting Curve'); xlabel('Time (s)');
ylabel('Height (m)'); hold off;
```

Appendix G

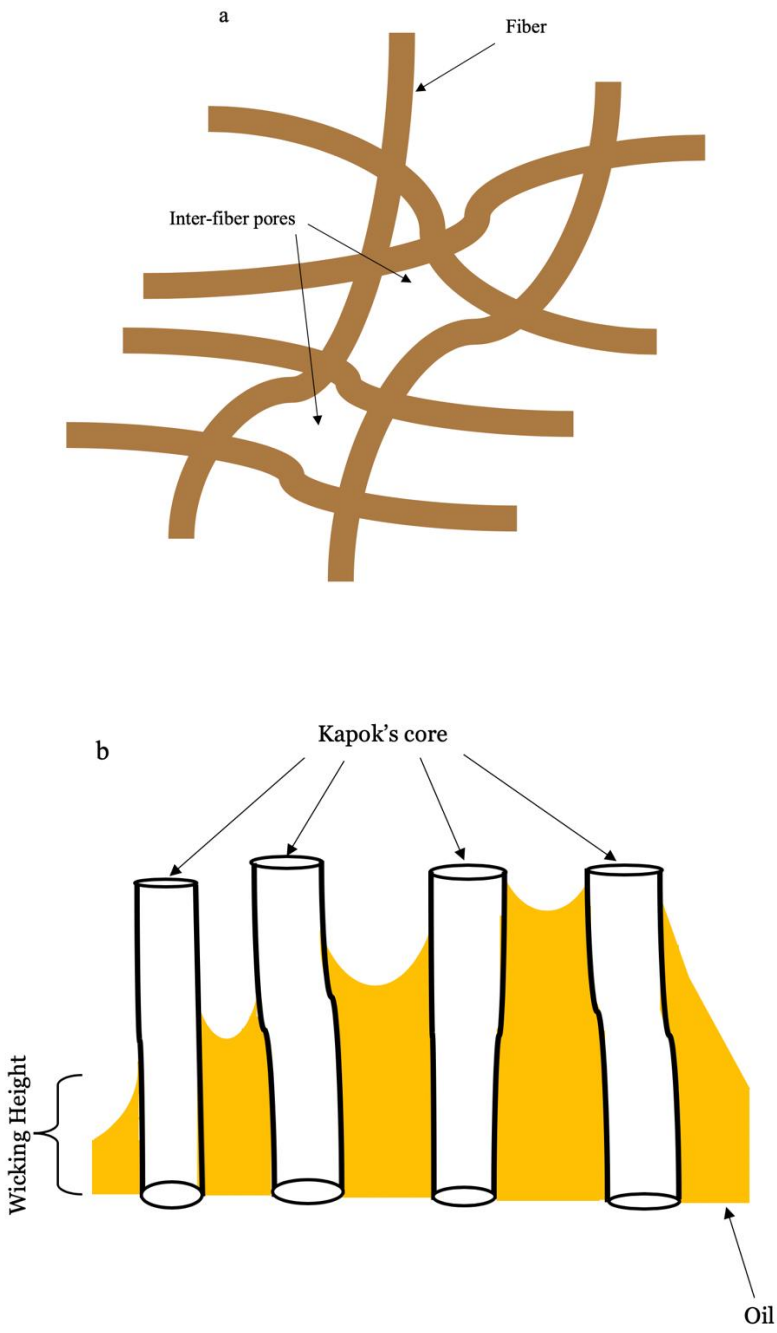

Figure G.1 Kapok Structure; a) Inter-fiber pores and b) kapok's hollow structure.

Appendix H

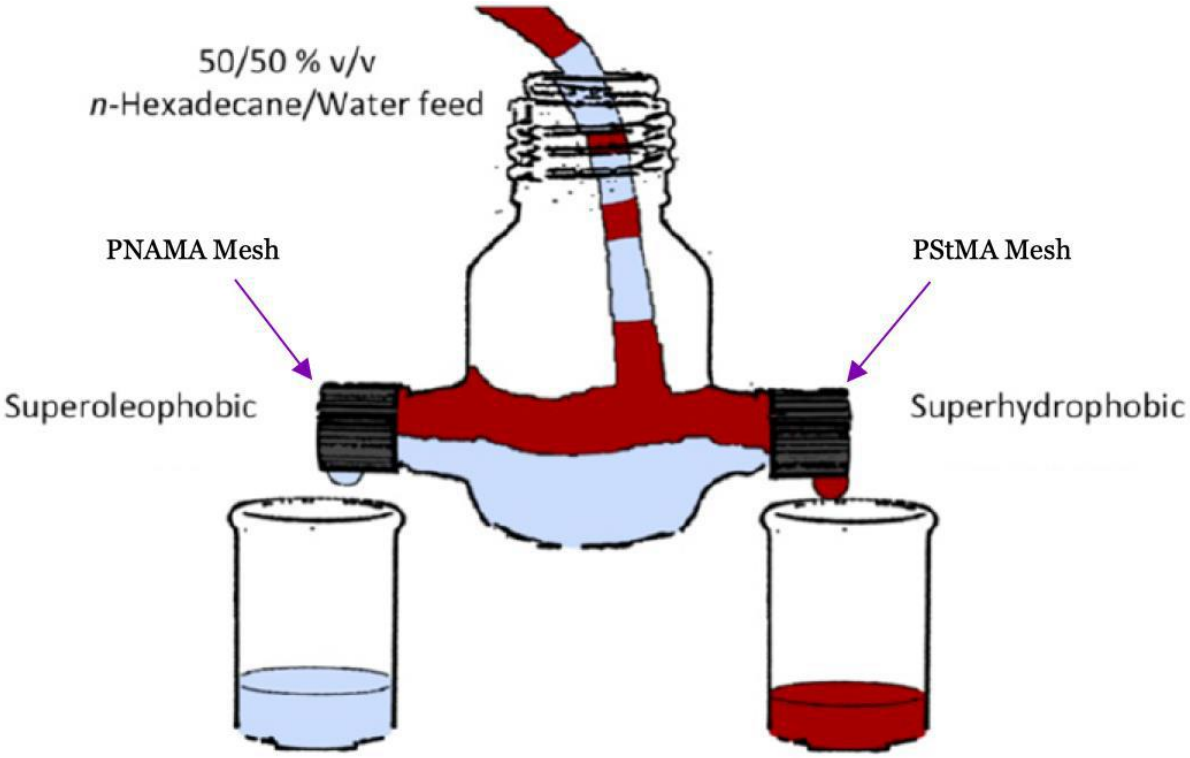

Figure H.1 Oil/water separation system using two antagonistic polymer brush-functionalized meshes [109].

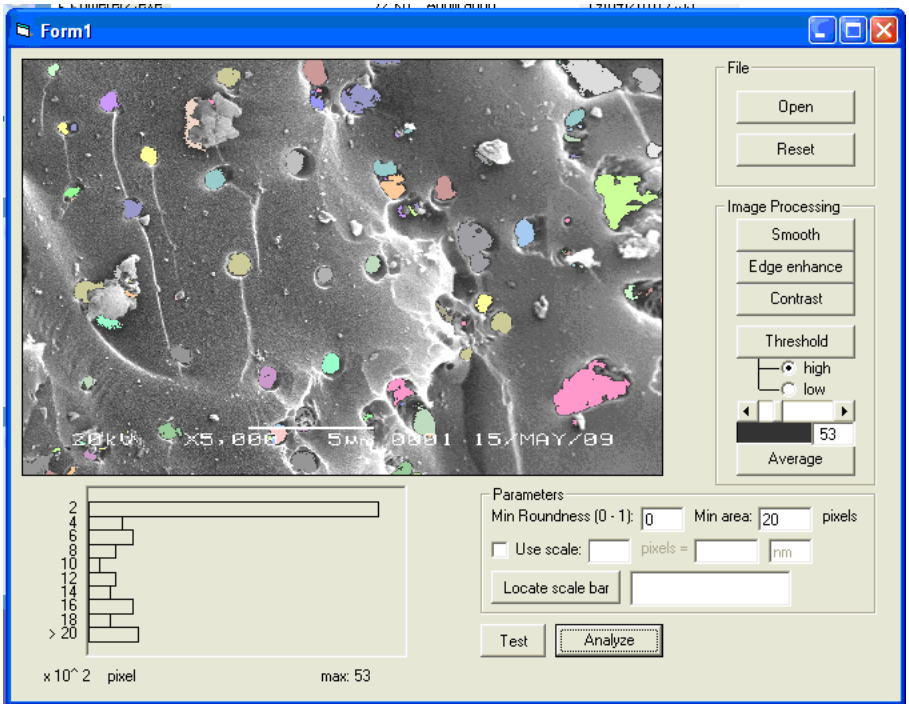

Figure H.2 Screenshot of the pore size measurement program [178].